Establishment of a highly sensitive detection method for neurotransmission disturbances and elucidation of neurotoxicity mechanism, using neonicotinoids as model compounds

(ネオニコチノイドをモデルとした、神経伝達撹乱の高感度検出法の確立と神経毒性メカニズムの解明)

Anri Hirai

Contents

Abbreviations

ACC:	anterior cingulate cortex
ACE:	acetamiprid
Ach:	acetylcholine
ADI:	acceptable daily intake
AOP:	adverse outcome pathway
Aq:	cerebral aqueduct
AUC:	area under the curve
BBB:	blood-brain barrier
BW:	body weight
C.C.:	cross-correlation
CE:	collision energy
CLO:	clothianidin
CV:	coefficient of variation
DA:	dopamine
dc-ACE:	*N*-descyano-acetamiprid
DG:	dentate gyrus
dm-ACE:	acetamiprid-N-desmethyl
dm-dc-ACE:	*N*-desmethyl-descyano-acetamiprid
DMSO:	dimethyl sulfoxide
DPP:	2,4-diphenyl-pyranylium
DRN:	dorsal raphe nuclei
DW:	distilled water
EPA:	Environmental Protection Agency
EPM:	elevated plus maze
ESI:	electrospray ionization

EU: European Union

EZM: elevated zero maze

IDL: instrument detection limit

IEG: immediate early gene

IMI: imidacloprid

IS: internal standard

KEs: key events

LC/MS/MS: liquid chromatography mass spectrometry

LD_{50}: median lethal dose

LOAEL: lowest observed adverse effect level

LOD: limit of detection

LOQ: limit of quantification

MAs: monoamine neurotransmitters

MDL: method detection limit

MeOH: methanol

MRM: multiple reaction monitoring

nAChRs: nicotinic acetylcholine receptors

N-acetyl-ACE: *N*-acetyl-acetamiprid

N-acetyl-dm-ACE: *N*-acetyl-desmethyl-acetamiprid

NNs: neonicotinoid pesticides

NOAEL: no observed adverse effect level

OECD: Organisation for Economic Co-operation and Development

PFA: paraformaldehyde

PB: phosphate buffer

PV: parvalbumin

Py-Tag: 2,4,6-triethyl-3,5-dimethyl pyrylium trifluoromethanesulfonate

RN: raphe nuclei

ROI:	region of interest
RT:	retention time
SD:	standard deviation
SEM:	standard error
SOM:	somatostatin
SSRIs:	selective serotonin reuptake inhibitors
STD:	standard
TEA:	triethylamine
TRAP:	targeted recombination in active populations
VIP:	vasoactive intestinal peptide
3-MT:	3-methoxytyramine HCl
4-OHT:	4-hydroxytamoxifen

Notes

Some of the contents of this dissertation have been published in the articles below:

List of publications related to the dissertation

(I) Hirai A, Sugio S, Nimako C, Nakayama SMM, Kato K, Takahashi K, Arizono K, Hirano T, Hoshi N, Fujioka K, Taira K, Ishizuka M, Wake H, Ikenaka Y. Ca^{2+} imaging with two-photon microscopy to detect the disruption of brain function in mice administered neonicotinoid insecticides. Sci. Rep., 12 (1), 1–13, 2022.

(II) Hirai A *, Yamazaki R*, Kobayashi A, Kimura T, Nomiyama K, Shimma S, Nakayama SMM, Ishizuka M, Ikenaka Y. Detection of changes in monoamine neurotransmitters by the neonicotinoid pesticide imidacloprid using mass spectrometry. Toxics, 10 (11), 696, 2022.

*Both authors contributed equally to this work.

(III) Hirai A, Toda C, Yohannes YB, Collins N, Tamba M, Nomiyama K, Eguchi A, Hoshi N, Hirano T, Nakayama SMM, Ishizuka M, Ikenaka Y. Role of brain monoamines in acetamiprid-induced anxiety-like behavior. Toxicology, 505, 153839, 2024.

The contents of ***Chapter 1*** and ***3*** have been published in *Scientific Reports* as (I).

The contents of ***Chapter 2-1*** have been published in *Toxics* as (II).

The contents of ***Chapter 2-2*** have been published in *Toxicology* as (III).

Preface

Human populations are ubiquitously exposed to chemicals through various sources, including consumer products, the food supply, and environmental media. Such exposure occurs even among individuals not professionally engaged in handling chemicals. Despite the prevalence of chemical exposure, comprehensive risk assessments for human health remain limited, underscoring the need for large-scale, longitudinal epidemiological studies, such as biomonitoring (Calafat et al., 2006). For instance, while numerous epidemiological studies suggest an association between pesticide exposure and the etiology of Parkinson's disease, inconsistent exposure data and insufficient evidence preclude the establishment of a causal relationship (Freire et al., 2012; Vellingiri et al., 2022). Similarly, exposure to environmental contaminants, including heavy metals and pesticides, has been linked to an elevated risk of Alzheimer's disease. However, the absence of reliable biomarkers for retrospective exposure assessment hinders the development of early diagnostic methods (Rahman et al., 2020). Thus, while extensive monitoring is imperative, elucidating the kinetics and toxic mechanisms of individual chemicals is equally critical for interpreting epidemiological findings and guiding risk management efforts. It is noteworthy that a large proportion of chemicals have not yet been fully characterized with respect to their mammalian toxicity and their mechanisms, emphasizing the urgent need for further research in this field.

Neurotoxicity affecting higher brain functions, such as emotional and cognitive behaviors, presents a particularly complex challenge due to the intricacies of the underlying mechanisms. The transmission of signals between neurons, glial cells, and neurotransmitters within the brain is a dynamic process involving complex interactions. Disruption of these networks, whether between neurons or between neurons and glial cells, can compromise higher-order brain functions. One critical component of these networks is the neurotransmitter pathway responsible for "signal transmission," which mediates the transduction of extracellular signals, such as neurotransmitters, into intracellular responses, ultimately modulating gene expression (Costa et al., 2001). The impact of chemicals targeting these neurotransmitter pathways on emotional and cognitive behaviors has been demonstrated, even at concentrations that do not induce histopathological changes (Moser,

2010). However, given the multifactorial nature of behavior, which integrates processes ranging from central neurotransmission to peripheral signaling, unraveling the precise relationship between neurotransmission deficits and their impact on emotional and cognitive functions remains a considerable challenge.

Neonicotinoid pesticides (NNs) are a class of neuroreceptor modulators that act as agonists at nicotinic acetylcholine receptors (nAChRs). Since their introduction in the 1990s, the use of NNs has expanded rapidly due to their efficacy and wide applicability (Bass et al., 2015; Jeschke et al., 2011; Klingelhöfer et al., 2022). In recent years, exposure to NNs have been implicated as a potential contributing factor to bee colony collapse disorder, a phenomenon marked by the sudden disappearance of bees (Sánchez-Bayo et al., 2016). In response, regulatory agencies, including the European Union (EU) and the United States Environmental Protection Agency (EPA), have implemented measures to restrict NN usage. However, these measures have not been universally adopted, with their application remaining prevalent in many other regions (Zhang et al., 2022).

NNs are characterized by their high water solubility, which classifies them as systemic pesticides. This property enables NNs to be absorbed by plants through water uptake. Additionally, NNs exhibit a prolonged environmental half-life, allowing their persistence in soil, surface water, and groundwater for extended periods (Thompson et al., 2020). Empirical studies have reported the presence of NNs in agricultural surface waters across several regions (Stehle et al., 2023), as well as in commercial teas and juices (Li, D et al., 2020; Ly et al., 2022; Suzuki et al., 2021). Furthermore, trace amounts of NNs have been detected in human biological samples, including the urine of newborns (Ichikawa et al., 2019; Taira, K et al., 2021), suggesting that exposure to low doses of NNs is a common occurrence.

In contrast, recent *in vivo* studies have demonstrated that clothianidin (CLO), a commonly used NNs, induces anxiety-like behaviors in mice even at doses below the no observed adverse effect level (NOAEL) (Hirano et al., 2018). Despite these observations, the precise mechanisms underlying NNs-induced neurotoxicity remain unclear. As the acceptable daily intake (ADI) for humans is typically estimated using NOAEL data, these findings underscore the necessity for further research to elucidate the neurotoxic

mechanisms of NNs. Such research will enable the refinement of toxicity assessments and the establishment of more accurate risk management strategies.

According to the Organisation for Economic Co-operation and Development (OECD) guidelines for neurotoxicity testing (OECD, 1997, 2004), behavioral tests for higher brain function are not included as routine screening tests in neurotoxicity evaluations for all chemicals. Instead, tests for higher brain function are performed only when general tests, such as histopathology and spontaneous locomotor activity evaluations, show symptoms that indicate potential neurotoxicity. This suggests that the effect of neurotransmission disturbances on emotional and cognitive behaviors may be overlooked in current toxicity tests.

Furthermore, the evaluation of higher brain function typically relies on behavioral tests. While such tests are essential, they have limitations, including insufficient sensitivity for detecting neurotoxic effects, particularly developmental toxicity (Claudio et al., 2000; European Food Safety Authority, 2013). This issue is compounded by the necessity for large-scale animal experiments to address inter-individual variability, presenting additional challenges in terms of ethical considerations and experimental feasibility. Consequently, the utilization of behavioral tests alone is considered inadequate for the comprehensive detection of neurotoxicity. Accordingly, there is an imperative to elucidate the mechanisms underlying neurotoxicity and to establish more sensitive and reliable testing systems. These advancements would enable the accurate evaluation of the effects of neuroreceptor modulators on emotional and cognitive behaviors.

In the evaluation of chemical substances, the adverse outcome pathway (AOP) concept is critical. The AOP describes the causal relationships among key events (KEs) occurring at the molecular, cellular, organic, and organismal levels in the expression of adverse effects caused by chemical substances on human health. By conceptualizing toxicity as a series of pathways, the AOP framework enables a deeper understanding of toxicity mechanisms. These pathways are typically initiated by the interactions of chemicals with biomolecules, progress through KEs at various levels, and result in the development of adverse effects. This framework not only facilitates the risk assessment of

individual chemicals, but also enables the identification of significant KEs in pathways associated with neurological diseases. Furthermore, by integrating multiple AOPs that share common KEs into a comprehensive network, the AOP framework provides insights into the complex interactions and mechanisms of toxicity (Bal-Price et al., 2017). Collecting additional data on AOPs is essential, as these findings enable predictive risk assessments for combined exposures to multiple chemicals, reflecting the complexities of real-world environments.

Accordingly, this study focused on NNs as a model compound to investigate neurotoxicity. The research was conducted with the following objectives: in *Chapter 1*, the effects of NNs on emotional-cognitive behavior were examined, while *Chapter 2* elucidated the relationship between the NNs-induced behavioral changes and alterations in monoamine neurotransmitters (MAs). The subsequent chapter, *Chapter 3*, investigated changes in neural activity under conditions of arousal, and the final chapter, *Chapter 4*, identified brain regions where neural activity was altered *in vivo*. To achieve these objectives, this study employed innovative approaches not yet widely utilized in the toxicology field, including *in vivo* Ca^{2+} imaging using two-photon microscopy and transgenic mice. The integration of these methodologies was undertaken to facilitate a comprehensive understanding of AOP at multiple levels: neurotransmitters, neurons, brain regions, and behavior.

Through these efforts, this study seeks to elucidate the mechanisms of neurotoxicity and establish a highly sensitive testing system to detect disturbances in neurotransmission. The findings of this study are expected to contribute to the development of advanced methods for assessing neurotoxicity, thereby improving the accuracy and comprehensiveness of chemical risk evaluations.

Chapter 1

Neonicotinoids transfer into the brain and the assessment of behavioral changes

1. Introduction

NNs are pesticides with a nicotine-like structure that act as nicotinic acetylcholine receptor (nAChR) agonists. The nAChRs are abundantly expressed in the central nervous system of insects, and when NNs bind to them, the excitation is sustained, resulting in insecticidal effects (Taillebois et al., 2018; Tomizawa et al., 2000). Due to the varying properties of nAChRs, NNs have a higher affinity for insect nAChRs than for mammalian nAChRs (Tomizawa et al., 2003); therefore, NNs have been considered to be highly selective, with low toxicity to mammals and non-target species (Lansdell et al., 2000; Matsuda et al., 2001; Tomizawa et al., 2003, 2005). These circumstances, coupled with their flexible application in sprays and seed treatments, have led to the widespread use of NNs, accounting for more than 25% of the global market (Bass et al., 2015; Klingelhöfer et al., 2022; Stehle et al., 2023; Thompson et al., 2020).

NNs have been detected in the urine of Japanese people; even in those without occupational exposure (Ikenaka et al., 2019; Ueyama et al., 2015). Researchers have reported a correlation between the detection rate of NNs in urine and the domestic shipment volume in Japan of some NNs, such as thiamethoxam (Ueyama et al., 2015). Moreover, acetamiprid (ACE), one of the NNs, has been identified in its metabolized form as acetamiprid-N-desmethyl (dm-ACE) in the urine of extremely low-birth-weight infants collected within 48 h and 14 days after birth (Ichikawa et al., 2019). The aforementioned findings suggest that humans may be chronically exposed to NNs, despite not being engaged in NN-associated occupations, such as agriculture. On the other hand, Hirano *et al.* found that CLO at 5 mg/kg body weight (BW), which is the concentration below the NOAEL (47.2 mg/kg BW), increased anxiety-like behavior during the elevated plus-maze (EPM) test in mice (Hirano et al., 2018). NNs exert their effects by modulating nAChRs at low concentrations without causing histopathological changes (Hirano et al., 2018). This eventually affects emotional and cognitive behaviors. Since it is difficult to assess the effects of NNs on emotional and cognitive behaviors in higher mammals such as humans, it is necessary to understand the mechanism of action of the chemical substance and conduct the appropriate toxicological effect assessment. However, the mechanism of neurotoxicity of NNs is still not understood in detail.

Therefore, this study focused on ACE, which is used worldwide and, as mentioned above, has been detected in human urine. The lowest NOAEL calculated in toxicity tests in mice was 20.3 mg/kg/day in an 18-month carcinogenicity test (European Food Safety Authority, 2016; Food Safety Commission, 2014). The lowest-observed-adverse-effect level (LOAEL) and NOAEL in mice in a general pharmacological study of the central nervous system were 20 mg/kg and 10 mg/kg, respectively, and a decrease in spontaneous locomotor activity was observed at the LOAEL level (Food Safety Commission, 2014). In light of these factors, the dose concentration of ACE was set at 20 mg/kg in this study. Following the study of Kimura-Kuroda et al. (2012), I also administered nicotine as a typical nAChRs agonist and tried to compare it with ACE. Since nicotine is a positive control, I administered nicotine at two different concentrations, half or tenth of the oral median lethal dose (LD_{50}). EPM tests were performed 1 hour after administration of these nAChRs agonists to assess the level of neurotoxicity due to ACE exposure. Furthermore, the levels of ACE and its metabolites in the mouse brain were quantified to ascertain the transfer of ACE to the brain and its distribution within the brain.

2. Material and methods

2.1. Chemicals

ACE was purchased from Cosmo Bio Co., Ltd. (100% purity, Tokyo, Japan) and Kanto Chemical Co., Inc. (Tokyo, Japan). ACE-d6 and dm-ACE-d3 were purchased from Hayashi Pure Chemical Industries, Ltd. (Osaka, Japan). dm-ACE was purchased from Sigma-Aldrich (St. Louis, MO, USA). *N*-descyano-acetamiprid (dc-ACE), *N*-desmethyl-descyano-acetamiprid (dm-dc-ACE), *N*-acetyl-acetamiprid (*N*-acetyl-ACE), and *N*-acetyl-desmethyl-acetamiprid (*N*-acetyl-dm-ACE) were synthesized by the Toho University. Nicotine (97% purity), isoflurane, formic acid (99% purity), acetic acid (99.7% purity), and sodium acetate (98.5% purity) were purchased from Fujifilm Wako Pure Chemicals Co., Inc. (Tokyo, Japan). In addition, I purchased magnesium sulfate from Agilent Technologies Japan, Ltd. (Tokyo, Japan). All other reagents were purchased from Kanto Chemical Co., Inc. (Tokyo, Japan).

2.2. Animals

All the animal experiments were approved by the Experimental Committee of the Faculty of Veterinary Medicine, Hokkaido University. All animal experiments were performed in accordance with the Guide for the Care and Use of Laboratory Animals, in conformity with the Association for the Assessment and Accreditation of Laboratory Animal Care International (AAALAC; approval number: 18-0061). Male C57BL/6J mice (7 weeks old) were obtained from CLEA Japan, Inc. (Tokyo, Japan) and were kept in a 12 h light/dark cycle at a room temperature of 22 ± 1°C and humidity of 70 ± 5%. The mice were provided food (breeding solid feed for mice, rats, and hamsters: CE-2, CLEA Japan, Inc., Tokyo, Japan) and tap water, ad libitum. I changed the feed and water twice a week. The mice cages were changed once a week.

2.3. EPM tests

Following a 1-week acclimation period, I randomly divided the mice into four groups: the control group (group C), the ACE group (group A), a low concentration nicotine group (group L), and a high concentration nicotine group (group H). ACE was dissolved in distilled water (DW) to 2 mg/mL, and nicotine to 0.033 mg/mL or 0.165 mg/mL. At 9 weeks of age, I orally administered DW, ACE (20 mg/kg BW), low-dose nicotine (0.33 mg/kg BW), and high-dose nicotine (1.65 mg/kg BW) to groups C, A, L, and H, respectively, under light anesthesia with isoflurane. Sonde (FUCHIGAMI Co., Ltd., Kyoto, Japan) was used to administer a 10 mL/kg BW dose. The ACE dose used in the current study was inferred from the NOAEL of the ACE in the toxicity tests (Food Safety Commission, 2014). Furthermore, the nicotine dose was based on the oral LD_{50} of mice, as described in the International Peer Reviewed Chemical Safety Information (Landoni, 1991), and was calculated as 1/10 and 1/2 LD_{50}. Approximately 1 h after administration, I subjected the mice to the EPM tests.

The EPM test is comprised of walled (closed arms) and wall-less passages (open arms) (two each). This behavioral test uses the equilibrium between curiosity in a novel environment and fear of heights as a measure of anxiety-like behavior (Walf et al., 2007; Yamaguchi et al., 2005a). Following chemical administration, the EPM test was performed after keeping the mice in a dark room for 1 h, for groups C, A, L, and H (n = 10 each, in accordance with a previous study (Biala et al., 2006)). The EPM apparatus (length, 29.5 cm; width, 6 cm; wall height, 15 cm; and height, from floor; 41.5 cm) was set up high off the floor such that the closed arms and open arms were at a 90° angle. The brightness of the light within the apparatus was set at 20 lx. Each mouse was allowed to move freely for 5 min in the maze. Mice were not placed into the EPM apparatus in a blinded manner, but the behavioral analysis was conducted using SMART 3.0 (Panlab, S.L., Barcelona, Spain) and the effect of subjectivity is considered to be minimal. The distance and time traveled, the number of entries into the arm, and the rate of arm selection (the number of entries into each arm / total number of entries into the open and closed arms) were used as indicators of anxiety-like behavior, and the number of moves between zones and the total distance traveled were used as indicators of activity. Entry into each zone was defined as when the mouse's center of gravity entered the area.

2.4. Sample preparation using QuEChERS method for liquid chromatography/mass spectrometry (LC/MS/MS) analysis of ACE and its metabolites

Groups C (n = 5) and A (n = 8) were euthanized, dissected, and sampled after EPM tests. I conducted euthanasia via cervical dislocation under deep isoflurane anesthesia. At necropsy, whole blood and organs, such as the cerebral cortex, hippocampus, striatum, and liver, were collected and stored at -20°C.

The pretreatment for LC/MS/MS analysis was performed differently for organs and blood. I extracted and purified ACE and its metabolites from tissues using the QuEChERS method (Anastassiades et al., 2003; Lehotay et al., 2007; Liu, X et al., 2011). Approximately 10 mg of tissue samples obtained from the target organs were weighed into 1.5 mL tubes. I then added 1 mL acetonitrile containing 1% acetic acid and a 50 μL internal standard master mix containing ACE-d6 and dm-ACE-d3 (100 ppb) to the tissue sample.

The samples were homogenized using a Tissue Lyser (1 min, 30/s; Retsch, QIAGEN K.K., Tokyo, Japan) and two zirconia beads (2.0 mm; Tokyo Garasu Kikai Co., Ltd., Tokyo, Japan). Following homogenization, the tissue homogenate was centrifuged at 10,000 x*g* for 5 min. The supernatant was carefully transferred to a 15 mL tube. Subsequently, I added 3 mL of sodium acetate buffer (0.1667 g/mL), 2 mL DW, and 4 g magnesium sulfate (MgSO4) to the supernatant. The sample was vortexed thoroughly and centrifuged at 10,000 x*g* for 10 min. I eventually diluted a 20 µL aliquot of the supernatant in 180 µL of DW, containing 1% formic acid. It was then subjected to LC/MS/MS analysis.

I prepared the blood specimens by measuring 50 µL of whole blood into a 1.5 mL tube and topping it up to the 1.5 calibrated mark using DW. The extraction and purification process of the blood samples followed a similar QuEChERS protocol adopted for tissue samples (as explained before). However, I diluted 100 µL of the supernatant from whole blood extract in 100 µL of DW, containing 1% formic acid for LC/MS/MS in the final stage.

2.5. LC/MS/MS measurement conditions for the analysis of ACE and its metabolites

I quantified the concentrations of ACE and its metabolites from the extracts of tissues and whole blood using an Agilent 1290 Infinity ultra-high performance liquid chromatography system (Agilent Technologies Japan, Ltd., Tokyo, Japan), coupled with an Agilent 6495 triple quadrupole mass spectrometer (Agilent Technologies Japan, Ltd., Tokyo, Japan). The UK Phenyl HT column measured 150 × 2 mm and 3.0 µm particle size (Intact, Kyoto, Japan). The temperature was set at 60°C. I used DW containing 0.1% formic acid and 10 mM ammonium acetate as the mobile phase A. In contrast, methanol containing 0.1% formic acid and 10 mM ammonium acetate were used as phase B. The analytes were separated at a flow rate of 0.6 mL/min. The gradient was initiated at 1% B, increased linearly to 95% B from 0.5 min to 4 min, maintained at 95% B for 5 min, returned to 1% B, and equilibrated for 5.5 min before the next injection. The injection volume was 20 µL. Furthermore, I conducted the ionization using the positive mode of the electrospray ionization (ESI) method. Table 1 summarizes the retention times (RT), multiple reaction monitoring (MRM) transitions, and collision energies (CE) for each analyte.

I performed the quantification using the internal standard method. Seven calibration points were used to plot the standard curves for quantification, and the average coefficient of determination was >0.99. I calculated the limit of quantification (LOQ) and limit of detection (LOD) of the analytes as 10 × SD/S and 3.3 × SD/S, respectively (Table 2). While SD represents the standard deviation (SD) of the five repetitions of the standard solution, S represents the slope of the calibration curve. I checked the peak shape for the analysis. A peak with a signal-to-noise ratio > 10 was adopted as the peak.

2.6. Statistical analysis

I conducted statistical analyses using Excel (2016) and JMP (SAS Institute Inc., Cary, NC, USA). I performed the Steel test to analyze EPM test results. Data are presented as the mean ± standard error (SEM), and the significance level was set at $P < 0.05$.

3. Results

3.1. EPM tests

I measured the percentage of the distance traveled and the time spent in each arm, the number of entries, the rate of arm selection, the number of movements between the zones, and the total distance traveled (Fig. 1). The less time mice stayed in the open arm and, conversely, the more time they stayed in the closed arm, the more anxiety-like behavior was observed.

The distance traveled in the open arms was 24.4 ± 3.1%, 21.0 ± 5.5% (P = 0.7663), 27.9 ± 4.3% (P = 0.8575), and 15.6 ± 3.2% (P = 0.2128) for groups C, A, L, and H, respectively (Fig. 1a); the time spent in the open arms was 31.9 ± 3.7% for group C, 24.5 ± 6.3% for group A (P = 0.5568), 37.6 ± 4.9% for group L (P = 0.6632), and 21.0 ± 4.3% for group H (P = 0.2807) (Fig. 1b). The number of entries was 24.3 ± 2.3 times, 14.1 ± 1.6 times (P = 0.0098), 20.2 ± 1.8 times (P = 0.4519), and 13.1 ± 2.8 times (P = 0.0336) for groups C, A, L, and H, respectively (Fig. 1c). The rate of open arms selection was 50.8 ± 2.9% for group C, 43.3 ± 2.7% for group A (P = 0.3607), 53.0 ± 3.6% for group L (P =

0.8573), and 34.6 ± 5.3% for group H (P = 0.0807) (Fig. 1d). There was a significant difference in the number of entries for groups A and H compared to that for group C.

The distance traveled in the closed arms in groups C, A, L, and H was 56.0 ± 3.2%, 63.0 ± 5.3% (P = 0.0.5568), 54.4 ± 4.1% (P = 1), and 69.7% ± 4.0% (P = 0.0962), respectively (Fig. 1e). The time spent was 42.4 ± 3.7% for group C, 57.4 ± 6.4% for group A (P = 0.1141), 41.8 ± 4.3% for group L (P = 0.9953), and 60.6 ± 6.1% for group H (P = 0.0807) (Fig. 1f). And the number of entries for groups C, A, L, and H was 22.8 ± 1.2 times, 18.3 ± 1.8 times (P = 0.1429), 18.0 ± 1.9 times (P = 0.1535), and 20.1 ± 2.7 times (P = 0.4509), respectively (Fig. 1g). The rate of closed arms selection was 49.2 ± 2.9% for group C, 56.7 ± 2.7% for group A (P = 0.3607), 47.0 ± 3.6% for group L (P = 0.8573), and 65.4 ± 5.3% for group H (P = 0.0807) (Fig. 1h). There was no significant difference found.

The number of movements between the zones was 94.0 ± 4.7 times, 64.6 ± 6.1 times (P = 0.0071), 76.5 ± 5.7 times (P = 0.0804), and 66.4 ± 10.2 times (P = 0.1047) for groups C, A, L, and H, respectively (Fig. 1i), with a significant decrease in groups A. The total distance traveled in groups C, A, L, and H was 1096 ± 42.1 cm, 940.9 ± 79.1 cm (P = 0.4067), 1061 ± 72.1 cm (P = 0.8959), and 1019 ± 74.8 cm (P = 0.9284), respectively (Fig. 1j), with no significant difference.

3.2. Concentrations of ACE and its metabolites in tissue

I measured the concentrations of ACE and its metabolites in the cerebral cortex, hippocampus, striatum, liver, and blood of mice in groups C and A, 1 h after ACE administration. I could not detect ACE and its metabolites in any organs or blood samples from group C. Conversely, ACE and several of its metabolites were detected in all target samples from group A. Only the concentrations for Group A are shown in Table 3.

In group A, the mean concentrations of ACE in the cortical, hippocampal, striatal, liver, and blood tissues were 8.37 ± 0.53 μg/g, 7.47 ± 0.37 μg/g, 9.04 ± 0.51 μg/g, 19.2 ± 1.1 μg/g and 6.48 ± 0.27 μg/mL, respectively. Moreover, the mean concentrations of dm-ACE in the cortical, hippocampal, striatal, liver, and blood tissues were 3.45 ± 0.32 μg/g, 3.39 ± 0.21 μg/g, 3.46 ± 0.14 μg/g, 14.9 ± 0.88 μg/g, and 5.54 ± 0.30 μg/mL, respectively. *N*-

acetyl-dm-ACE was also detected in the blood (63.6 ± 0.26 ng/mL). Other peaks with S/N > 10 were detected for dc-ACE and *N*-acetyl-dm-ACE in the liver, and in various brain regions and the liver, respectively (Table 3). However, dm-dc-ACE and *N*-acetyl-ACE were not detected in any organs.

4. Discussion

ACE acts as an agonist of nAChRs, which are pentameric ligand-dependent ion channels. There are various subtypes of nAChRs; α4β2 hetero-pentamers and α7 homo-pentamers being the most frequently expressed subtypes in the vertebrate brain (Gotti et al., 2006). The α4β2 and α7 subtypes have two and five acetylcholine binding sites, respectively, where acetylcholine binds to induce the depolarization of the postsynaptic membrane (Matsuda et al., 2020). However, the agonistic effects of NNs depend on the type of NN and the nAChR subtype to which it binds. For example, ACE reportedly acts as a partial agonist of the α7 subtype (Cartereau et al., 2018).

I observed the distribution of ACE and dm-ACE in the cerebral cortex, hippocampus, and striatum 1 h after the acute oral administration of ACE (Table 3). ACE and its metabolites have been previously detected in the brain (Ford et al., 2006). The accumulation of ACE in different brain regions has also been investigated (Terayama et al., 2016). However, to the best of my knowledge, there are no studies comparing the concentration of ACE in different brain regions with its metabolites. The results in this study provide new evidence to support the hypothesis that NNs and their metabolites cross the blood-brain barrier (BBB) and are widely distributed in the brain.

NNs generally undergo metabolic activation (Tomizawa et al., 2005), thus necessitating the pharmacokinetics of not only the parent compound but also its metabolites. The major metabolite detected in the brain and blood was dm-ACE. However, I also detected *N*-acetyl-dm-ACE (Table 3). Based on findings from previous studies that compared NN metabolism in rats, dogs, cats, and humans, dm-ACE, the primary metabolite of ACE, *N*-acetyl-ACE, and *N*-acetyl-dm-ACE are likely to be detected (Khidkhan et al., 2021). Cation-π interactions are required for agonists to bind to nAChRs in mammals, but insect nAChRs have cationic sub-sites (Tomizawa et al., 2005). NNs have nitro or cyano

substituents and are not protonated under physiological conditions. Cationic nicotine and other compounds have a higher affinity for mammalian nAChRs. In contrast, for insect nAChRs, NNs have a higher affinity than nicotine because the substituents of NNs interact with cationic sub-sites (Tomizawa et al., 2005). Therefore, these substituents play an important role in establishing selective toxicity to insect nAChRs. Hence, dc-ACE and dm-dc-ACE with deconjugated cyano substituents may have a higher affinity for mammalian nAChRs. However, I failed to detect a significant amount of dc-ACE and dm-dc-ACE, thus suggesting that the selective toxicity of metabolites may not be as high as that of the parent compound.

In addition to ACE, I could detect high concentrations of dm-ACE in the mice brain. dm-ACE exerts modulatory effects on nAChRs. Therefore, the aforementioned neuronal disruption might have been partly caused by dm-ACE. This necessitates studying the effect of dm-ACE on neuronal activity and brain function to clarify the contribution of dm-ACE to ACE-mediated neurotoxicity.

The EPM test is a conflict model in which curiosity from being in a novel environment is in equilibrium with the anxiety and fear resulting from exposure to heights in the open arms. Moreover, it is widely used for behavioral analysis of rodents (Walf et al., 2007; Yamaguchi et al., 2005a). In this research, I placed the mice for 1 hour in darkness during the light period. The brightness of the EPM in this study was set at approximately 20 lux because dark illumination is considered appropriate for observing anxiety-like behavior, i.e., a reduction in open-arm exploratory behavior, since bright illumination conditions have been reported to suppress open-arm exploratory behavior (Jones et al., 2001). However, since the sudden change from a light environment to a dark environment is a stressor, I acclimated mice by keeping them in the dark environment for a certain period of time. In behavioral studies, it is important that mice receive consistent treatment prior to testing (Jones et al., 2001). Therefore, in this study, mice in the control and exposed groups were placed in the dark environment for the same amount of time to eliminate the effects of stressors caused by environmental changes.

Previous studies have shown that exposure to NNs can induce anxiety-like behaviors (Ford et al., 2006; Hirano et al., 2018). I observed a significant decrease in the number of

entries into the open arms and in the movements between the zones (Fig. 1c, i), and the rate of open arms selection tended to decrease (P = 0.3607). In other words, an increase in anxiety in the ACE group (20 mg/kg BW, p.o.) was observed 1 h after administration. Only a weak trend of increased distance traveled and time spent in the closed arm in the ACE group (P = 0.5568 and 0.1141, respectively) existed. This could be because these parameters in the ACE group showed bimodal results. In future studies, implementing more distinct dosing concentrations and larger numbers of mice may help evaluate the effects of ACE on behavior in more detail. Clothianidin and thiamethoxam activate the α4β2 or α7 subtypes of nAChRs in the rat striatum and induce dopamine release (Faro et al., 2019). Considering the variation of nAChR sensitivity among different NNs (Cartereau et al., 2018), it is unclear if ACE activates α4, α7, or otherwise. The behavioral changes described above could be the result of changes in MAs or other substances, and they will be examined in detail in *Chapter 2*.

In addition, the effects of nicotine exposure on behavior vary, depending on the animal species, age, sex, strain, and dose (Biala et al., 2006; Faro et al., 2019; Rodrigues et al., 2010). The subcutaneous injection of nicotine into adult male C57BL6/J mice significantly increases anxiety-like behavior at a dose of 0.05 mg/kg but not at a dose of 0.1 mg/kg or 0.25 mg/kg (Akinola et al., 2019). I observed no significant changes in the low concentration nicotine group (0.33 mg/kg BW, p.o.), 1 h after the treatment. However, there was a significant decrease in the number of entries into the open arms (Fig. 1i) and a strong trend of decreasing rate of open arms selection (P = 0.0807) in the high nicotine group (1.65 mg/kg BW, p.o.), similar to what was observed in the ACE group. The distance traveled and time spent in the closed arm tended to increase (P = 0.0962 and 0.0807, respectively). Therefore, the effects of nicotine on behavior may not be dose dependent. Low and high doses may increase anxiety-like behaviors. However, medium doses may not cause any behavioral changes. The metabolism of nicotine in mice is extremely rapid. Following an intraperitoneal administration of 1.0 mg/kg, the half-life in the blood and brain was approximately 7 min and 20 min for nicotine and cotinine, respectively (Petersen et al., 1984). The latter is a major metabolite of nicotine (Petersen et al., 1984). In addition, when injected subcutaneously, the half-life of nicotine was approximately 20 min (Akinola et al., 2019). I measured the nicotine group 1 h after administration to standardize the

measurement time for all groups. However, a change in the measurement time may produce different results.

There was no significant change in the total distance traveled in any of the groups. In other words, at the concentrations used in this study, the administration of ACE or nicotine did not change mice activity.

5. Summary

In summary, ACE and its metabolites have been demonstrated to be transferred to various regions of the brain, including the hippocampus and striatum, within one hour of oral administration. Furthermore, ACE increased anxiety-like behavior, even at the NOAEL levels in the toxicity tests, a dose at which adverse effects are not expected to occur. This effect was also observed at concentrations of nicotine that were half the LD50.

This is a novel report that compares the distribution of ACE in different brain regions along with metabolites. It also reinforces previous studies showing that NOAEL levels of NNs increase anxiety-like behavior. In order to elucidate this mechanism, I will investigate MAs and changes in neural activity in *Chapter 2* and subsequent chapters.

6. Figures and tables

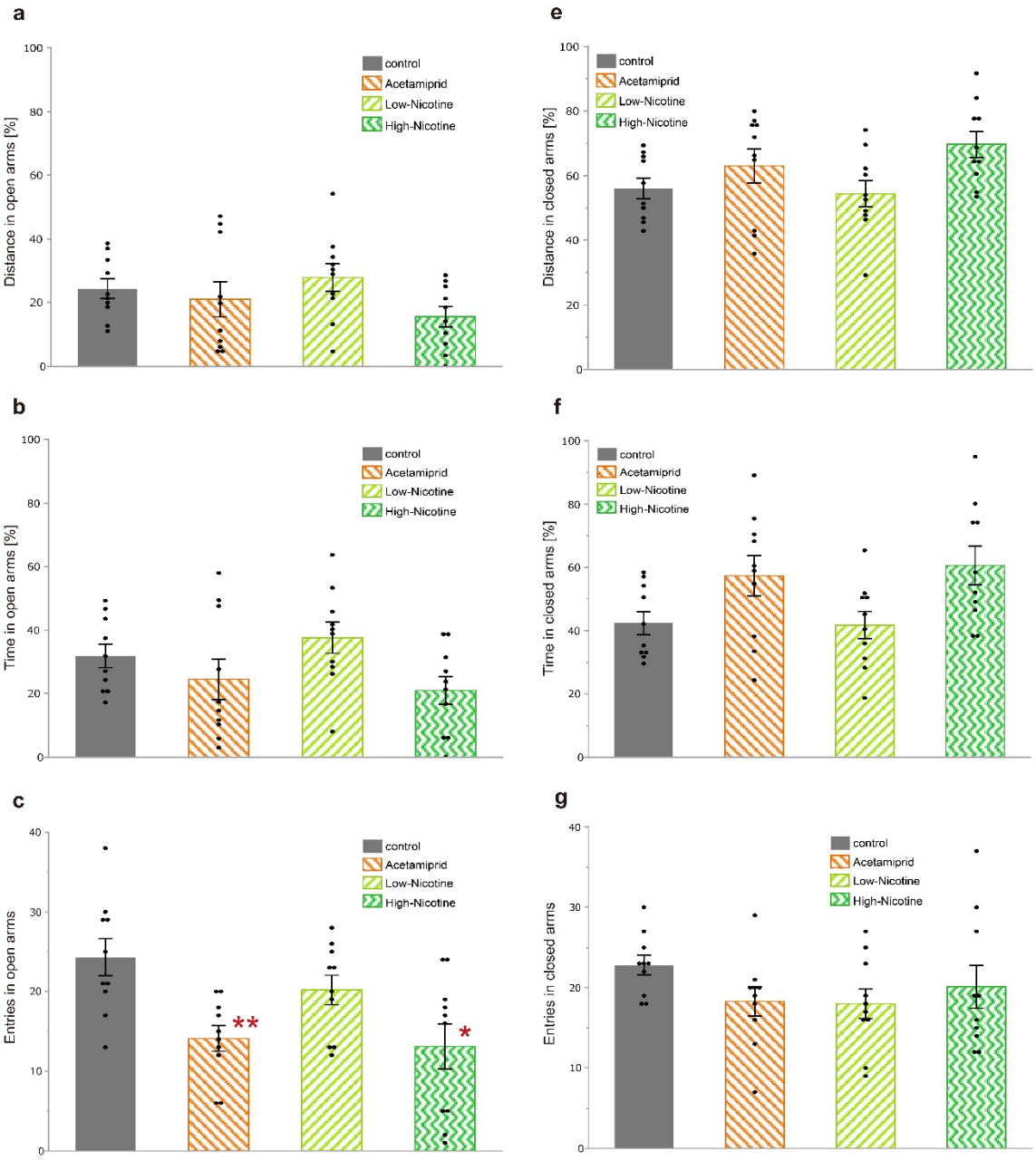

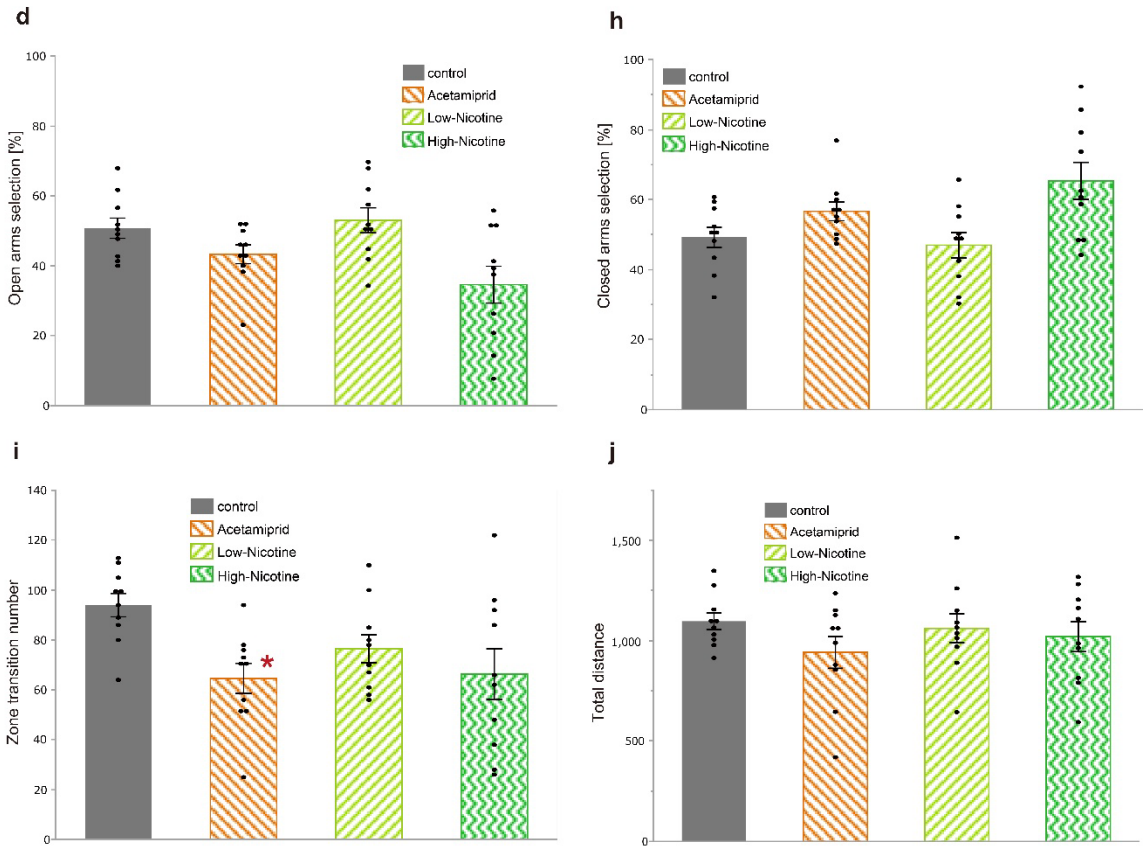

Figure 1. Behavioral effects of acute exposure of 20 mg/kg acetamiprid and 0.33 or 1.65 mg/kg nicotine in the EPM tests.

The ACE group (group A) and the high concentration nicotine group (group H) exhibited a significant reduction in (c) entries into open arms. There was no significant difference in (a) distance traveled in open arms; (b) time spent in open arms; (d) rate of open arms selection; (e) distance traveled in closed arms; (f) time spent in closed arms; (g) entries into closed arms; (h) rate of closed arms selection; (i) the number of movements between zones; and (j) total distance traveled in the EPM.

Data are represented as mean ± SEM of each group (n = 10 each). *P < 0.05, **P < 0.01, Steel test.

Table 1. LC/MS parameters for ACE and its metabolites.

Target ion is the product ion listed in the top column of each compound. Other product ions are used as qualifier ions.

Compound	RT [min]	MRM Transition [m/z]		CE [V]
		Precursor Ion	Product Ion	
ACE	3.3	233.1	126.0	24
			56.3	16
ACE-d6	3.3	229.2	125.9	28
			62.2	16
dm-ACE	3.0	209.1	125.8	20
			72.9	52
dm-ACE-d3	3.0	212.2	126.2	24
			89.9	36
dc-ACE	2.2	198.0	126.1	28
			90.1	44
dm-dc-ACE	1.8	184.0	126.1	20
			73.0	60
N-acetyl-ACE	3.1	199.0	126.1	20
			56.2	20
N-acetyl-dm-ACE	2.7	185.0	126.0	20
			107.1	24

Table 2. LOQ and LOD of ACE and its metabolites.

Compound	LOQ [ng/mL]	LOD [ng/mL]
ACE	0.472	0.156
dm-ACE	1.16	0.382
dc-ACE	1.35	0.445
dm-dc-ACE	1.28	0.423
N-acetyl-ACE	0.955	0.315
N-acetyl-dm-ACE	1.02	0.336

Table 3. The concentration of ACE and dm-ACE in organs and blood of the ACE group. Data are expressed as mean ± SEM (n = 8). N.D., not detected.

Compound	Concentration				
	Cortex [μg/g]	**Hippocampus [μg/g]**	**Striatum [μg/g]**	**Liver [μg/g]**	**Blood [μg/mL]**
ACE	8.37 ± 0.53	7.47 ± 0.37	9.04 ± 0.51	19.2 ± 1.1	6.48 ± 0.27
dm-ACE	3.45 ± 0.32	3.39 ± 0.21	3.46 ± 0.14	14.9 ± 0.88	5.54 ± 0.30
dc-ACE	N.D.	N.D.	N.D.	0.0795 ± 0.0040	N.D.
dm-dc-ACE	N.D.	N.D.	N.D.	N.D.	N.D.
N-acetyl-ACE	N.D.	N.D.	N.D.	N.D.	N.D.
N-acetyl-dm-ACE	0.258 ± 0.0062	0.259 ± 0.0067	0.317 ± 0.042	0.248 ± 0.012	0.0636 ± 0.00026

Chapter 2

Analysis of brain monoamines using two methods and the relationship between behavioral tests and brain monoamines.

Chapter 2-1

Detection of changes in monoamine neurotransmitters by neonicotinoids using DPP derivatization

1. Introduction

MAs is a general term for neurotransmitters with a single amino group, and they are known to regulate brain functions such as behavior, memory, emotion, and learning. For example, the dopamine (DA) is known to be involved in motor control and learning, while serotonin is known to be involved in anxiety and memory (Nieoullon et al., 2003). Thus, MAs play an important role in the regulation of brain function, and abnormalities in their functioning are thought to be involved in the development of neurological disorders such as depression, anxiety disorders, and Parkinson's disease (Hamon et al., 2013; Morilak et al., 2004; Ohama et al., 1976).

Some chemicals exert their toxic effects by acting on receptors in the central nervous system, disrupting neurotransmitters such as MAs. The changes in neurotransmitters cause detrimental effects on the body, most of which manifest as abnormalities in higher brain functions, such as behavior, memory, and learning, without histopathological changes (Kanno, 2016). NNs are among the chemicals known to disrupt neurotransmitters; for example, Oliveira *et al.* (2010) reported that intracerebral administration of CLO and thiamethoxam enhanced DA release in the striatum. These changes in MAs in the brain are suspected to be responsible for the NNs-induced behavioral changes, but few studies have investigated the effects of NNs on MAs, and thus, insufficient knowledge currently exists. As suggested in *Chapter 1*, ACE has been shown to transfer to the brain 1 hour after administration and to increase anxiety-like behavior. Based on these findings, this chapter focuses on MAs as a candidate mechanism underlying the behavioral changes induced by NNs. It also examines imidacloprid (IMI), another widely used NN, for which limited knowledge exists regarding its effects on MAs.

Current neurotoxicity studies focus on symptom observation, behavioral tests, and histopathological examinations after the administration of test substances to evaluate toxicity, making it challenging to detect neurodisruptions, including MA abnormalities. It is essential to use a simple, highly sensitive, and quantitative detection method for more accurate toxicity assessment (Yoshimura, 1993). LC/MS/MS is a detection method for measuring substances in a highly sensitive and quantitative manner by combining mass spectrometry, which ionizes substances in a sample and measures the mass/charge ratio specific to each substance, with high-performance liquid chromatography. Despite the

necessity of a certain level of expertise, this method allows for the detection of neural alterations, including abnormalities in MAs, which cannot be detected by conventional methods.

There have been several previous studies on the detection of MAs using LC/MS/MS (Liu, R xia et al., 2018; Mabrouk et al., 2011; Sørensen et al., 2019; Zhu et al., 2011). However, the octadecylsilyl columns used for liquid chromatography of MAs have weak retention, resulting in low ionization efficiency and difficulty in separating impurities. Therefore, the detection sensitivity of this technology is not high. Since neurotransmitters, including MAs, exert their effects in minute amounts, more sensitive analytical methods are required to detect their fluctuations. It has been reported that the use of tetrafluoroborate salt of 2,4-diphenyl-pyranylium (DPP), a MA derivatization reagent, increases the ionization efficiency and enables highly sensitive MA detection (Esteve et al., 2016; Shariatgorji et al., 2014, 2015; Shimma et al., 2016). Thus, the localization of a wide variety of molecular species can be visualized by performing mass spectrometry on tissue sections. DPP is part of the pyrilium group and reacts with the amino group of MAs (Fig. 2). Although there are no examples of LC/MS/MS applications, this reagent has the potential to be used for highly sensitive analyses of MAs in LC/MS/MS. Therefore, the main objective of this study was to investigate the effect of NNs on MA production in the brain by applying DPP to LC/MS/MS analysis.

2. Material and methods

2.1. Chemicals

IMI was purchased from Kanto Chemical Co., Inc. (Tokyo, Japan). DA, 3-methoxytyramine HCl (3-MT), 3-methoxytyramine-d4 HCl, and serotonin were purchased from Sigma-Aldrich (St. Louis, MO, USA). Serotonin-d4 hydrochloride and histamine were purchased from Toronto Research Chemicals, Inc. (Toronto, ON, Canada), and dopamine-d4 and histamine-d4 were purchased from WATARAI Co., Ltd. (Kanagawa, Japan). DPP, which was originally purchased from Sigma Aldrich (St. Louis, MO, USA),

was donated by Associate Professor Shuuichi Shimma, Department of Biotechnology, Graduate School of Engineering, Osaka University. Corn oil and formic acid were purchased from Wako Pure Chemicals Co., Inc. (Tokyo, Japan); dimethyl sulfoxide (DMSO) was purchased from Nacalai Tesque, Inc. (Kyoto, Japan); triethylamine (TEA) was purchased from Tokyo Chemical Industry Co., Ltd. (Tokyo, Japan); and methanol (MeOH) was purchased from Kanto Chemical Co., Inc.

2.2. Animals

All of the animal experiments were approved by the Experimental Committee of the Faculty of Veterinary Medicine, Hokkaido University. All of the animal experiments were conducted in accordance with the Guide for the Care and Use of Laboratory Animals and with the Association for the Assessment and Accreditation of Laboratory Animal Care International (AAALAC; approval number: 18-0061). Male C57BL/6NCrSlc mice aged 10–12 weeks were obtained from Sankyo Labo Service Co., Inc. (Tokyo, Japan) and kept in a 12-h light/dark cycle (7:00 a.m. to 7:00 p.m.: light, 7:00 p.m. to 7:00 a.m.: dark) at a room temperature of 22 ± 1°C and humidity of 70 ± 5%. Food (breeding solid feed for mice, rats, and hamsters: CE-2, CLEA Japan, Inc., Tokyo, Japan) and tap water were provided to the mice ad libitum. The food and water were changed twice a week, and the cages were changed once a week. The experimental procedures were conducted after an acclimation period of at least two weeks.

2.3. Open field (OF) tests

The mice (n = 24) were randomly divided into three treatment groups (n = 8/group, following the previous study (Biala et al., 2006): control, low-dose, and high-dose groups. IMI dissolved in 2.5% (*v/v*) DMSO in corn oil was orally administered to the low-dose group at 10 mg/kg BW and to the high-dose group at 50 mg/kg BW. The control group received 2.5% (*v/v*) DMSO in corn oil orally at a dose of 10 mL/kg BW. Oral administration with sonde (FUCHIGAMI Co., Ltd., Kyoto, Japan) was performed under mild isoflurane anesthesia. Afterward, the mice were placed in individual cages in a dark

room. The OF tests were then conducted 1 h after oral dosing. All IMI administrations and behavioral tests were performed during the light cycle of the housing facility. The dose of IMI used in this experiment was set at 10 mg/kg (low-dose group), which is the NOAEL, and approximately 46 mg/kg (high-dose group), which is the LOAEL (Bayer CropScience K.K., 2017).

The OF test is a test system that evaluates activity and anxiety levels using exploratory behavior and responsiveness in novel environments. The OF was performed using a square open field box for mice (Panlab, S.L., Barcelona, Spain). The apparatus consisted of a 45 cm × 45 cm square floor surface and 40 cm walls. The central 22.5 cm × 22.5 cm floor of the apparatus was set as the center area and the remaining floor as the side areas. The brightness was set such that the center of the device was approximately 20 lx.

One mouse was allowed to freely explore the apparatus for 5 min. I was aware of the group allocation, but their behavior was objectively analyzed using SMART 3.0 (Panlab, S.L., Barcelona, Spain). The distance traveled, number of area movements, average movement speed, and resting time were used to measure activity, and the time spent in the center area was used as an index of anxiety-like behavior. The average movement speed was the average movement speed during the activity time (5 min minus resting time).

2.4. EPM tests

The mice (n = 24) were randomly divided into control, low-dose, and high-dose groups (n = 8/group, following previous study (Biala et al., 2006)), and they were administered IMI in accordance with the methods described in *section 2.3.* The EPM tests were conducted 1 h after administration.

The EPM test is a behavior test used to evaluate anxiety behavior. The EPM was performed using an elevated plus maze for mice (Panlab, S.L., Barcelona, Spain). The apparatus consisted of an aisle with walls (closed arm) and an aisle without walls (open arm) crisscrossing each other at a height of 40 cm above the floor. The length of each passage was 29.5 cm, the width was 6 cm, and the height of the closed-arm wall was 15 cm. The brightness was set such that the center of the device was 20 lx.

One mouse was allowed to freely explore the apparatus for 5 min as in the OF test. SMART 3.0 (Panlab, S.L., Barcelona, Spain) was used to analyze the behavior, and the ratio of the time spent in the open arms to the measurement time and the ratio of the number of entries into the open arms to the number of entries into both arms were used as indicators of anxiety-like behavior.

2.5. LC/MS/MS measurement conditions for the MA analysis

Among the MAs, there were seven to be measured: DA, 3-MT, l-DOPA, norepinephrine, normetanephrine, serotonin (tryptophan metabolite), and histamine (histidine metabolite), all belonging to the tyrosine metabolism system. However, l-DOPA, norepinephrine, and normetanephrine were poorly derivatized by DPP, making accurate quantification difficult. Therefore, the final four MAs to be measured were DA, 3-MT, serotonin, and histamine.

An Agilent 1290 Infinity UHPLC system (Agilent Technologies Japan, Ltd., Tokyo, Japan) was used for LC, and an Agilent 6495 triple quadrupole mass spectrometer (Agilent Technologies Japan, Ltd., Tokyo, Japan) was used for MS. A 100 mm × 3.0 mm InertSustain AQ-C18 column with a particle size of 1.9 μm (GL Science, Tokyo, Japan) was used, and the temperature was set to 60°C. DW containing 0.1% formic acid was used for mobile phase A, and acetonitrile containing 0.1% formic acid was used for mobile phase B. The analytes were separated at a flow rate of 0.8 mL/min. The gradient was started at 10% B, increased linearly to 95% B from 0.5 min to 4 min, maintained at 95% B for 1 min, and then returned to 10% B and equilibrated for 0.5 min before the next injection. The injection volume was 20 μL, and ESI was performed in positive mode. RT, MRM transition, and CE for each analyte are listed in Table 4.

2.6. Determination of the optimal reaction conditions for the DPP derivatization

The preparation of DPP solution was based on the method of Shimma et al. (Shimma et al., 2016). DPP was adjusted to 10 mg/mL with methanol and made into a DPP solution. As a dilution solvent, 8.1 mL of methanol, 5.4 mL of DW, and 9 μL of TEA were mixed. The derivatization reagent was a solution made by mixing the resulting diluted solvent and DPP

solution to a composition of 69:6 DPP mix. Then, standard (STD) solutions of each target MA were mixed and diluted with 70% MeOH containing 0.1% formic acid to prepare a 1 ppm STD solution (hereafter, called STD mix). The same procedure was followed for the internal standard (IS) to obtain a 1 ppm IS solution (hereafter, called IS mix).

Each 10 μL of the DPP mix and STD mix were combined and derivatized at room temperature (about 25°C), 40°C, or 60°C. These mixtures were collected after 1, 2, 3, 4, 5, and 6 h, diluted with 80 μL of DW, and analysed by LC/MS/MS to determine the optimal time and temperature for the DPP derivatization reaction.

2.7. Calculation of instrument detection limit (IDL) and method detection limit (MDL)

The IDL was calculated by repeating the measurement seven times with a standard solution corresponding to the lowest concentration (4 ppt) of the STD in the calibration curve. The SD was then calculated from the obtained analytical value using the formula below (1).

To calculate the MDL, IS mix was added to mouse brain extract and diluted with MeOH until near the limit of quantification. After the diluted solution was derivatized with DPP, it was analyzed by the prescribed operation, and the obtained analytical value was converted to sample concentration. This operation was repeated seven times, and the MDL was calculated from the SD at that time using the formula below (2):

$$\text{IDL} = 2 \times s \times 1.943, \quad (1)$$

$$\text{MDL} = 2 \times s \times 1.943, \quad (2)$$

where s is the SD and 1.943 is t (6, 0.05) (i.e., the Student's t-value with six degrees of freedom, risk rate 5% (one-sided)). The IDL and analytical MDL are listed in Table 5. In addition, the accuracy and precision of this analytical method are listed in Table 6.

2.8. Organ collection for the MA concentration measurement

The mice (n = 24) were randomly divided into three treatment groups (n = 8/group): control, low-dose, and high-dose groups. Each group received 2.5% (*v/v*) DMSO in corn

oil or IMI dissolved in 2.5% (*v/v*) DMSO in corn oil, as described above. One hour after administration, cardiac blood sampling was performed under deep isoflurane anesthesia, followed by euthanasia by cervical dislocation.

The brain was sectioned using a brain matrix (stainless steel, mouse (40–75 g) coronal; CellPoint Scientific Inc., Gaithersburg, MD, USA) in coronal sections containing the striatum (Bregma 1.00 mm to 0.00 mm) and a coronal section containing the hippocampus (Bregma -3.00 mm to -4.00 mm). The sections were visually checked and then sampled by punching out tissue using a disposable biopsy punch (φ2 mm; Kai Industries Co., Ltd., Tokyo, Japan). The hippocampus was separated from the abovementioned section using tweezers and then sampled. Other regions (olfactory bulb, cerebral cortex, brainstem, and cerebellum) were also isolated and sampled. Each brain region was kept in 1.5 mL tubes (olfactory bulb, striatum, and hippocampus) or 2.0 mL tubes (cerebral cortex, brainstem, and cerebellum), flash frozen in liquid nitrogen, and stored at -80°C. Blood obtained by cardiac puncture using the needle filled with heparin was kept on ice and then centrifuged (4,000 x*g*, 10 min, 4°C). The plasma was stored at -80°C. The brain and plasma samples were used to measure MA levels.

2.9. DPP derivatization for the measurement of MA concentrations in brain tissue

I used the brains that had been collected in *section 2.8.* First, 200 ppb, 20 µL (for striatum); 10 ppb, 20 µL (for hippocampus); or 100 ppb, 20 µL (for olfactory bulb, cerebral cortex, brainstem, and cerebellum) of IS mix (1 ppm in 70% MeOH containing 0.1% formic acid; diluted with MeOH as appropriate) was added as an internal standard to 1.5 mL tubes (olfactory bulb, striatum, and hippocampus) and 2.0 mL tubes (cerebral cortex, brainstem, and cerebellum) containing each brain region. Two zirconia beads (2.0 mm; Toray Industries, Inc., Tokyo, Japan) were placed in each 1.5 mL tube, and one zirconia bead (5.0 mm; Bio-medical Science Co, Ltd., Tokyo, Japan) was placed in each 2.0 mL tube. Ice-cold 0.05% acetonitrile formate was added (100 µL for olfactory bulb; 200 µL for striatum and hippocampus; 300 µL for cortex and brainstem; 400 µL for cerebellum) and homogenized in a Tissue Lyser (30/s, 1 min; QIAGEN K.K., Tokyo, Japan). Then, each

tube was centrifuged (10,000 x*g*, 10 min, 25°C). Ten microliters of the supernatant and 10 μL of the DPP mix were added to 8 tubes, and the derivatization reaction was conducted in a thermal cycler at 60°C for 4 h. After completion of the reaction, 80 μL of DW was added to each tube for dilution, and the target four MAs referred in *section 2.5.* were quantified by LC/MS/MS using an internal standard method. Each peak shape was checked for the analysis; a peak with a signal-to-noise ratio >10 was adopted as the peak. Other than that, it was marked as "N.D. (not detected)."

2.10. DPP derivatization for the measurement of plasma MA concentrations

The plasma stored at -80°C was thawed, 50 μL was sampled in a 1.5 mL tube, and 20 μL of IS mix (100 ppb) was added. Fifty microliters of ice-cold 0.05% formic acid acetonitrile was then added, and the mixture was centrifuged (10,000 x*g*, 10 min, 25°C). Ten microliters of the supernatant and 10 μL of the DPP mix were added to 8 tubes, and the derivatization reaction was conducted in a thermal cycler at 60°C for 4 h. After completion of the reaction, 80 μL of DW was added to each tube, and the target substances were measured by LC/MS/MS. Each dataset was checked similarly to *section 2.9.*

2.11. Statistical analysis

Statistical analysis was performed using Excel (2019) and JMP (SAS Institute Inc., Cary, NC, USA). Analysis of variance was performed using the Bartlett test ($P < 0.025$). The Tukey-HSD test was used for comparison of reaction times, and the Dunnett's test was used for comparison between groups in the results of behavioral tests and measurements of MA concentrations. Data are presented as mean ± SEM, and the criterion for significant difference was $P < 0.05$.

3. Results

3.1. OF tests

The OF results are shown in Figure 3. In the OF group, there was a significant decrease in the distance traveled from 1304 ± 55 cm in the control group and 1202 ± 77 cm in the low-dose group to 195 ± 24 cm in the high-dose group (Fig. 3a, $P < 0.0001$). The number of area movements was 30 ± 7 times in the control group, 21 ± 4 times in the low-dose group, and 2 ± 1 times in the high-dose group, with a significant decrease in the high-dose group (Fig. 3b, $P = 0.0004$). In the center area, the mean movement speed was 9.27 ± 0.86 cm/s in the control group, 9.45 ± 0.61 cm/s in the low-dose group, and 2.19 ± 0.72 cm/s in the high-dose group. In the side area, the mean movement speed was 6.46 ± 0.19 cm/s in the control group, 6.29 ± 0.20 cm/s in the low-dose group, and 3.20 ± 0.20 cm/s in the high-dose group; in both areas, there was a significant decrease in mean movement speed in the high-dose group (Fig. 3c,d, $P < 0.0001$). The resting time was 43.4 ± 2.22% in the control group, 47.30 ± 2.93% in the low-dose group, and 92.67 ± 1.60% in the high-dose group, with a significant increase in the high-dose group (Fig. 3e, $P < 0.0001$). Although the average time spent in the center area was higher in the high-dose group (17.91 ± 11.45%) than in the control group (7.38 ± 2.09%) and low-dose group (4.96 ± 1.31%), the differences were not statistically significant (Fig. 3f).

3.2. EPM tests

The EPM results are shown in Figure 4. The percentage of time spent in the open arm was 45.80 ± 5.24% in the control group, 27.86 ± 3.68% in the low-dose group, and 70.20 ± 9.60% in the high-dose group, and the percentage of distance spent in open arms was 38.95 ± 4.76%, 23.56 ± 3.85% and 63.25 ± 9.62%, in the control group, low-dose group, high-dose group, respectively. For these parameters, there was a significant increase in the high-dose group compared to the control group (Fig. 4a,b, $P < 0.05$). In contrast, the percentages of open arm entries were 53.27 ± 2.09% in the control group, 44.93 ± 2.48% in the low-dose group, and 63.52 ± 11.31% in the high-dose group, which were not significantly different (Fig. 4c). The total distance traveled in the control, low-dose and high-dose group was 1140.7 ± 41.08 cm, 1021.7 ± 51.91 cm and 214.1 ± 28.49 cm, respectively, was significantly less in the high-dose group than in the control group (Fig. 4d, $P < 0.0001$).

3.3. Determination of the optimal reaction conditions for the DPP derivatization

MA concentrations at each reaction time are shown in Figure 5. For each substance, the concentration (area value) increased in a time-dependent manner. For all of the substances except histamine, the highest concentration was obtained 6 h after the start of the reaction, but there was no significant difference between this time and 4 h. Thus, the reaction time was set to 4 h.

MA concentrations at each reaction temperature are shown in Figure 6. The concentration increased in a temperature-dependent manner, and the reaction efficiency was maximal at 60°C for all of the substances. Therefore, the reaction temperature was set to 60°C.

3.4. MA concentrations in brain tissue

Using the analytical method established in this study, I measured MA concentrations in various regions of the brain. The measurement sites were the olfactory bulb, striatum, hippocampus, cerebral cortex, brain stem and cerebellum, and the results were compared between the control and exposed groups (Table 7).

There was a significant dose-dependent reduction in DA in the olfactory bulb (low-dose group, $P = 0.0061$; high-dose group, $P = 0.0004$), and DA was significantly reduced in the cerebellum in the high-dose group ($P = 0.0007$). In addition, a dose-dependent decreasing trend was observed in the striatum, although there was no significant difference between groups. In the olfactory bulb, 3-MT was significantly decreased in the high-dose group ($P = 0.0011$), while it was significantly elevated in the high-dose group ($P = 0.0159$). Histamine levels were significantly decreased in the striatum in both the low-and high-dose groups ($P < 0.0001$). Significant decreases were also observed in the olfactory bulb (low-dose and high-dose groups) and cerebellum (high-dose group) (olfactory bulb, low-dose group: $P = 0.0271$, high-dose group: $P = 0.037$; cerebellum, high-dose group: $P = 0.013$). Serotonin was significantly reduced in the striatum, from 438.0 ± 44.8 ng/g in the control group to 193.3 ± 33.7 ng/g in the low-dose group and 320.2 ± 14.8 ng/g in the high-dose

group (low-dose group, $P < 0.0001$; high-dose group, $P = 0.0391$, compared to the control group). At the other sites, no significant difference was observed for any of the MAs.

3.5. MA concentrations in plasma

The results of the measurements of MA concentrations in the plasma are shown in Table 8. Histamine was reduced in a dose-dependent manner in the IMI: 131 ± 32.78 ng/mL in the control group, 58.90 ± 6.88 ng/mL in the low-dose group, and 45.08 ± 3.43 ng/mL in the high-dose group (low-dose group, $P = 0.03$; high-dose group, $P = 0.0099$). There were no significant changes in 3-MT and serotonin levels, and DA was not detected.

4. Discussion

NNs such as IMI are known to exhibit selective toxicity to many pests with low toxicity to mammals. However, in recent years, mammalian toxicity, especially the effects on affective cognitive behavior, has been reported. Hirano et al. (Hirano et al., 2018) administered a single oral dose of CLO, a type of NN, to mice and performed EPM. As a result, the anxiety levels of the mice increased in a dose-dependent manner. The same investigators found that anxiety-like behavior was also increased by CLO below the NOAEL. Yoneda *et al.* (2018) also reported that long-term administration of dinotefuran to mice caused a dose-dependent increase in activity. Chronic administration of IMI has been reported to cause a decrease in spontaneous locomotion, an increase in resting time, and depression (Abd-Elhakim et al., 2018; Bhardwaj et al., 2010; Lonare et al., 2014); since MAs regulate brain functions such as behavior, memory, emotion, and learning, MA disruption may be involved in the development of those symptoms.

In this study, I first confirmed the effects of acute exposure to IMI on affective and cognitive behaviors using OF and EPM in mice, assessing exploratory behavior and responsiveness to novel environments as indicators of activity, and anxiety levels. Normally, animals exposed to a novel environment avoid the center of the device (center area) and perform exploratory behavior near the wall in the OF tests. In contrast, animals which are administered benzodiazepine anxiolytic drugs increase their exploratory

behavior in the center area (Bruhwyler, 1990). These effects are thought to be a state representing release of behavioral inhibition that is based on anxiety and fear in a novel environment (Yamaguchi et al., 2007). However, it is difficult to conclusively evaluate anxiety levels using this test system alone, and it is important to include other test systems. In the present study, the distance traveled, number of area movements, average speed of movement, and resting time were used to measure activity, while the time spent in the center area was used as an index of anxiety-like behavior. As a result, the distance traveled, number of area movements, and average speed of movement were significantly reduced in the high IMI-dose group. In contrast, the resting time was markedly increased in the high-dose group. The time spent in the center area did not significantly change in either group. These results indicate that the administration of high-dose IMI caused a decrease in activity. These results are consistent with those of the previous studies.

In contrast, no anxiety-like behaviors were observed in the EPM. The EPM was utilized to assess anxiety by taking advantage of the fact that mice prefer the wall side of an enclosure and avoid heights (Yamaguchi et al., 2005b). On the open arm, mice feel fear and anxiety due to exposure to heights; thus, I can evaluate their anxiety levels by measuring the time and distance spent on the open arm or the number of intrusions. In this study, there was no significant change in the entries into the open arm between the control and exposed groups, but the time and distance spent in the open arm increased in the high-dose group. However, because the total distance traveled was significantly less in the high-dose group, these results did not reflect a decrease in anxiety levels, but rather a decrease in activity and an increase in rest time, which might have increased the time spent in the open arms.

Since the results of the behavioral tests showed that IMI caused a decrease in activity, the next step in this study was to measure MAs in the brains of IMI-exposed mice using LC/MS/MS. Prior to these measurements, in this study, I investigated the appropriate LC/MS/MS analytical conditions for the determination of MA neurotransmitters using the derivatizing reagent DPP. DPP specifically reacts with MAs, and its use in MSI has been reported (Esteve et al., 2016; Shariatgorji et al., 2014, 2015; Shimma et al., 2016). DPP derivatization for MSI requires a reaction time of at least 24 h at room temperature (Esteve

et al., 2016; Merdas et al., 2021), but a shorter reaction time is essential to establish a simpler analytical method for LC/MS/MS. Therefore, I investigated the optimal reaction time and temperature and found them to be 60°C and 4 h. The extraction process before derivatization utilized the method of Maeda et al. (Maeda et al., 2016), with modifications, to establish an analytical method for measuring MAs via DPP derivatization. The LODs of conventional LC/MS/MS methods for MA analysis in brain tissue were reported as 125 ppt to 3 ppb for 3-MT, 114 ppt to 4 ppb for DA, and 132 ppt to 44 ppb for serotonin (González et al., 2011; Huang et al., 2014; Kim et al., 2014; Sørensen et al., 2019; Tareke et al., 2007; Zhu et al., 2011). However, the detection of histamine in brain tissue by LC/MS/MS has not been reported. In addition, these methods require pretreatment such as ion-exchange solid-phase extraction and drying under nitrogen gas to achieve highly sensitive measurements (Huang et al., 2014; Sørensen et al., 2019; Tareke et al., 2007). The MDL established in this study was 2.08 ppt for 3-MT, 24.9 ppt for DA, 9.82 ppt for histamine, and 1.51 ppt for serotonin, achieving much higher detection sensitivity than conventional methods. I was able to simplify the pretreatment process, as I only needed to derivatize the extracts after brain tissue homogenization. In this study, only four MAs were measured, but it is believed that the simultaneous detection of more MAs could be realized in the future.

The measurement of MAs in each brain region of the IMI-exposed mice by DPP derivatization LC/MS/MS showed that DA was significantly decreased in the cerebellum and olfactory bulb, and serotonin and histamine were significantly decreased in the striatum. DA is a neurotransmitter involved in motor coordination, feelings of pleasure, motivation, and learning (Nieoullon et al., 2003). In behavioral testing, DA is particularly involved in voluntary movement. There are four projection pathways in the central DA nervous system, among which the substantia nigra-striatal pathway plays an important role in motor regulation. In general, enhanced DA release in the striatum increases spontaneous locomotor activity, while DA suppression decreases this activity (Hagino et al., 2015). In the present study, a decrease in DA concentration in the striatum was expected because a decrease in activity was observed in the IMI-exposed group in the behavioral test. However, there was no significant change in DA concentration in the striatum of the exposed group.

A possible reason for this finding was the large variability in the control group. The Bartlett test for DA in the striatum was used to determine equivariance, and the results showed that the variances were different between groups. There was convergence of variance in the high-dose group, which may be due to neural disturbance caused by IMI administration, but the reasons are unknown. Note that the decrease in serotonin and histamine levels in the striatum was not dose-dependent. There are 2 possible reasons, which are as follows: (1) dose-dependent changes in the balance between secretion and synthesis due to feedback control and receptor downregulation; (2) secondary changes in MA levels due to other non-dose-dependent changes induced by IMI.

Acute exposure to a high dose of nicotine has been reported to decrease spontaneous locomotor activity in mice and rats (Akinola et al., 2019; Prus et al., 2008). Additionally, nAChRs are desensitized in the presence of nicotine, which is an agonist (Robinson et al., 2006). The release of DA in the striatum involves nAChRs being expressed on the dopaminergic nerves (Cachope et al., 2014). Furthermore, a previous study by Kimura-Kuroda et al. reported that both IMI and nicotine exhibit agonist activity toward mammalian nAChRs *in vitro* (Kimura-Kuroda et al., 2012). In other words, IMI may act as an agonist and desensitize nAChRs, or act as a partial agonist, thereby suppressing the release of DA into the synaptic cleft and reducing spontaneous movements. However, since the decrease in activity in this study was only observed in the high-dose group, I cannot exclude the possibility that this effect is secondary to other stresses caused by exposure to high levels of NN. Although CLO, another NN, has been reported to induce DA release in the striatum of rats (de Oliveira et al., 2010), it has been reported to decrease activity in behavioral tests in mice (Hirano et al., 2018). There are also *in vitro* studies that reported that CLO enhanced ACh-induced currents, while IMI suppressed them (Li, P et al., 2011). Although a simple comparison cannot be made because of differences in dosing methods and animal species, the differences in changes to DA and behavior between CLO and IMI may be due to differences in affinity and agonist activity for nAChRs.

Interestingly, DA and 3-MT were significantly decreased in the olfactory bulb in the IMI-exposed group. There is a population of approximately 10% DA-activating interneurons within the glomerular layer of the mammalian olfactory bulb (Pignatelli et al., 2005). In Parkinson's disease, which is caused by the loss of DA-activating nerves in the

substantia nigra-striatal pathway and the depletion of DA in the striatum, olfactory disturbances are often observed (Doty, 2012). The role of DA in olfaction is complex, but it has been reported that blocking dopaminergic nerves projecting from the substantia nigra to the olfactory bulb causes olfactory dysfunction (Höglinger et al., 2015). This indicates that changes in DA concentration in the olfactory bulb may cause olfactory dysfunction, and that IMI may affect olfaction by acting on the olfactory bulb of mice.

In addition, a significant decrease in DA was observed in the cerebellum, a brain region involved in motor and cognitive functions in the high-dose group. While DA is not a predominant neurotransmitter in the cerebellum, previous studies have suggested that the cerebellum is implicated in psychiatric disorders, such as schizophrenia (Flace et al., 2021; Yeganeh-Doost et al., 2011), which are characterized by dysregulation of DA. The involvement of cerebellar DA in IMI-induced anxiety-like behavior remains to be investigated, but it is possible that other cognitive functions may be affected.

It should be noted that the analysis of norepinephrine, whose precursor is dopamine, was unsuccessful in this study due to the low derivatization efficiency. However, previous studies have indicated that nicotine increases norepinephrine release (Morse, 1989) and that nicotine-induced anxiety-like effects can be reversed by α1-adrenergic receptor antagonists (Zarrindast et al., 2000). Consequently, further investigation into the role of norepinephrine in anxiety-like effects induced by IMI, a nicotine analog, is suggested.

Histamine levels were significantly decreased in the striatum, cerebellum, and olfactory bulb of the exposed group in the present study. Histamine is synthesized in the hypothalamic raphe nucleus and is projected to most areas of the brain, where it plays a role in arousal, cognition, and feeding behavior in the central nervous system. Although the relationship between NNs and the decreased activity observed in behavioral tests is unknown, to date there have been no reports of NN affecting histamine, and to the best of my knowledge, this is the first time that NN has been shown to affect histamine levels. Furthermore, there was a significant decrease in plasma histamine levels in the exposed group in this study. Histamine in the blood is mainly stored in mast cells and basophils, and its release is known to induce inflammation and allergic reactions. There are reports of increased blood histamine levels in Alzheimer's disease patients and decreased blood

histamine levels in schizophrenia patients (Antón Alvarez et al., 1996; Fernández-Novoa et al., 2001). This suggests that histamine in the blood not only acts as an inflammatory mediator but is also a biomarker for central nervous system diseases. In the present study, histamine levels were also decreased in both the brain and the plasma, suggesting that histamine changes in the central nervous system are reflected in the blood. While the investigation of the effects on peripheral nAChRs is necessary, histamine and other blood MAs could be used as simple biomarkers in neurotoxicity studies in the future.

In the cerebellum, histamine has been reported to enhance motor performance in rats by activating H2 receptors (He et al., 2012; Song et al., 2006). In this study, a significant decrease in histamine was observed in the high-dose group, which may be related to the reduced activity observed in the OF and EPM tests.

A significant decrease in serotonin was also observed in the striatum; however, the effects of IMI on serotonin have been studied only in a few previous studies. Selective serotonin reuptake inhibitors (SSRIs) are the primary treatment for depression, and serotonin is widely known to be important in anxiety (Mohammad-Zadeh et al., 2008). However, no anxiety-like behavior was observed in the EPM in this study. Serotonin has been implicated in a variety of behaviors beyond anxiety, with serotonin depletion having been demonstrated to enhance responses to external stimuli and increase aggression (Lucki, 1998). Further research is necessary to elucidate the effects of IMI-induced serotonin depletion, although it is possible that it affects behaviors other than anxiety and activity examined here.

5. Summary

In this study, I improved the ionization efficiency by using DPP, and clarified the effect of NN administration on the distribution and concentration of MAs in the brain.

The results of behavioral tests showed that IMI administration caused a decrease in activity in mice. Furthermore, I measured the concentration of MAs in various parts of the brain and a decreasing but not significant trend of DA was observed in the striatum, which

is believed to be involved in spontaneous movements. However, decreases in 3-MT and DA in the olfactory bulb, and decreases in serotonin and histamine in the striatum were detected. In particular, changes in DA in the olfactory bulb occurred at the NOAEL dose, indicating that MA disruption is caused by low level of IMI. Furthermore, the measurement of blood MA levels showed a significant decrease in histamine in the exposed group. This paralleled the brain levels, indicating that blood histamine levels may be a biomarker reflecting the effects of CNS diseases (Coelho et al., 1991; Gholipoor et al., 2013).

Although I was unable to identify the cause of the effect of IMI on activity, I was able to show, for the first time by LC/MS/MS quantification using DPP derivatization, that NN alters MA concentrations in various parts of the brain, even at a low-dose exposure.

6. Figures and tables

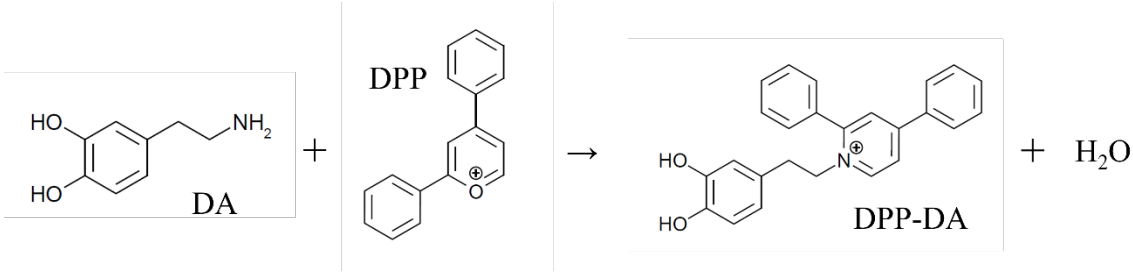

Figure 2. Chemical reaction of DPP-derivatization.

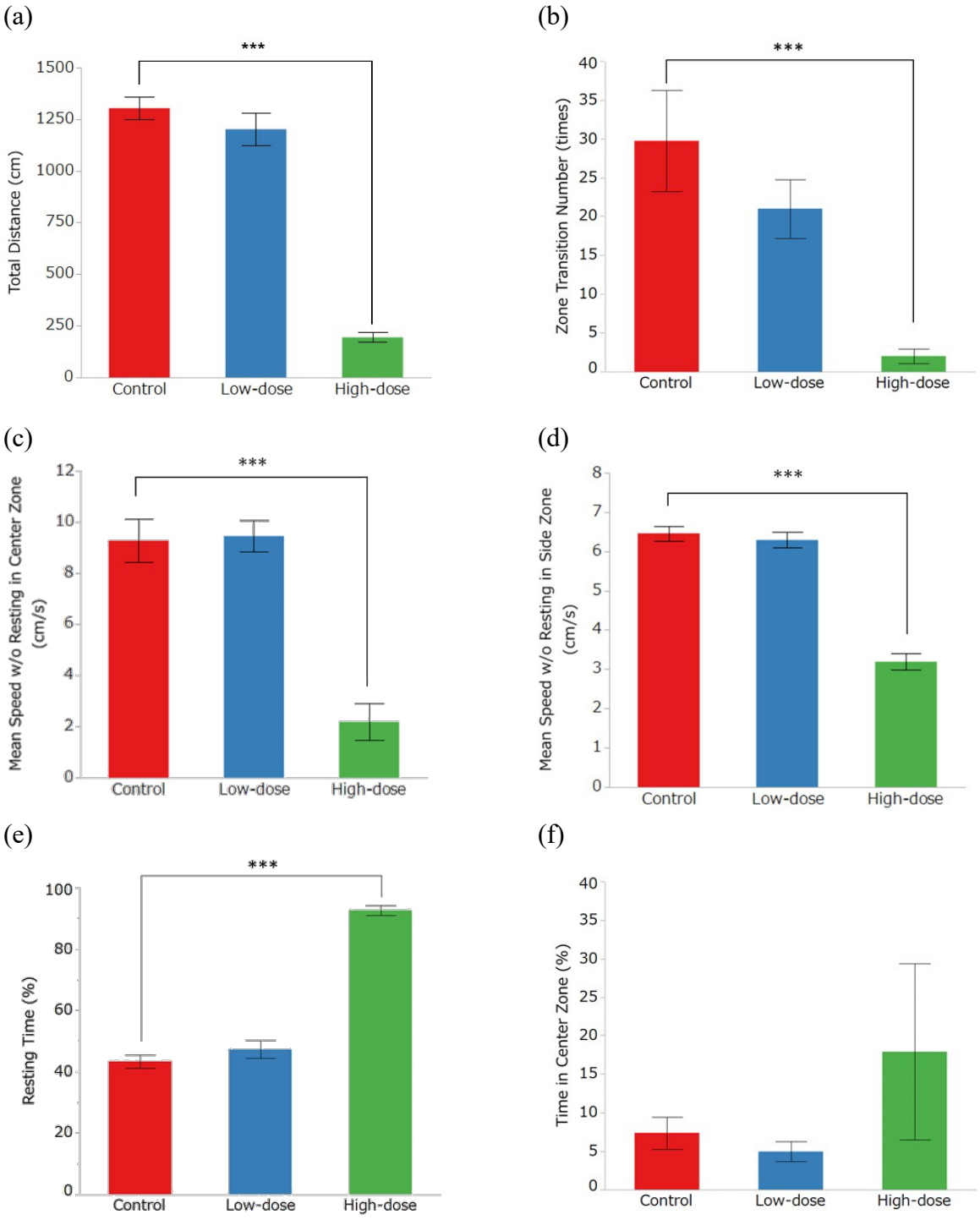

Figure 3. Behavioral effects of IMI administration in the OF tests.

(a) Total distance, (b) zone transition number, and mean speed without resting in (c) center zone and (d) side zone were significantly lower in the high-dose group than in the control

group. (e) Resting time was significantly higher in the high-dose group than in the control group. (f) There were no significant differences among all groups in the time in center zone. Bar graphs indicate the mean ± SEM (n = 8 each). *** $P < 0.001$, Dunnett's test.

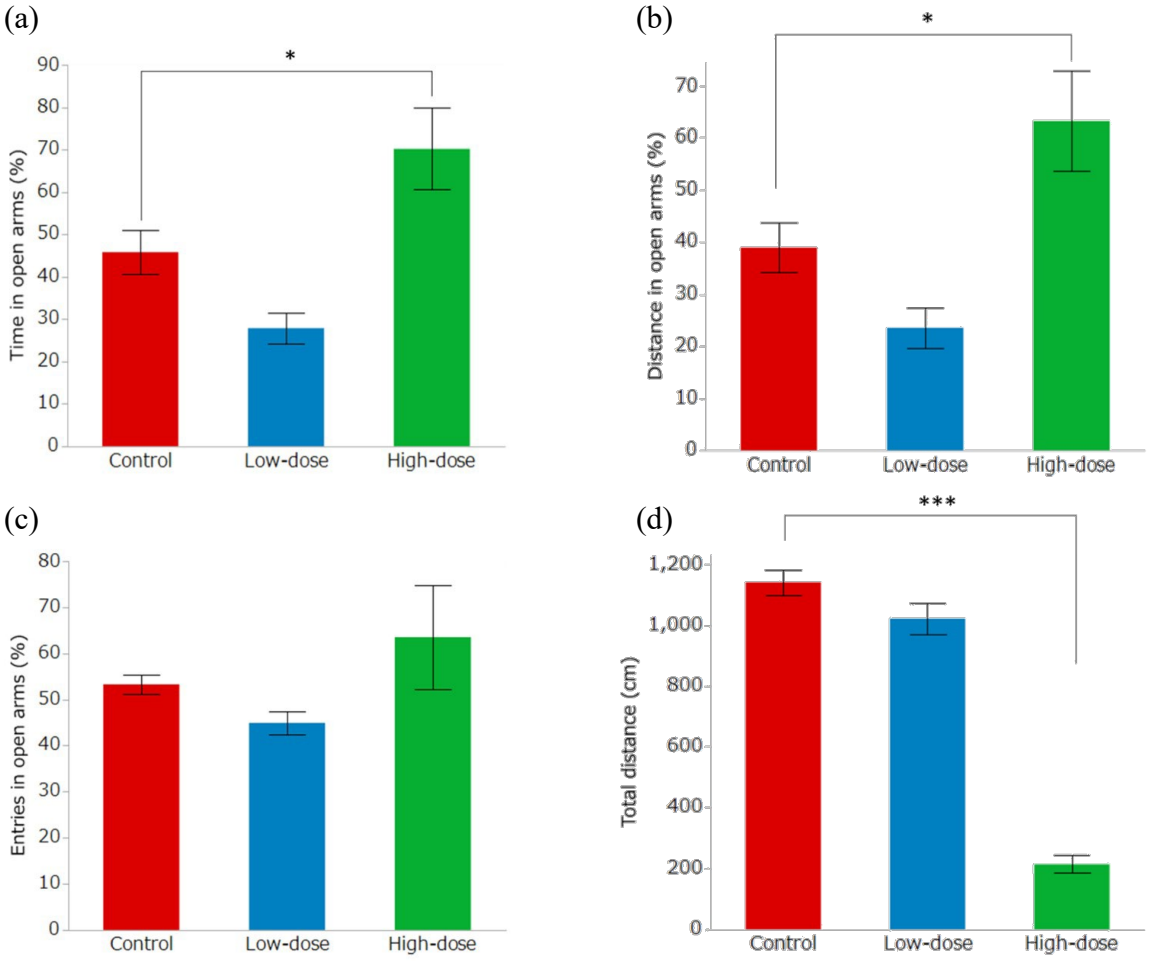

Figure 4. Behavioral effects of IMI administration in the EPM tests.

The percentage of time (a) and distance (b) spent in the open arm were significantly higher in the high-dose group than in the control group. (c) There were no significant differences in the percentage of entries in the open arm. (d) The total distance traveled was significantly decreased in the high-dose group.

Bar graphs indicate the mean ± SEM of each group (n = 8 each). * $P < 0.05$, *** $P < 0.001$, Dunnett's test.

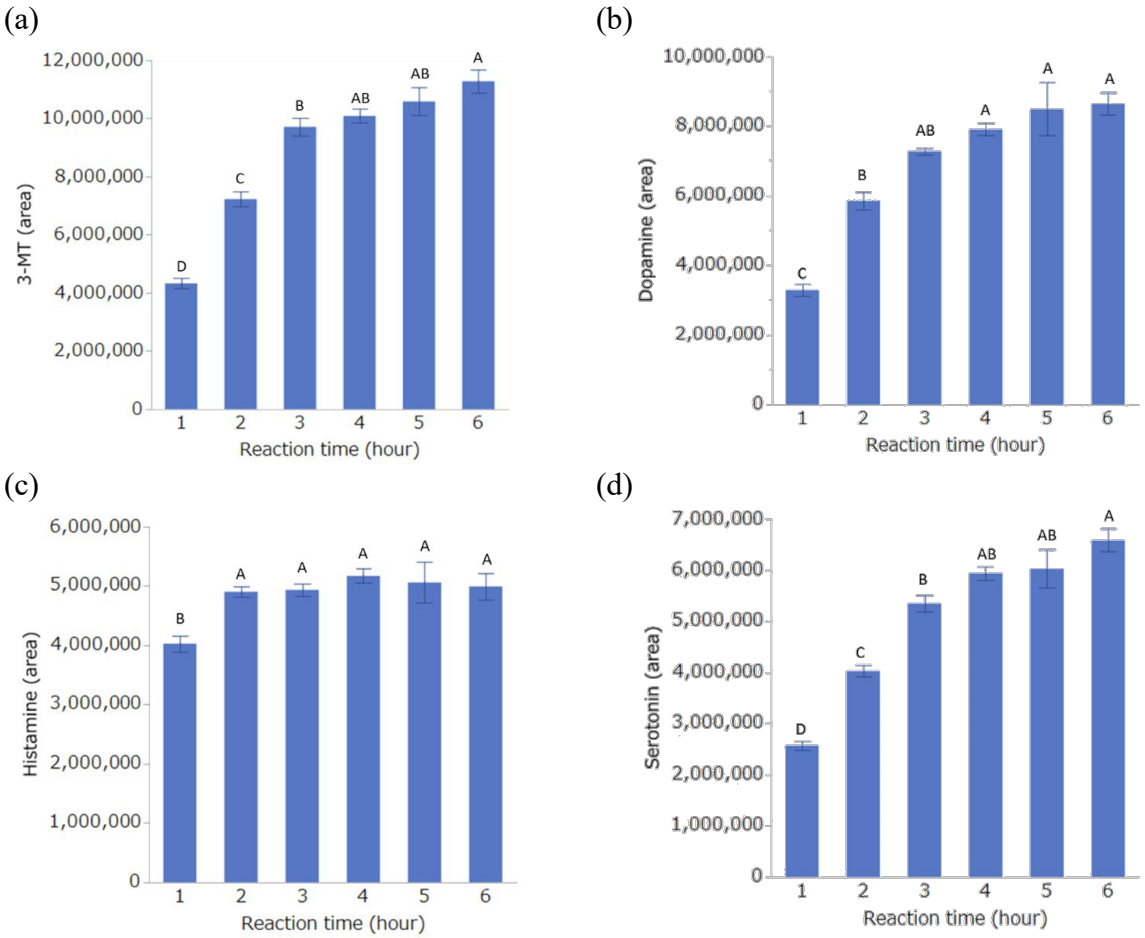

Figure 5. Effect of reaction time on derivatization with DPP.

Detection of 3-MT (a), dopamine (b), histamine (c), and serotonin (d) by LC/MS/MS. Bar graphs indicate the mean ± SEM of each condition (n = 5 per condition).

Different characters indicate significant differences, while identical characters indicate non-significant differences, as determined by Tukey-HSD tests.

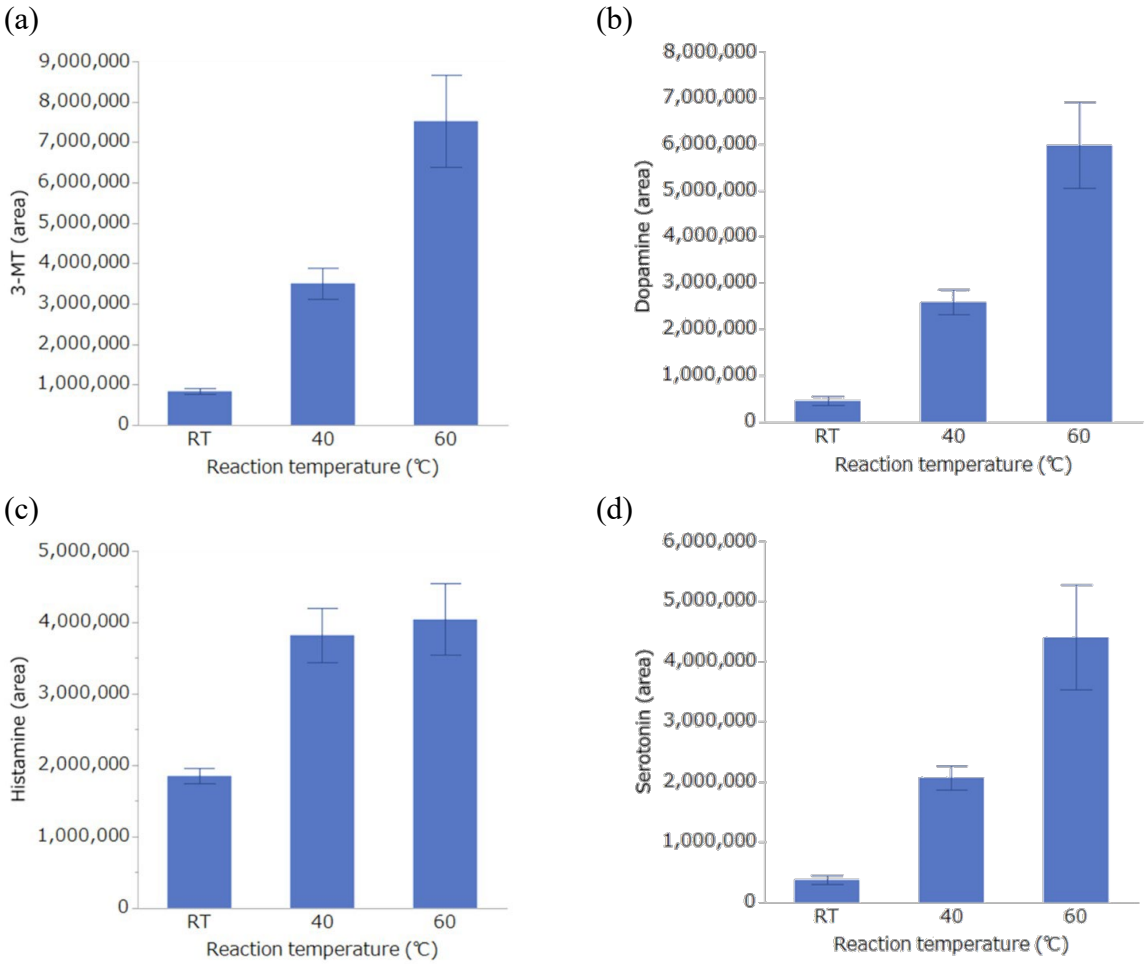

Figure 6. Effect of reaction time on derivatization with DPP.

Detection of 3-MT (a), dopamine (b), histamine (c), and serotonin (d) by LC/MS/MS. Bar graphs indicate the mean ± SEM of each condition (n = 5 per condition).

Table 4. MRM parameters for determination of MAs.

Target ion is the product ion listed in the top column of each compound. Other product ions are used as qualifier ions.

Compound	RT [min]	MRM Transition [m/z]		CE [V]
		Precursor Ion	Product Ion	
DPP-3-MT	3.030	383.1	151.2	24
			91.0	60
DPP-Dopamine	2.860	369.0	233.3	24
			233.2	20
DPP-Histamine	2.060	327.0	95.1	32
			233.4	28
			68.1	72
DPP-Serotonin	2.930	392.0	160.0	32
			232.3	20
DPP-3-MT-d4	3.030	387.3	156.2	24
			96.0	68
DPP-Dopamine-d4	2.860	372.1	232.1	28
			140.9	28
			94.5	56
DPP-Histamine-d4	2.060	330.0	232.2	24
			99.1	36
DPP-Serotonin-d4	2.930	395.0	164.2	24
			232.1	16

Table 5. IDL and MDL for MAs.

Compound	IDL [ppt]	MDL [ppt]
3-MT	0.90	2.08
Dopamine	4.48	24.9
Histamine	3.24	9.82
Serotonin	0.91	1.51

Table 6. The accuracy, precision and linearity of MA analytical method.

These values were calculated from the measurement results and calibration curve used to calculate the MDL.

Accuracy was represented as the mean ± SEM of seven times measurements, and linearity was shown as R^2 on the calibration curve. CV: coefficient of variation.

Compound	Accuracy [%]			Precision [CV%]	Linearity [R^2]
	0.2 ppb	2 ppb	20 ppb		
3-MT	99.6 ± 8.3	98.4 ± 6.5	104.4 ± 5.5	64.8	0.9998
Dopamine	135.8 ± 8.2	100.9 ± 3.1	100.2 ± 3.5	31.3	0.9998
Histamine	269.4 ± 6.7	90.1 ± 4.1	100.4 ± 0.4	26.9	0.9995
Serotonin	155.4 ± 28.0	94.7 ± 3.5	98.9 ± 2.2	11.6	0.9999

Table 7. The concentration of MAs in different parts of brain.

Values represent the mean ± SEM of each group (n = 8 each). * $P < 0.05$, ** $P < 0.01$, *** $P < 0.001$, Dunnett's test; † $P < 0.025$, Bartlett test.

Brain Region	Control	Low-Dose	High-Dose
3-MT [ng/g]			
Striatum	747.3 ± 88.0	807.4 ± 137.1	595.6 ± 39.9
Hippocampus	6.1 ± 1.2	5.0 ± 0.6	4.9 ± 1.0
Cortex	66.7 ± 15.6	69.0 ± 15.8	56.5 ± 5.2 †
Cerebellum	3.1 ± 0.2	3.7 ± 0.1	4.4 ± 0.45 *
Brain stem	13.0 ± 0.9	11.9 ± 0.6	13.9 ± 1.2
Olfactory bulb	72.4 ± 5.1	62.4 ± 3.3	51.8 ± 1.4 **†
Dopamine [ng/g]			
Striatum	9747.0 ± 1580.2	9364.5 ± 1458.3	8283.8 ± 515.5 †
Hippocampus	67.9 ± 8.7	46.3 ± 8.8	43.0 ± 9.6
Cortex	418.0 ± 103.4	457.7 ± 116.7	294.3 ± 34.7 †
Cerebellum	20.2 ± 1.6	16.7 ± 0.7	13.7 ± 0.7 ***†
Brain stem	123.0 ± 7.3	106.6 ± 7.3	116.9 ± 8.0
Olfactory bulb	407.8 ± 20.0	331.9 ± 16.7 **	304.8 ± 10.1 ***
Histamine [ng/g]			
Striatum	452.8 ± 28.3	133.7 ± 28.5 ***	198.1 ± 12.2 ***
Hippocampus	53.3 ± 6.8	48.3 ± 4.8	39.6 ± 5.3
Cortex	64.1 ± 4.9	57.9 ± 4.1	55.9 ± 4.5
Cerebellum	60.9 ± 4.0	54.7 ± 3.2	44.9 ± 4.0 *
Brain stem	65.3 ± 10.4	63.5 ± 4.8	60.8 ± 5.6
Olfactory bulb	155.9 ± 16.2	112.9± 8.6 *	115.3 ± 7.6 *
Serotonin [ng/g]			
Striatum	438.0 ± 44.8	193.3 ± 33.7 ***	320.2 ± 14.8 *†
Hippocampus	704.0 ± 78.3	800.0 ± 51.7	651.3 ± 55.8
Cortex	546.6 ± 40.0	565.6 ± 41.9	481.3 ± 24.8
Cerebellum	370.1 ± 36.8	404.4 ± 30.5	260.8 ± 24.5

Brain stem	1348.0 ± 56.8	1407.9 ± 49.9	1288.4 ± 69.4
Olfactory bulb	666.8 ± 26.8	662.2 ± 43.3	616.9 ± 38.1

Table 8. The concentration of MAs in the plasma.

Values represent the mean ± SEM of each group (n = 8 each). * $P < 0.05$, ** $P < 0.01$, Dunnett's test. N.D., not detected.

[ng/mL]	**Control**	**Low-Dose**	**High-Dose**
3-MT	0.91 ± 0.13	0.99 ± 0.078	1.05 ± 0.13
Dopamine	N.D.	N.D.	N.D.
Histamine	131 ± 32.78	58.90 ± 6.88 *	45.08 ± 3.43 **
Serotonin	1235 ± 261	1460 ± 580	1075 ± 159

Chapter 2

Analysis of brain monoamines using two methods and the relationship between behavioral tests and brain monoamines

Chapter 2-2

Elucidation of the role of brain monoamines in neonicotinoids-induced anxiety-like behavior by LC/MS/MS analysis using Py derivatization

1. Introduction

As indicated in *Chapter 1* and *Chapter 2-1*, NNs at NOAEL or LOAEL levels induce behavioral changes such as increased anxiety-like behavior in mice (Hirano et al., 2018) and elevated dopamine release in the striatum (de Oliveira et al., 2010; Faro et al., 2019; Yoneda et al., 2018). Given that abnormalities in the MA system can lead to the development of psychiatric disorders, including depression, anxiety disorders, and Parkinson's disease (Hamon et al., 2013; Morilak et al., 2004; Ohama et al., 1976), it is hypothesized that MAs is involved in the mechanism of NNs-induced behavioral changes. However, as previously stated, the effects of NNs on the mammalian central nervous system remain unclear, and there are particularly limited reports on how the impact of NNs on MAs affects behavior *in vivo*. This chapter is thus focused on the effects of ACE, which was indicated in *Chapter 1* to increase anxiety-like behavior, on MA production and whether this affects behavior.

Dopamine is reportedly involved in nicotine-induced anxiety-like behavior (Zarrindast et al., 2012), and various types of NNs increases striatal dopamine levels (de Oliveira et al., 2010; Faro et al., 2019; Yoneda et al., 2018). However, few studies have examined the effects of ACE on MAs. Although the hippocampus is associated with memory, it is also important for anxiety (Bannerman et al., 2004): it has been reported that injection of dopamine receptor antagonists into the dorsal or ventral hippocampus reduces nicotine-induced anxiety-like behavior (Nasehi et al., 2011; Zarrindast et al., 2010), and that the cholinergic system in the hippocampus can modulate anxiety (Degroot et al., 2002; Mineur et al., 2013).

Several previous studies, including *Chapter 1* and *Chapter 2-1*, have reported that NNs cause a decrease in activity as well as an increase in anxiety-like behavior in the EPM (Hirano et al., 2021; Kubo et al., 2022). Additionally, the index of activity in the EPM is also affected by anxiety (Shepherd et al., 1994); for example, freezing, which refers to immobility in mice and rats, is known to be a defensive response (Blanchard et al., 2003) that may affect activity in the EPM. The serotonergic system is involved in freezing (da Silva Soares et al., 2019), and the major dopaminergic pathways, including the nigrostriatal pathway, and dopaminergic neurons in the hippocampus are innervated by serotonergic nerves originating in the raphe nuclei (RN) (Alex et al., 2007; Moore et al., 1975). The RN

is another brain region that is critically involved in anxiety, and stimulation of serotonergic neurons in the RN increases anxiety-like behavior via the release of hippocampal serotonin (Abela et al., 2020; Ohmura et al., 2014). In addition, nAChRs are also expressed in the RN, and nicotine increases the firing frequency of serotonergic neurons in the RN (Garduño et al., 2012). These studies suggest that MAs in the striatum, hippocampus, and RN may play an important role in NNs-induced anxiety-like behavior.

It has been established that derivatization improves detection sensitivity in the MA analysis using mass spectrometry (Shikano et al., 2022; Taira, S et al., 2021). Derivatization with DPP was performed in *Chapter 2-1*. There are several other types of reagents used for derivatization, among which 2,4,6-triethyl-3,5-dimethyl pyrylium trifluoromethanesulfonate (Py-Tag) provides a rapid and highly efficient reaction (Shikano et al., 2022; Taira, S et al., 2021). The Py-Tag reagent reacts with primary amine groups, such as DPP, and possesses the advantages of shorter reaction times than DPP and commercial availability, facilitating ease of acquisition. Against this background, in this study, I sought to clarify the involvement of MAs in ACE-induced behavioral changes by examining the correlation between the behavioral effects of ACE and MAs in the brain by MA analysis using Py derivatization, as well as serotonin production in the RN, which plays an important role in anxiety.

2. Material and methods

2.1. Chemicals

ACE was purchased from Cosmo Bio Co., Ltd. (100% purity, Tokyo, Japan). Dopamine, 3-MT, and 3-MT-d4 HCl were purchased from Cerilliant Corporation (Round Rock, TX, USA). Serotonin was purchased from Sigma-Aldrich Co. LLC (St. Louis, MO, USA); histamine and serotonin-d4 hydrochloride from Toronto Research Chemicals, Inc. (Toronto, ON, Canada); and dopamine-d4 and histamine-d4 from Cambridge Isotope Laboratories, Inc. (Tewksbury, MA, USA). Py-Tag for histamine was purchased from TAIYO NIPPON SANSO CORPORATION (Tokyo, Japan); formic acid and sucrose from FUJIFILM Wako Pure Chemical Corporation (Osaka, Japan); L-ascorbic acid and Triton™

X-100 from Sigma-Aldrich Co. LLC (St. Louis, MO, USA); 4% paraformaldehyde phosphate buffer solution (PFA/PB) from Bioenno Lifesciences (Santa Ana, CA, USA); goat anti-serotonin IgG antibodies from Abcam plc. (Cambridge, UK); Alexa Fluor™ 594 donkey anti-goat IgG (H+L) from Invitrogen; Thermo Fisher Scientific, Inc. (Waltham, MA, USA). All other chemicals and solvents were purchased from Kanto Chemical Co., Inc. (Tokyo, Japan).

2.2. Animals

All animal experiments were approved by the Experimental Committee of the Faculty of Veterinary Medicine, Hokkaido University, and were conducted in accordance with the ARRIVE guidelines, as well as the Guide for the Care and Use of Laboratory Animals and with the As-sociation for the Assessment and Accreditation of Laboratory Animal Care International (AAALAC; approval date: 17th March 2022, approval number: 22-0024).

Male C57BL/6J mice (11-weeks-old) were obtained from Japan SLC, Inc. (Shizuoka, Japan). They were maintained at 22 ± 1°C (room temperature), 70 ± 5% humidity, and a 12-h light/dark cycle (8:00–20:00; light, 20:00–8:00; dark), with food (breeding solid food for mice, rats, and hamsters: CE-2, CLEA Japan, Inc., Tokyo, Japan) and tap water available *ad libitum*. Food and water were changed twice a week, and cages were changed once a week. Experiments were performed after at least one week of acclimation.

2.3. Elevated zero maze (EZM) tests

Mice (n = 41) were randomly divided into two groups: control (n = 20) and ACE (n = 21) groups. These number of mice in each group was calculated based on a previous study using similar behavioral test (Biala et al., 2006). The ACE group received oral ACE dissolved in normal saline at 20 mg/kg BW, which was estimated to be the NOAEL of ACE in mice (Food Safety Commission, 2014), while the control group received saline at 10 mL/kg BW. These doses were administered under light anesthesia with isoflurane using

sonde (FUCHIGAMI, Kyoto, Japan). After administration, mice were placed individually in a dark room for 30 min, and their behavior was observed in the EZM for 5 min.

The EZM apparatus has a 0-shaped corridor, placed at 50 cm from the floor, with an outer diameter of 46 cm and an inner diameter of 35 cm, and this corridor is divided into four areas. Alternating areas are surrounded by a 17-cm high wall (closed arm), while the others are without walls (open arm). This apparatus was placed in a quiet room with no human access during tests, surrounded on all sides by a white enclosure, and the light intensity inside the enclosure was kept at 20 lx. Behavior was automatically recorded and analyzed by SMART 3.0 (Panlab, S.L., Barcelona, Spain), and mice were defined as having entered the zone when their center of gravity entered each area. All administrations and behavioral tests were performed during the light cycle (12:00-18:00), ensuring that there was no group bias. The EZM tests measured the percentage of time and distance in open arms and the number of entries into open arms as an index of anxiety-like behavior, and the total distance traveled as an index of activity. Mice that fell out of the EZM apparatus during testing were excluded from this and subsequent LC/MS/MS analyses.

2.4. Py derivatization for the measurement of MA concentration in brain tissue

Immediately after the behavioral tests were performed, mice were euthanized by cervical dislocation under deep isoflurane anesthesia. Brains were sampled and visually dissected on an ice-cold tray using tweezers and spatulas into 6 brain regions, primarily containing the following areas: hippocampus (including both dorsal and ventral parts), striatum, brainstem, cerebellum, cerebral cortex, and thalamus (including hypothalamus). The regions sampled are shown in Figure 7, and I refer to them in this study as the above six brain regions that each primarily contains. Samples were flash frozen in liquid nitrogen and stored at -20°C until further use.

Approximately 10 mg of the sample was weighed into a 1.5 mL tube to which 200 μL of 0.05% formic acid in acetonitrile and 0.5 mM ascorbic acid solution and 20 μL of an internal standard master mix (100 ppb) containing dopamine-d4, 3-MT-d4, histamine-d4, and serotonin-d4 were added. This tube was homogenized with two zirconia beads (2.0 mm; Toray Industries, Inc., Tokyo, Japan) in a Tissue Lyser (30/s, 1.5 min; QIAGEN K.K.,

Tokyo, Japan), the tissue homogenate was centrifuged at 10,000 x*g* for 10 min, and the supernatant was carefully transferred to a new tube. Then, to derivatize the MAs, 20 μL of Py-Tag for histamine, a derivatization reagent, was added to 30 μL of this supernatant, vortexed, and incubated at 50°C for 15 min using a thermal cycler. Finally, 70 μL of this derivatized sample was diluted with 50 μL of DW and analyzed by LC/MS/MS.

2.5. LC/MS/MS measurement conditions for MA analysis

The LC and MS apparatus used to measure MA concentrations were an Agilent 1290 Infinity ultra-high performance LC system and an Agilent 6495 triple quadrupole mass spectrometer, respectively (Agilent Technologies Japan, Ltd., Tokyo, Japan). The column used was a 150 × 2.1 mm Kinetex Biphenyl column with 2.6 μm particle size (Phenomenex Inc., Torrance, CA, USA), and the temperature was set at 60°C.

Using DW containing 0.1% formic acid as mobile phase A and methanol containing 0.1% formic acid as mobile phase B, the analytes were separated at a flow rate of 0.2 mL/min until 0.8 min and 0.4 mL/min after 0.8 min at an injection volume of 5 μL. The gradient was started at 5% mobile phase B. After a linear increase of B to 75% from 0.8 min to 17 min, the mobile phase B was switched to 100% and maintained until 18.5 min. It was then returned to 5% B and equilibrated for 1.5 min until the next injection. Table 9 shows the RT, MRM transition, and CE for each analyte. ESI was performed in positive mode.

2.6. Anti-serotonin staining

Two groups of mice were randomized: control (n = 6) and ACE (n = 7) groups. Solutions, methods of administration, and concentrations administered were the same as those used in the behavioral test. In brief, 30 min after administration, mice were cervically dislocated under deep anesthesia with isoflurane and immediately perfusion fixed with 0.9% NaCl with 10 mg/L heparin, and whole brains were sampled. The sampled brains were shaken at 4°C in 4% PFA/PB overnight, then replaced with 30% sucrose in 0.1 M phosphate buffer

(PB) and shaken again at 4°C overnight. After fixation, frozen sections were prepared by embedding in O.C.T. Compound (Sakura Finetek Japan Co., Ltd., Tokyo, Japan) and freezing in liquid nitrogen. Frozen sections were stored at -20°C until sectioning; then, after cryostat thinning to 50 μm thickness, they were stored at 4°C in 0.1 M PB until staining. Sections were then blocked with 4% Triton™ X-100 and incubated with goat anti-serotonin IgG antibody (1:1000) overnight at room temperature with protection from light. After incubation with Alexa Fluor™ 594 donkey anti-goat IgG (H+L) (1:500) as a secondary antibody for 2 h at room temperature, the slides were mounted with DAPI Fluoromount-G® (Southern Biotechnology Associates Inc., Birmingham, AL, USA).

The prepared slides were observed using an all-in-one fluorescence microscope, BZ-9000 (KEYENCE CORPORATION, Osaka, Japan), and slides containing the middle part of the dorsal RN (DRN) (Bregma -4.54 mm to -4.90 mm (Abrams et al., 2004)), were visually identified for all mice. These slides were observed using a confocal laser-scanning microscope, Zeiss LSM 700 (Carl Zeiss Co., Ltd., Tokyo, Japan; objective lens: × 20), and fluorescence images of 8 z-stacks (3.05 μm interval) of the DRN were captured. The maximum intensity projections of these z-stacks were used for image analysis. All image data were mixed so that groups were not recognized, and cell counts were performed in a blinded manner using Fiji Image J (1.53e; NIH, Java 1.8.0_172; 64 bit) (Schindelin et al., 2012).

2.7. *Statistical analysis*

Microsoft Excel (2016) and JMP (SAS Institute Inc., Cary, NC, USA) were used for statistical analysis. Non-parametric tests were used for experiments in which there were data sets that did not show either normal distribution or homogeneity of variance; the Wilcoxon test was used to compare behavioral test results, the Steel test to compare MA concentrations, and the Spearman's rank correlation coefficient test to analyze the correlation between behavioral test results and MA concentrations or BW. The number of cells in the RN showed a Gaussian distribution and homogeneity of variance in both groups

and was assessed by one-tailed t-test. All data are presented as mean ± SEM, and the significance level was set at $P < 0.05$.

3. Results

3.1. EZM tests

The results of EZM tests are shown in Figure 8. During the test, the control group spent 17.94 ± 1.37% of the total time in the open arms and the ACE group spent 14.15 ± 1.69% of the total time, showing a decreasing trend (Figure 8a, $P = 0.0569$). The control group traveled 19.30 ± 1.30% of the total distance in the open arms, while the ACE group traveled 16.04 ± 1.85%, showing no significant difference (Fig. 8b, $P = 0.0951$). The entries into the open arms were 22.45 ± 1.47 times in the control group and 13.76 ± 1.53 times in the ACE group (Fig. 8c, $P = 0.0001$), and the total distance traveled was 1431 ± 43.66 cm in the control group and 1120 ± 66.19 cm in the ACE group (Fig. 8d, $P = 0.0026$), wherein a significant decrease was observed in the ACE group. The correlation coefficients between mouse BW and time in the open arms and total distance were -0.06 and 0.26, respectively (Fig. 9). Neither of these coefficients was significant ($P = 0.7182$, 0.0963), indicating that BW did not significantly affect anxiety-like behavior and activity in the EZM.

3.2. MA concentrations in several brain regions

Dopamine, 3-MT, histamine, and serotonin concentrations in the hippocampus, striatum, and brainstem were measured by LC/MS/MS analysis (Figures 10–12). In the cerebellum, cerebral cortex and thalamus, it should be noted that the sampled brain regions were extensive, and only a small subset was used for measurements. This limitation reduced the accuracy of region-specific analyses in those brain regions. In the calculation of the mean and SEM, the concentrations of undetected samples were treated as zero.

The concentrations of dopamine, 3-MT, histamine, and serotonin in the hippocampus were 0.0049 ± 0.0008, 0.0019 ± 0.0002, 0.012 ± 0.001, and 0.13 ± 0.007

ng/mg in the control group, and 0.012 ± 0.002, 0.011 ± 0.002, 0.011 ± 0.002, and 0.68 ± 0.1 ng/mg in the ACE group, respectively (Fig. 10a–d).

In the striatum, the concentrations of dopamine, 3-MT, histamine, and serotonin were 1.7 ± 0.3, 0.27 ± 0.03, 0.12 ± 0.02, and 0.26 ± 0.01 ng/mg in the control group, and 3.1 ± 0.5, 0.66 ± 0.1, 0.11 ± 0.02, and 0.80 ± 0.1 ng/mg in the ACE group, respectively (Fig. 11a–d).

In contrast, in the brainstem, dopamine was detected in only three mice in the control group (0.0027 ± 0.002 ng/mg) and eight mice in the ACE group (0.0083 ± 0.005 ng/mg) (Fig. 12a); 3-MT was detected in only one mouse in the ACE group (0.00022 ± 0.001 ng/mg). Histamine and serotonin levels were 0.032 ± 0.006 and 0.014 ± 0.004 ng/mg in the control group, and 0.037 ± 0.007 and 0.15 ± 0.03 ng/mg in the ACE group, respectively (Fig. 12b, c).

Dopamine in the cerebellum of the ACE group, 3-MT in the cerebellum and cerebral cortex of both groups, and serotonin in the cerebellum of the control group were not detected (Table 10). In other brain regions, each MA was detected in more than two mice, and the mean concentrations are shown in Table 10.

In the hippocampus and striatum, dopamine ($P = 0.0049$ and 0.0460), 3-MT ($P < 0.0001$ and $P = 0.0005$), and serotonin ($P < 0.0001$ for both) levels were significantly increased in the ACE group. There was no significant difference in the concentration of histamine in the striatum ($P = 0.2154$) of the two groups, while it tended to decrease in the hippocampus ($P = 0.0535$). In the brainstem, cerebellum, and cerebral cortex, only serotonin concentration was significantly increased in the ACE group ($P < 0.0001$, $P = 0.0057$ and 0.0127, respectively). In the thalamus, levels of all four MAs were significantly increased (dopamine: $P = 0.0011$, 3-MT: $P = 0.0047$, histamine: $P = 0.0210$, and serotonin: $P < 0.0001$).

3.3. Correlation analysis of EZM test results and MA concentrations

Correlations were examined for two parameters of the behavioral test: time in open arms as a representative index of anxiety-like behavior and total distance as a representative index of activity, and each of the four LC/MS/MS analysis results: concentrations of

dopamine, 3-MT, histamine, and serotonin in the hippocampus, striatum, and brainstem (Figures 13–15).

The correlations between 3-MT and dopamine and between 3-MT and serotonin were significant in the hippocampus and striatum of both the control (hippocampus: P = 0.0305 and 0.0027, striatum: P = 0.0016 and 0.0081, respectively) and ACE groups (hippocampus: P = 0.0011 and 0.0004, striatum: P = 0.0444 and 0.0006, respectively), and between dopamine and histamine only in the striatum of both groups (control: P = 0.0435, ACE: P = 0.0343), while histamine and serotonin levels were correlated only in the brainstem of both groups (control: P = 0.0067, ACE: P = 0.0054). The significant correlations observed only in the ACE group were between dopamine and serotonin in both the hippocampus (P = 0.0019) and striatum (P = 0.0132), between time spent in the open arms and serotonin in the hippocampus (P = 0.0305), and between time in open arms and dopamine in the striatum (P = 0.0320). In contrast, the correlations between dopamine and histamine (P = 0.0082), and between 3-MT and histamine (P = 0.0184) in the hippocampus, and between dopamine and serotonin in the brainstem (P = 0.0369) were significant only in the control group. Time spent in the open arms and total distance traveled were significantly correlated only in the control group (P = 0.0064). The other correlations were not significant.

3.4. Neuronal count of the DRN

In the DRN of the control group, 113 ± 10 neurons were stained with anti-serotonin antibodies (Fig. 16b). In contrast, 142 ± 9.3 neurons were stained in the ACE group (Fig. 16c). Thus, the number of neurons actively producing serotonin in the DRN was significantly increased in the ACE group (P = 0.0307).

4. Discussion

In this study, four MAs, dopamine, 3-MT, histamine, and serotonin, were measured in different brain regions using LC/MS/MS, and the correlation between these levels and behavioral test results was plotted for each mouse. Dopamine, 3-MT, and serotonin levels

were significantly increased in the hippocampus and striatum, and striatal dopamine and hippocampal serotonin levels, in particular, were significantly correlated with time spent in the open arms, an index of anxiety-like behavior, in the ACE group.

Although NNs are known to affect dopamine transmission (Faro et al., 2019; Yoneda et al., 2018), reports on the involvement of the dopaminergic system in NNs-induced anxiety-like behavior are limited. Expression of dopamine transporters responsible for dopamine clearance in the striatum are reduced in Parkinson's disease patients, which correlates with the severity of anxiety symptoms (Erro et al., 2012). Dopamine signaling in the hippocampus and striatum is involved in the anxiogenic-like effects of nicotine (Nasehi et al., 2011; Zarrindast et al., 2010, 2012, 2015). I observed that increased striatal dopamine concentrations significantly increased the occurrence of anxiety-like behaviors, highlighting the importance of striatal dopamine in anxiety-like behaviors induced by NNs, which are structurally similar to nicotine.

The serotonergic system is also widely known to be involved in anxiety; for example, the SSRIs are typical anti-depressants (Żmudzka et al., 2018). Previous studies using social interaction tests have shown that microinjection of nicotine into the dorsal hippocampus induced anxiety-like behaviors, and this effect was reversed by serotonin receptor antagonists, but not by muscarinic receptor antagonists (Kenny et al., 2000). These studies suggest that hippocampal serotonin plays an important role in NNs-induced anxiety-like behavior; however, the present analysis was performed without separating the dorsal and ventral hippocampus, and further research is needed to determine which of these play a key role in NN-induced anxiety.

In this study, histamine levels did not show significant changes; however, a decreasing trend was observed in the hippocampus. The role of histamine in anxiety is thought to be complex (Haas et al., 2008); it has been reported that mice fed a diet low in L-histidine, which is necessary for histamine synthesis, show decreased histamine levels in the brain and increased anxiety-like behavior (Yoshikawa et al., 2014), while microinjection of histamine into the dorsal hippocampus induces anxiolytic effects (Zarrindast et al., 2006) and anxiogenic effects when injected in the ventral hippocampus (Rostami et al., 2006). Furthermore, as acute stress promotes histamine turnover in the striatum and other brain regions (Ito, 2000; Yoshitomi et al., 1986), measuring the

concentrations of metabolites may further clarify the role of histamine in NNs-induced anxiety-like behavior.

Significant correlations were also found between several MA concentrations. The correlations between the levels of dopamine and histamine in the striatum and between dopamine and 3-MT, and 3-MT and serotonin in both the hippocampus and striatum were significant in both the control and ACE groups. As 3-MT is a metabolite of dopamine, its correlation with dopamine is likely due to metabolism of the increased dopamine. The correlation between dopamine or 3-MT and histamine in the hippocampus was significant only in the control group but not in the ACE group; the correlation disappeared with the administration of ACE. This may have been due to the decreasing trend of hippocampal histamine, although levels of the other MAs were significantly increased.

Conversely, the correlation between dopamine and serotonin in the hippocampus and striatum was significant in the ACE group, but not the control group, suggesting that it was caused by ACE administration. Three major dopaminergic pathways, including the nigrostriatal pathway, are innervated by serotonin (Alex et al., 2007), and serotonergic stimulation of the striatum increases dopamine release (Dailly et al., 2004). Such innervations occur when the serotonergic tone is increased, rather than under physiological conditions (Alex et al., 2007). In light of these findings, the significant correlation between dopamine and serotonin observed only in the ACE group in this study may be the result of ACE increasing serotonin and modulating dopamine levels due to increased serotonergic tone.

The EZM, developed as an improvement on the EPM, is widely used to study anxiety-like behavior in rodents (Shepherd et al., 1994). This behavioral test uses a balance between curiosity about novel environments and fear of heights, and it is generally interpreted that the lesser time spent exploring in the open arm, the more fear avoidance behavior occurs, that is, a state of increased anxiety (Walf et al., 2007; Yamaguchi et al., 2005a). In contrast to the EZM, the EPM has open and closed arms that cross each other in a crisscross pattern, and the stay in the central area is difficult to interpret; the EZM resolved this issue by using a circular design for the arms (Shepherd et al., 1994). In this study, the administration of ACE tended to decrease the time spent in open arms in the EZM, indicating increased anxiety-like behavior. These results support previous findings

(Kubo et al., 2022; Rodrigues et al., 2010; Sano et al., 2016). In addition, entries into the open arms and total distance traveled were significantly reduced. The rate of entries into the open arms is one of the parameters that is a typical indicator of anxiety-like behavior, especially in the EPM; however, due to the absence of a center area and the placement of open and close arms proximal to each other in the EZM, the number of entries into the open arms is almost the same as those into the closed arms. Therefore, in the EZM, this parameter is similar to that of total distance traveled rather than an index of pure anxiety-like behavior. Another parameter that was significantly reduced, total distance traveled, is often interpreted as an indicator of activity. However, this index is affected not only by activity but also by anxiety (Shepherd et al., 1994), and freezing can also occur as a defensive response (Blanchard et al., 2003). In the present results, total distance traveled was significantly correlated with time spent in the open arms in the control group, rendering it difficult to separate the effects of anxiety and activity on this parameter. One limitation of this study is the gender of mice; women have been reported to be at greater risk of anxiety and depression than men (Altemus et al., 2014), but only male mice were used in this study. Interestingly, in the EPM, a behavior test similar to the EZM, it has been reported that female mice and rats show less anxiety than males (An et al., 2011; Börchers et al., 2022). It is unclear whether female mice are better suited to investigate the effects of anxiety because of this species difference, but further studies of sex differences in monoaminergic systems may reveal not only sex differences in anxiety, but also the mechanism of this species difference.

As mentioned, the serotonergic system plays an important role in anxiety, and serotonergic neurons that project to the forebrain, including the serotonergic neurons that innervate the dopamine pathways, are largely derived from the RN (Abela et al., 2020; Alex et al., 2007). The serotonergic system of the DRN, in particular, has been implicated in anxiety-related behaviors (Bouwknecht et al., 2007). In the DRN, nAChRs are expressed in both the serotonergic nerves and presynaptic glutamatergic neurons, and nicotine increases the firing frequency of approximately 80% of serotonergic neurons in the DRN (Mihailescu et al., 1998, 2002) and induces glutamate release via activation of the presynaptic α4β2 nAChRs subtypes (Garduño et al., 2012). It has also been reported that stimulation of serotonergic nerves in the RN increases anxiety-like behavior via release of

hippocampal serotonin (Abela et al., 2020; Ohmura et al., 2014). In this study, serotonin concentration in the brainstem, the brain region containing the RN, was increased in the ACE group, suggesting that ACE acts on the RN to increase serotonin levels.

However, a limitation of this study is that not all brain samples analyzed necessarily contained the RN because the RN is a very small region of the brainstem and was technically difficult to separate visually. Therefore, anti-serotonin staining, which was performed in this study for a more reliable examination of DRN serotonin production, revealed that the number of stained neurons was increased in the ACE group. This suggests that ACE treatment increased serotonin production in the DRN. Further, in the ACE group, there was a significant decrease in total distance traveled in the EZM; as activation of the serotonergic pathway from the DRN to the inferior colliculus has been reported to cause freezing (da Silva Soares et al., 2019), the results of this behavioral test may reflect freezing rather than a decrease in activity. Further studies on effects on the serotonergic system, as well as dose-response and sex differences, will provide more detailed information on the mechanisms by which ACE affects behavior.

5. Summary

In conclusion, ACE induced anxiety-like behavior 30 min after oral administration, and the results suggest that hippocampal serotonin and striatal dopamine play an important role in this behavioral change. Specifically, it is hypothesized that activation of serotonergic neurons in the DRN increases serotonin levels in projection regions, such as the hippocampus, which in turn modulates dopamine concentrations.

This study is the first to examine the effects of NNs on behavior using EZM and, to my knowledge, this is the first paper to evaluate these correlations, although the effects of NNs on MA or behavior are beginning to be investigated. Little attention has been paid to the effects of NNs on the serotonergic system in mammals, but further studies on the serotonergic system will be helpful in elucidating the mechanism of NNs-induced anxiety-like behavior.

6. Figures and tables

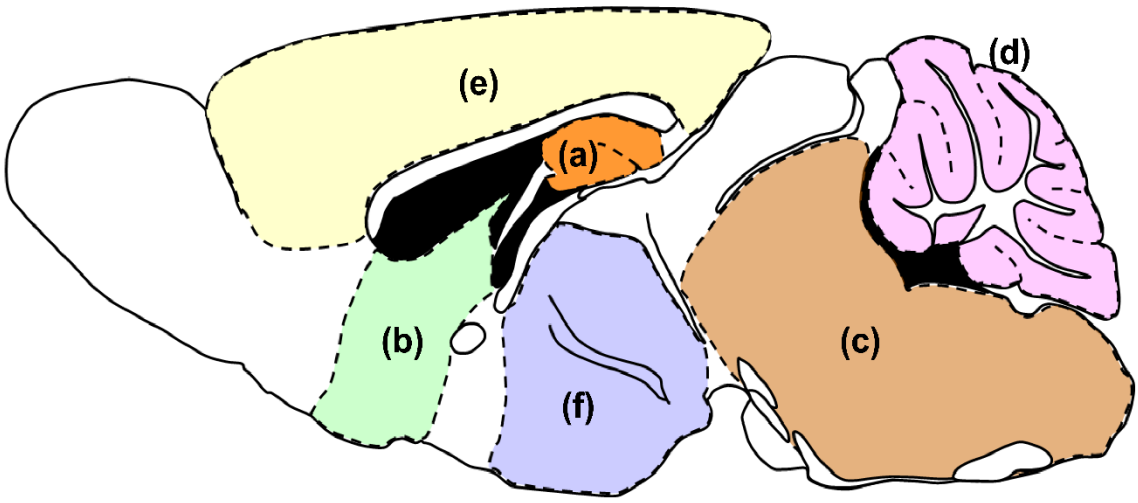

Figure 7. Brain regions sampled in this study.

This is an image diagram using a sagittal section of Lateral 0.48 mm, and each colored region represents a sampled site. In this study, (a) is referred to as the hippocampus, (b) as the striatum, (c) as the brainstem, (d) as the cerebellum, (e) as the cerebral cortex, and (f) as the thalamus.

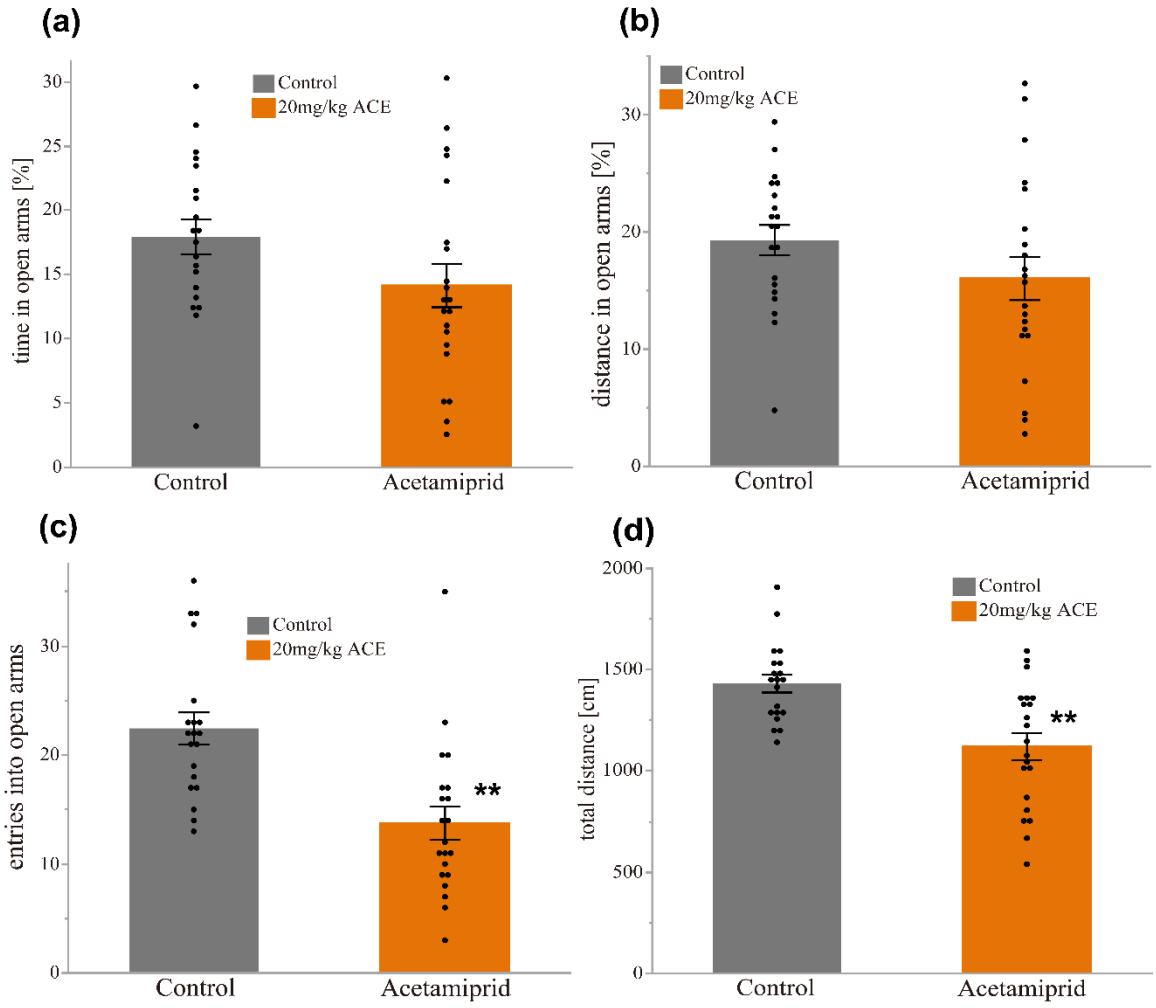

Figure 8. ACE-induced behavioral changes in the EZM tests.

(a) The percentage of time spent in the open arms tended to decrease in the ACE group. (b) The percentage of distance traveled in the open arms did not change significantly between the two groups. (c) The number of entries into the open arms and (d) the total distance traveled in the EZM were significantly lesser in the ACE group than the control.

Bar graphs represent the mean ± SEM of each group (control: $n = 20$, ACE: $n = 21$). ** $P < 0.01$, Wilcoxon test.

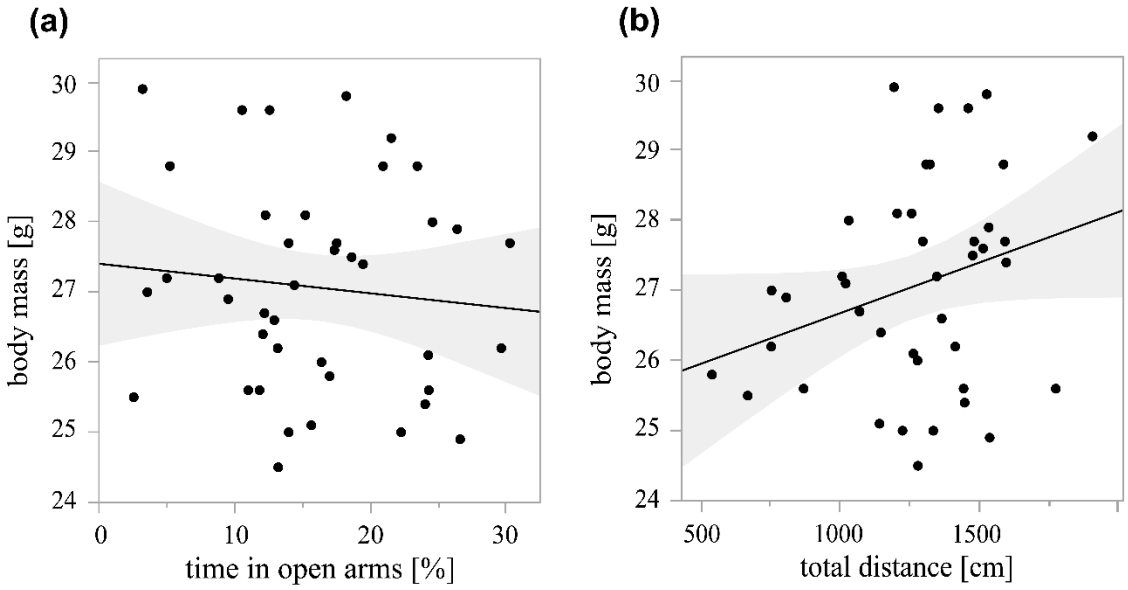

Figure 9. Scatterplot matrix of correlation between body mass and EZM test results. Mice from both groups (control: n = 20, ACE: n = 21) were combined to examine the correlation between body mass and (a) time in the open arms and (b) total distance in the EZM test. The Spearman's rank correlation coefficient test showed no significant differences.

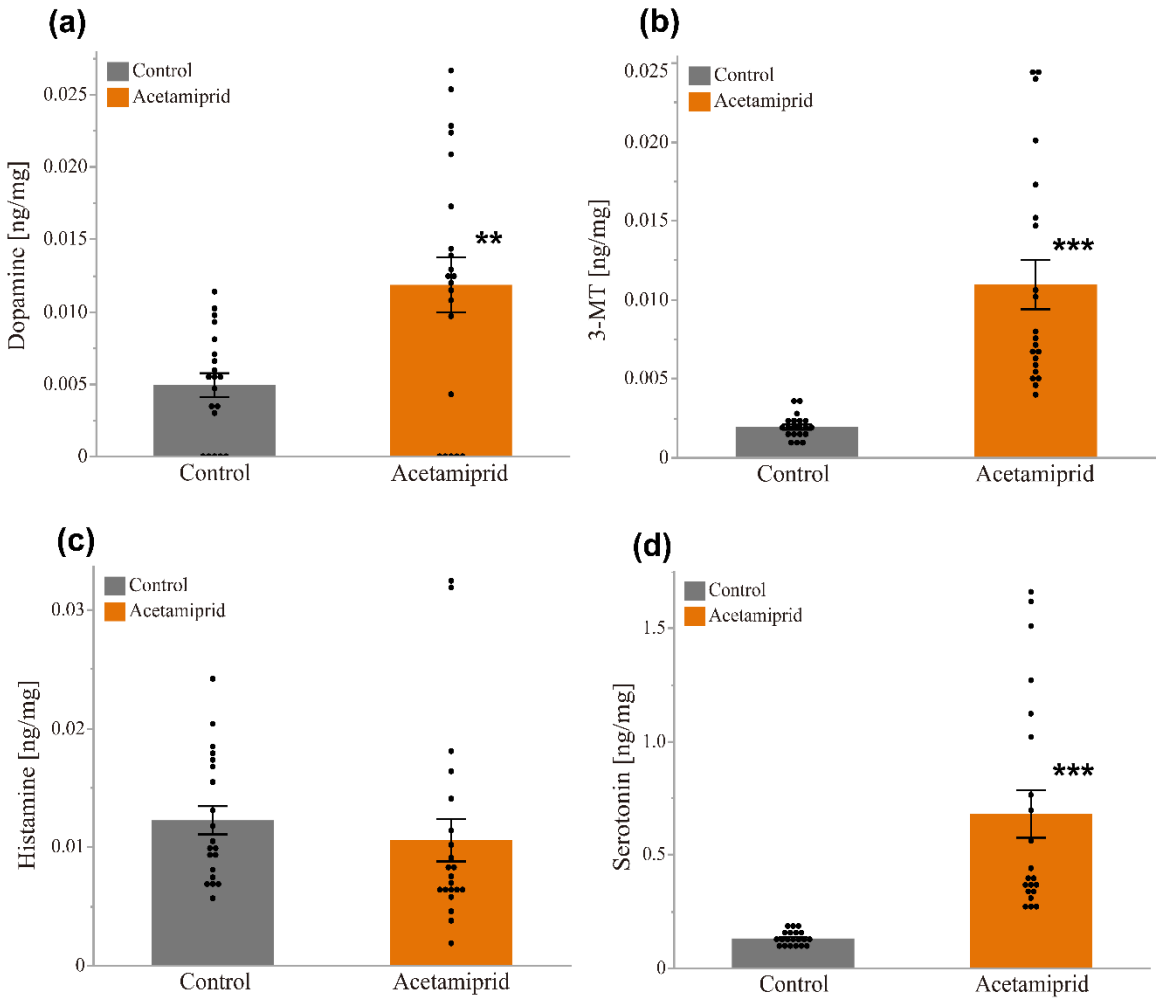

Figure 10. MA concentrations in the hippocampus.

The concentrations of (a) dopamine, (b) 3-MT, and (d) serotonin were significantly high in the ACE group. (c) The concentration of histamine tended to decrease in the ACE group. Bar graphs represent mean ± SEM of each group (control: $n = 20$, ACE: $n = 21$). ** $P < 0.01$, *** $P < 0.0001$, Steel test.

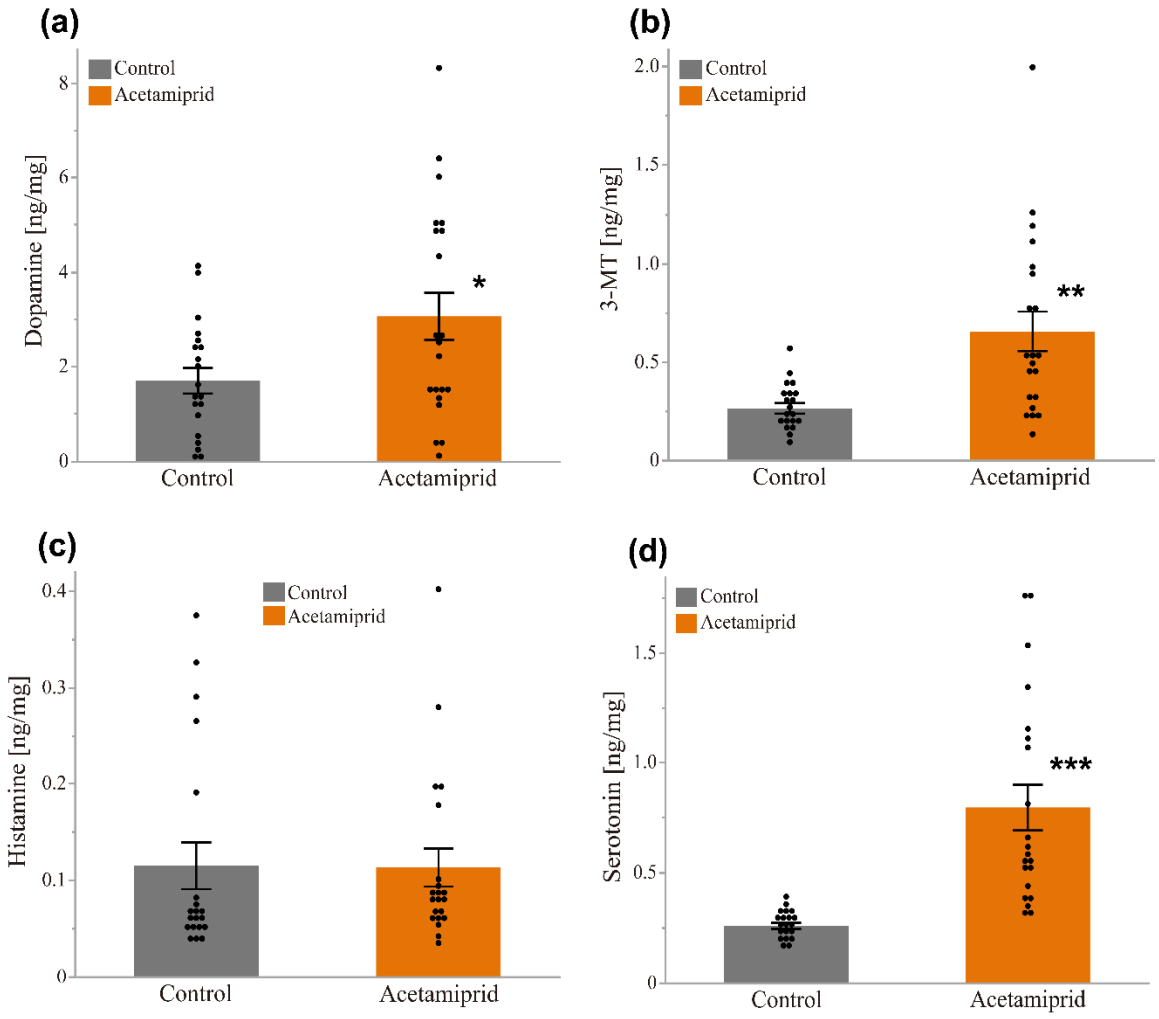

Figure 11. MA concentrations in the striatum.

The concentrations of (a) dopamine, (b) 3-MT, and (d) serotonin were significantly high in the ACE group. (c) The difference in histamine concentration was not significant.

Bar graphs represent mean ± SEM of each group (control: $n = 20$, ACE: $n = 21$). * $P < 0.05$, ** $P < 0.01$, *** $P < 0.0001$, Steel test.

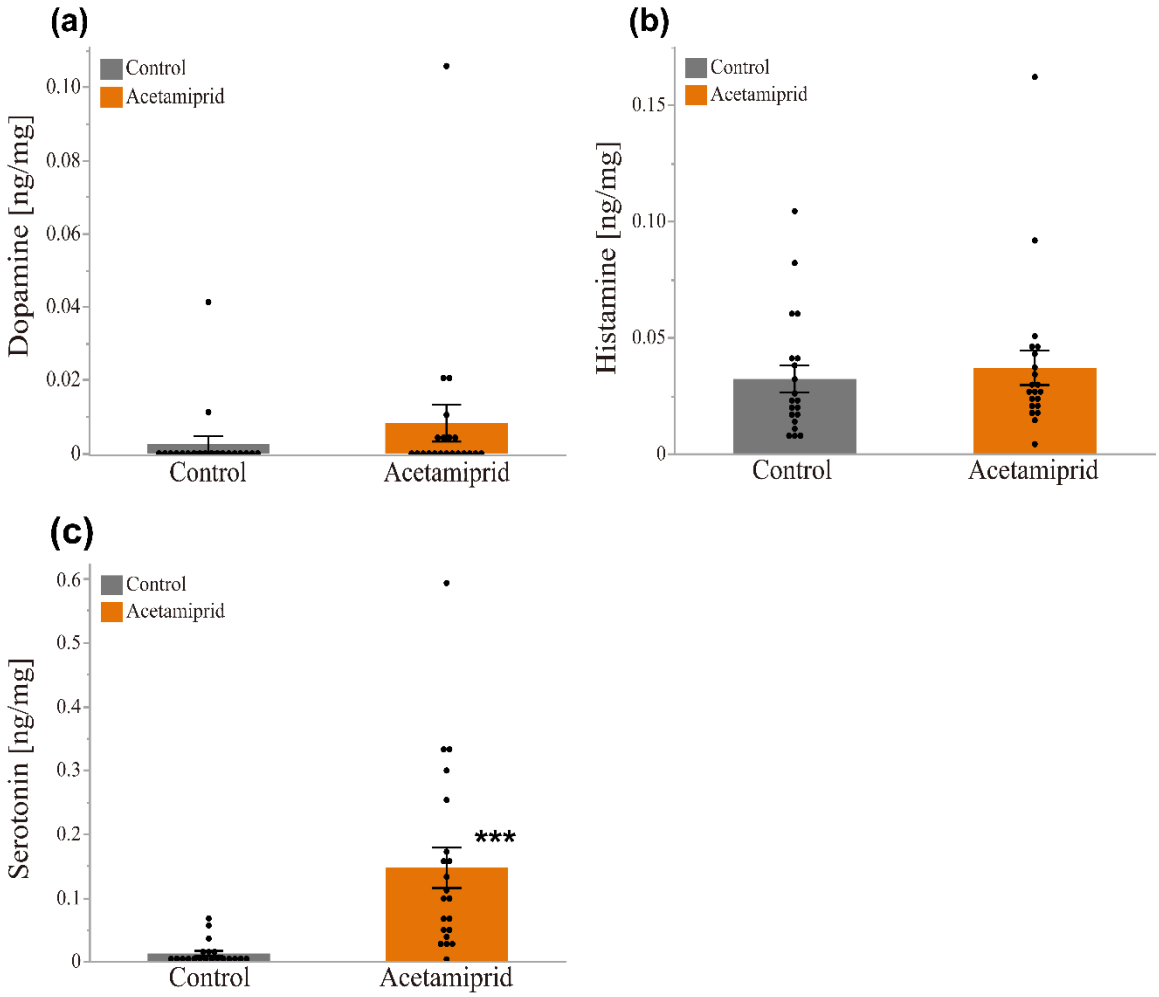

Figure 12. MA concentrations in the brainstem.

The concentration of (c) serotonin was significantly high in the ACE group. There was no significant difference in the concentration of (a) dopamine and (b) histamine between the two groups.

Bar graphs represent mean ± SEM of each group (control: n = 20, ACE: n = 21). *** $P <$ 0.0001, Steel test.

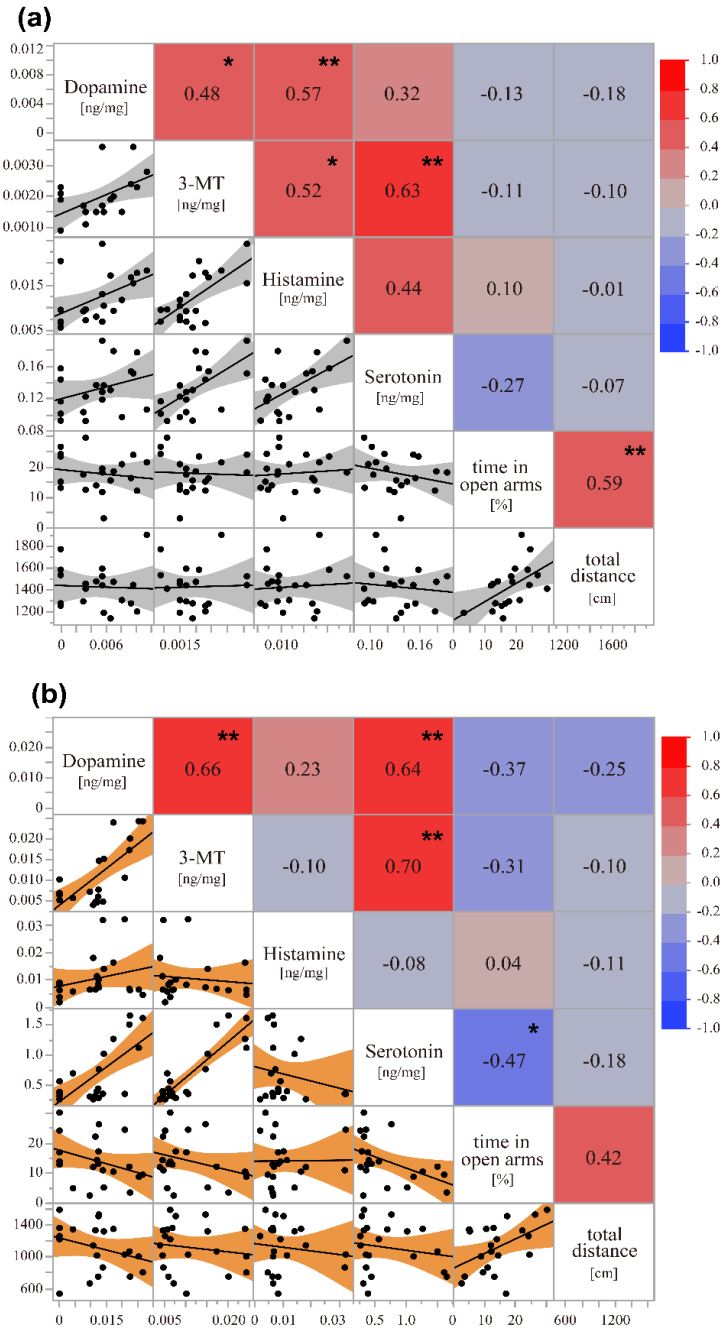

Figure 13. Scatterplot matrix of correlation between the results of EZM test and MA concentrations in the hippocampus.

The lower left half of the figures show the scatterplot matrix, and the upper right half show a heat map of the correlation coefficients. (a) In the control group (n = 20 each), five correlations were significant. (b) In the ACE group (n = 21 each), four correlations were significant. * $P < 0.05$, ** $P < 0.01$, Spearman's rank correlation coefficient test.

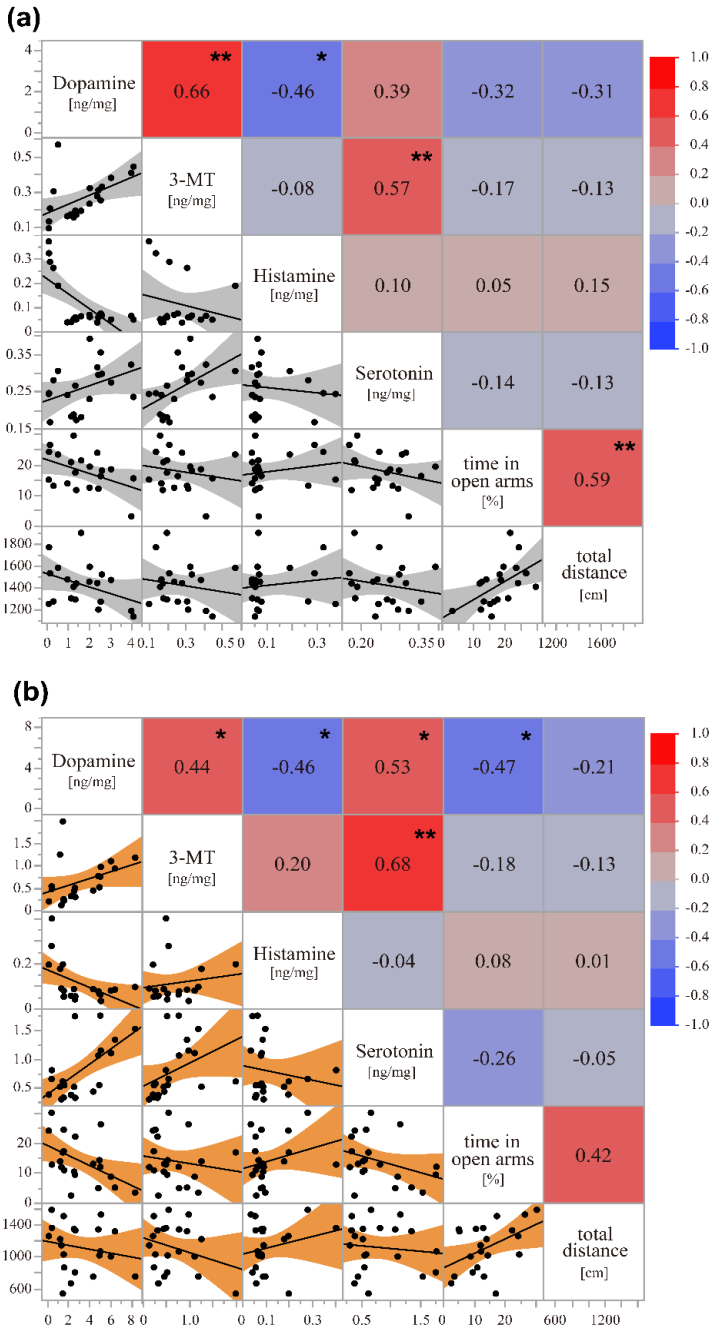

Figure 14. Scatterplot matrix of correlation between the results of EZM test and MA concentrations in the striatum.

The lower left half of the figures show the scatterplot matrix, and the upper right half show a heat map of the correlation coefficients. (a) In the control group (n = 20 each), four correlations were significant. (b) In the ACE group (n = 21 each), five correlations were significant. * $P < 0.05$, ** $P < 0.01$, Spearman's rank correlation coefficient test.

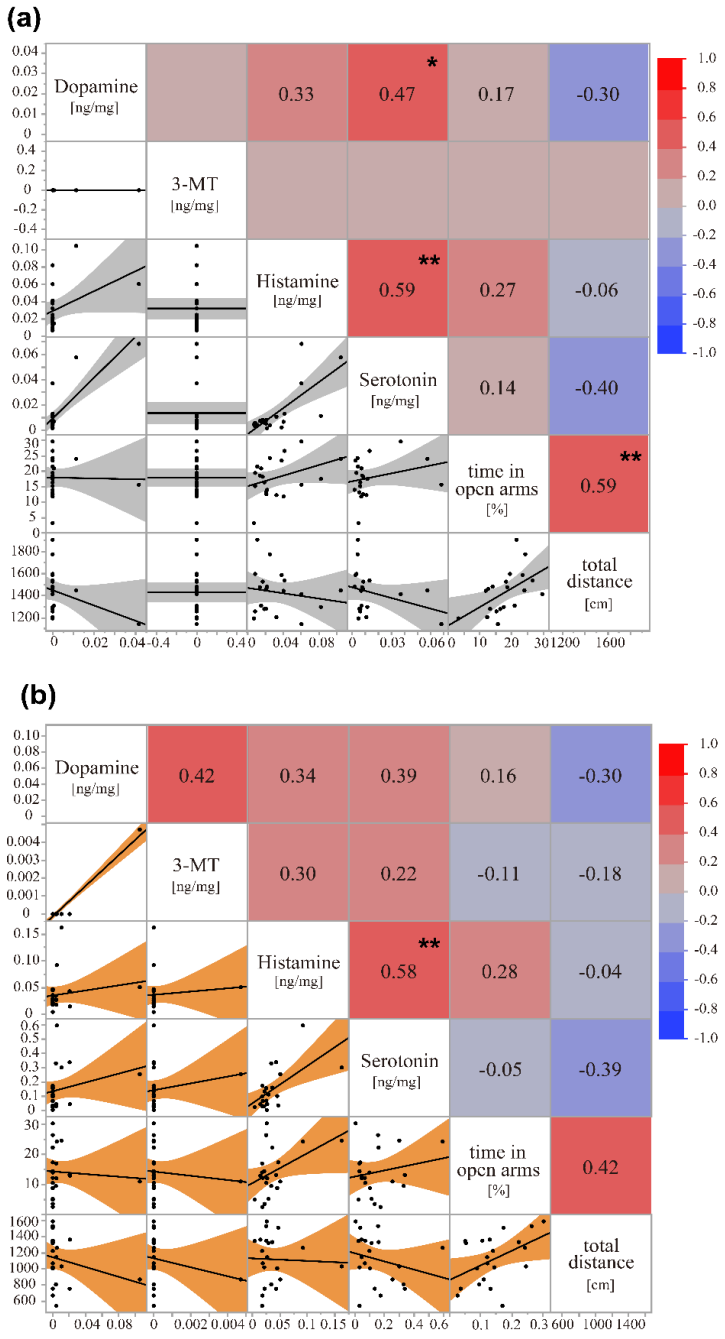

Figure 15. Scatterplot matrix of correlation between the results of EZM test and MA concentrations in the brainstem.

The lower left half of the figures show the scatterplot matrix, and the upper right half show a heat map of the correlation coefficients. (a) In the control group (n = 20 each), three correlations were significant. (b) In the ACE group (n = 21 each), only one correlation was significant. * $P < 0.05$, ** $P < 0.01$, Spearman's rank correlation coefficient test.

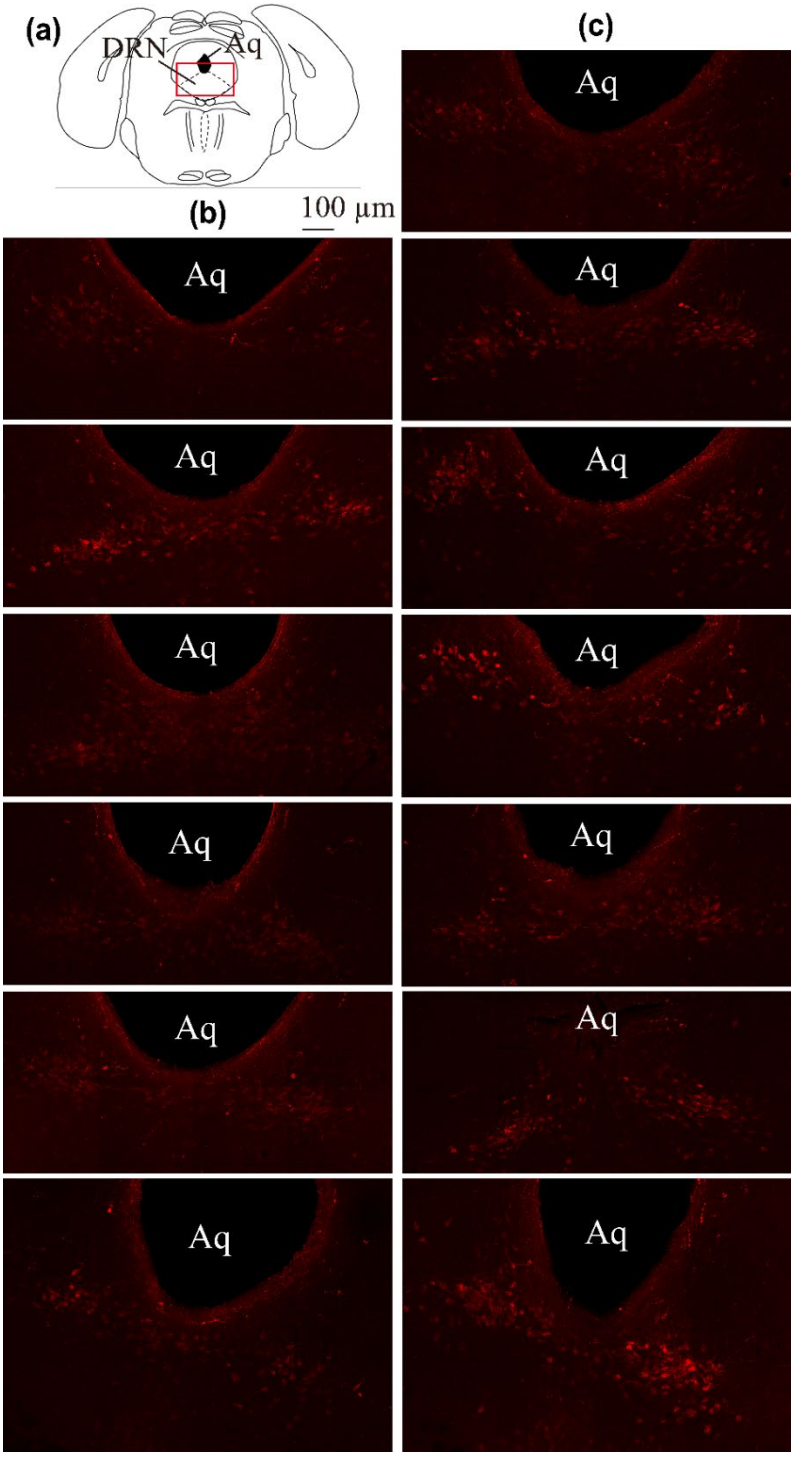

Figure 16. Anti-serotonin staining in the DRN.

(a) Observed area was circled in red. The maximum intensity projections of 8 z-stack red fluorescence images of the (b) control (n = 6) and (c) ACE (n = 7) groups are shown. Aq: cerebral aqueduct.

Table 9. Parameters in MA analysis by LC/MS/MS.

The product ion listed in the top row for each compound was used as the target ion, and the other product ions were used as qualifiers.

Compound	RT [min]	MRM Transition [*m/z*]		CE [V]
		Precursor Ion	Product Ion	
3-MT	14.5	342.31	192	28
			151.1	28
			91	60
3-MT-d4	14.5	346.41	192	16
			155	28
			95.1	48
Dopamine	14	328.31	192.3	24
			91.2	56
Dopamine-d4	14	332.41	192.2	20
			95.1	56
Histamine	7.7	286.21	192.3	24
			95.1	28
Histamine-d4	7.7	290.31	192.2	32
			99.1	32
Serotonin	14.3	351.41	192.1	20
			160	28
Serotonin-d4	14.3	355.41	192.1	20
			164	20

Table 10. MAs concentrations in the cerebellum, cerebral cortex and thalamus.

Values represent the mean ± SEM of each group (control: n = 20, ACE: n = 21). The concentrations of undetected samples were treated as 0 when calculating the mean and SEM. * $P < 0.05$, ** $P < 0.01$, Steel test. N.D., not detected.

	Cerebellum [ng/mg]		**Cerebral Cortex [ng/mg]**		**Thalamus [ng/mg]**	
	Control	**ACE**	**Control**	**ACE**	**Control**	**ACE**
Dopamine	0.00051 ± 0.0003	N.D.	0.0048 ± 0.002	0.0053 ± 0.002	0.0092 ± 0.003	0.065 ± 0.02**
3-MT	N.D.	N.D.	N.D.	N.D.	0.00041 ± 0.0003	0.011 ± 0.005**
Histamine	0.021 ± 0.002	0.021 ± 0.003	0.012 ± 0.002	0.0013 ± 0.002	0.050 ± 0.009	0.088 ± 0.01*
Serotonin	N.D.	0.00055 ± 0.0002**	0.0079 ± 0.002	0.021 ± 0.004*	0.033 ± 0.02	0.29 ± 0.07***

Chapter 3

In vivo Ca^{2+} imaging with two-photon microscopy to detect the disruption of brain function by neonicotinoids

1. Introduction

As indicated in the preceding chapters, NNs can alter MA levels in the brains of mice, which may subsequently affect behavior. This chapter therefore sought to investigate how NNs affect neural activity in awake mice by *in vivo* Ca^{2+} imaging using two-photon microscopy.

Two-photon microscopy, a laser scanning microscope, is a less invasive technique suitable for deep imaging, enabling the visualization of both the function and structure of neurons in living, awake animals (Nabekura et al., 2010). Inoculation of the mouse brain with an adeno-associated viral vector expressing GCaMP6f, a neuronal-specific fluorescent calcium indicator protein, results in alterations in the fluorescence intensity within neurons upon Ca^{2+} influx, allowing *in vivo* Ca^{2+} imaging using two-photon microscopy to capture changes in neural activity. This method facilitates detailed investigation of changes in neuronal activity *in vivo* during arousal. However, limitations such as the high cost and limited availability of equipment, as well as the necessity for skilled techniques mean that this technique is not yet widely utilized in toxicological research.

The somatosensory cortex is located in the anterior part of the parietal lobe and contributes to higher sensory functions by integrating signals received from sensory receptors and perceiving them as meaningful information (Akinola et al., 2019; Petersen et al., 1984). The information received by the sensory organs is relayed to the brain, processed, and then reintegrated. The details of this reintegration mechanism have not yet been elucidated. Nonetheless, the firing frequency, firing patterns, synchronized firing, and other factors presumably play a role in coding information and making connections between the segmented information and the information itself (Gray, 1994; Ioka, 2014; Metherate, 2004; Umeda et al., 2019).

The α4β2 and α7 subtypes are the commonly expressed nAChRs (Hritcu et al., 2007; Petersen et al., 1984). In the somatosensory cortex, nAChRs are expressed on inhibitory neurons and suppress both the excitatory neurons and inhibitory neurons that inhibit the excitatory neurons (Burwick, 2014; Buzsáki et al., 2012). For example, inhibitory neurons, such as vasoactive intestinal peptide (VIP)-expressing neurons, somatostatin (SOM)-expressing neurons, parvalbumin (PV)-expressing neurons, and excitatory neurons, such

as pyramidal neurons, are distributed in the prefrontal cortex. The aforementioned receptors are not expressed in pyramidal neurons. However, the α5, α7 and β2 subunits are reportedly expressed in VIP-, SOM-, and PV-expressing neurons (Koukouli et al., 2017). The VIP-expressing neurons inhibit SOM- and PV-expressing neurons. Furthermore, the SOM- and PV-expressing neurons inhibit pyramidal neurons (Koukouli et al., 2017). VIPs, SOMs, and pyramidal neurons are also expressed in layers II/III of the somatosensory cortex (Arroyo et al., 2014). In other words, NNs, which are nAChRs agonists, may alter neural activity in the somatosensory cortex and affect emotional cognitive behavior.

Accordingly, in this study, Ca^{2+} imaging by two-photon microscopy was conducted at three time points: before administration, 30 min, and 2 h after administration, with the objective of examining the changes in neuronal activity in the somatosensory cortex of mice over time, from immediately following exposure.

2. Material and methods

2.1. Chemicals

ACE was purchased from Cosmo Bio Co., Ltd. (100% purity, Tokyo, Japan) and Kanto Chemical Co., Inc. (Tokyo, Japan). Nicotine (97% purity) and isoflurane were purchased from Fujifilm Wako Pure Chemicals Co., Inc. (Tokyo, Japan). All other reagents were purchased from Kanto Chemical Co., Inc. (Tokyo, Japan).

2.2. Animals

All the animal experiments were approved by the Experimental Committee of the Faculty of Veterinary Medicine, Hokkaido University, and the Nagoya University Animal Care and Use Committee. All animal experiments were performed in accordance with the Guide for the Care and Use of Laboratory Animals, in conformity with the Association for the Assessment and Accreditation of Laboratory Animal Care International (AAALAC; approval number: 18-0061). Male C57BL/6J mice (7 weeks old) were obtained from CLEA Japan, Inc. (Tokyo, Japan) and were kept in a 12 h light/dark cycle at a room temperature

of 22 ± 1°C and humidity of 70 ± 5%. The mice were provided food (breeding solid feed for mice, rats, and hamsters: CE-2, CLEA Japan, Inc., Tokyo, Japan) and tap water, ad libitum. I changed the feed and water twice a week. The mice cages were changed once a week. Experiments were performed after at least one week of acclimation.

2.3. Craniotomy and inoculation with viral vectors for in vivo Ca^{2+} imaging

The brains of different sets of mice from all groups were surgically operated on at 8 weeks of age and used for Ca^{2+} imaging at 10 weeks of age. I placed a fixation plate on the heads of the mice to perform an *in vivo* imaging of the central nervous system. The mice were anesthetized by intraperitoneal administration of ketamine (74 mg/kg) and xylazine (10 mg/kg). Following shaving and disinfection of the parietal area, I incised the skin and exposed and cleaned the skull. Moreover, a custom-made metal plate was fixed to the skull using dental cement (G-CEM ONE; GC Co., Ltd., Gifu, Japan). The exposed skull was coated with acrylic-based dental resin cement (Super Bond; Sun Medical, Shiga, Japan).

After 1 day of recovery, the animals were subjected to craniotomy and inoculation with adeno-associated virus vectors. I immobilized the mice with a fixation plate in a stereotaxic instrument (SR-5M-HT, NARISHIGE, Tokyo, Japan) under isoflurane (1%) anesthesia. The skull above the somatosensory cortex (1.2 mm caudal to the cross suture and 1.5 mm lateral to the cross suture) was sectioned into a circle (2 mm in diameter) using a dental drill. The brain surface was exposed to a craniotomy (Masamizu et al., 2014). I used an adeno-associated viral vector expressing GCaMP6f, a neuron-specific fluorescent calcium indicator protein, adeno-associated virus 1-hSyn-GCaMP6f (Addgene), to visualize the neuronal activity in layers II/III of the cerebral cortex. I connected a glass pipette ((tip diameter: 10 μm) DGC-1; NARISHIGE, Tokyo, Japan) filled with diluted viral vector solution (1.0×10^{12} viral gram/mL) to a motorized microinjector (IM-31; NARISHIGE, Tokyo, Japan). The tip of the glass pipette was inserted at a depth of 250 μm from the brain surface, and 500 nL of the viral vector solution was injected. Following the injection, the glass pipette was held in place for 10 min and then withdrawn. This prevented leakage of the viral vector solution. The viral vectors were inoculated at three locations within the craniotomy window. Following inoculation, a custom-made circular cover glass

(Matsunami Glass Ind., Ltd., Osaka, Japan) was crimped to the craniotomy position. The edges of the glass were fixed with dental cement and dental resin cement to create the observation window.

2.4. In vivo Ca^{2+} imaging using two-photon microscopy

I randomly divided the mice into three groups: the ACE group (group A), a low concentration nicotine group (group L), and a high concentration nicotine group (group H). At 10 weeks of age, mice in groups A, L and H were orally administered ACE (20 mg/kg BW), low-dose nicotine (0.33 mg/kg BW), and high-dose nicotine (1.65 mg/kg BW), respectively. The determination of the concentration of each reagent, its preparation and administration to mice was conducted in the same procedure as previously described in *Chapter 1, section 2.3.*

I subsequently subjected them to *in vivo* Ca^{2+} imaging. I used two-photon microscopy (objective lens: × 10, XLPlan, NA 1.0, Zeiss, Tokyo, Japan; microscope; LSM 7 MP, Zeiss, Tokyo, Japan) and two-photon excitation laser (wavelength 950 nm. Ti: sapphire Chameleon Ultra II Laser; Coherent, Tokyo, Japan) for the *in vivo* Ca^{2+} imaging of neurons, distributed 200-250 μm deep from the brain surface. The mice were held on a dedicated fixation platform and placed under an objective lens. I conducted the imaging on awake mice. The imaging frame was 512 × 512 pixels (207.94 μm × 207.94 μm). I set the image acquisition speed to 0.39 s/frame (0.39 s/frame) and captured 1000 frames of continuous images (approximately 6 min). The imaging was performed for group A (n = 4), L (n = 4), and H (n = 3) before chemical administration and either 30 min or 2 h after chemical administration. The mice were continuously fixed on the microscope until the time of imaging (30 min after chemical administration) and were returned to their cages for imaging 2 h later (Fig. 17a).

I measured and quantified the frequency and area under the curve (AUC) of the Ca^{2+} transients in single neurons, and the correlation between activity in single neurons within the neuronal population, otherwise known as the cross-correlation (C.C.), before, 30 min, and 2 h after the administration of ACE and nicotine (low and high concentration). I initially determined the nature of the neurons expressing GCaMP6f, driven by the synapsin

promoter (Fig. 17a, b) (total of 120, 43, and 84 neurons in groups A, L, and H, respectively). In each mouse, I divided the neurons with high (high-AUC cell group) and low spontaneous activity (low-AUC cell group) according to whether the AUC was more or less than the median value. I then compared the properties of Ca^{2+} transients in each group (Fig. 17c, h, m).

The frequency of Ca^{2+} transients was calculated by dividing the total number of transients by the imaging time (seconds). Ca^{2+} transients and the C.C. were defined according to the previous study (Okada et al., 2021).

2.5. Imaging analysis

I used Fiji Image J (1.53e; NIH, Java 1.8.0_172; 64 bit) (Schindelin et al., 2012) and MATLAB R2019b (The MathWorks, Inc., Natick, MA, USA) to analyze the imaging data. TurboReg (Thévenaz et al., 1998) was used to compensate for the displacement of the focal plane. I used a semi-automatic algorithm to correlate the fluorescence intensity between adjacent pixels to define the region of interest (ROI) around the neuron. The ROI was visually confirmed. The fluorescence in the ROI was averaged over time, and background fluorescence was subtracted. I detected a Ca^{2+} response when the fluorescence intensity was two SD above the mean baseline, which was defined as the 35^{th} percentile of the total fluorescence intensity. In this study, the neurons that were commonly observed in all images captured before, 30 min, and 2 h after the administration were analysed.

Although *in vivo* Ca^{2+} imaging was not performed in a blinded manner, imaging analysis was thus performed using software such as MATLAB to minimize the effect of subjectivity.

2.6. Statistical analysis

I conducted statistical analyses using Excel (2016) and JMP (SAS Institute Inc., Cary, NC, USA). I performed the Steel test to analyze the Ca^{2+} imaging results. Data are presented as the mean ± SEM, and the significance level was set at $P < 0.05$.

3. Results

3.1. In vivo Ca^{2+} imaging using two-photon microscopy

The frequency and amplitude of Ca^{2+} transients and the C.C. of the neuronal population were measured (Table 11).

The amplitude of Ca^{2+} transients significantly decreased in the high-AUC cell group, 30 min and 2 h after ACE administration (Fig. 17d). In contrast, it significantly increased in the low-AUC cell group, 30 min after high-dose nicotine administration (Fig. 17n). However, low-dose nicotine administration did not show any detectable changes (Fig. 17i). Following NN administration, the frequency of Ca^{2+} transients significantly increased in the low-AUC cell group of the ACE group, but remained unchanged in all neural populations of the nicotine groups (Fig. 17e, j, and o). The C.C. of the neuronal population significantly decreased in all high-AUC cell groups and increased in all low-AUC cell groups, 30 min and 2 h after NN administration (Fig. 17f, k, and p). These results suggest that nicotine disrupts the synchronization of specific neuronal populations, with relatively limited effects on the amplitude and frequency of Ca^{2+} transients.

4. Discussion

In the somatosensory cortex, there is a mixture of neural populations whose activity likely increases and decreases with the activation of nAChRs. I roughly divided the mixed neural populations and calculated the AUC of the Ca^{2+} waveform before exposure, which was divided by the number of Ca^{2+} transients for each neuron. Moreover, I divided the neurons with AUC greater than and less than the median. I quantified the frequency of Ca^{2+} transients and their amplitude, as well as the synchronized firing of neurons in the somatosensory cortex, and observed significant changes in one or more of these parameters in all groups (Fig. 17).

Despite no significant change in the frequency of Ca^{2+} transients in Ca^{2+} imaging, neurons that changed beyond 2 SD before the treatment were observed in the nicotine groups (Fig. 17d, e). Possible reasons for the previously mentioned result are as follows: 1. there was no significant change in the frequency of Ca^{2+} transients in the somatosensory

cortex, 2. there was no detectable change at the time of measurement, or 3. no change was extractable by the AUC-based classification. While the amplitude of Ca^{2+} transients had significantly decreased in the high-AUC cell group of the ACE group (Fig. 17f), it significantly increased after 30 min in the low-AUC cell group of the nicotine-treated group (Fig. 17g). The increase in the amplitude of Ca^{2+} transients is said to be a phenomenon brought about by the superposition of action potentials (Chen et al., 2013), and *in vitro* studies have reported that ACE elicits a lower amplitude Ca^{2+} response than acetylcholine (Houchat et al., 2020). These results suggest that ACE causes Ca^{2+} influx through the activation of nAChRs in the somatosensory layers II/III. The synchronization of Ca^{2+} transients significantly decreased and increased in the high- and low-synchronized neural populations (Fig. 17h, i). Therefore, the neuronal activity was altered in both the highly and lowly activated neurons before imaging. Although the present study is an *in vivo* study, a previous study using cultured hippocampi demonstrated that the administration of nicotine increased synchronous firing (Djemil et al., 2020). Moreover, the β4 subunit is required for increased synchrony in the hippocampus (Djemil et al., 2020). Unlike the hippocampus, however, the somatosensory cortex does not express the β4 subunit (Gotti et al., 2006). Hence, the subtype variations might have contributed to the difference in results when compared with previous studies. Interestingly, I observed significant synchronous changes 2 h after administration in the nicotine group. The half-life of intraperitoneally administered nicotine in a mouse's brain is approximately 7 min and roughly 20 min for its metabolites (Petersen et al., 1984). Therefore, despite not reflecting a direct effect of nicotine on the nAChR somatosensory neurons, the results indicate a secondary effect, such as changes in neurotransmitters in different brain regions.

While the amplitude was significantly low in the high-AUC cell group of the ACE group, it was significantly high in the low-AUC cell group of the nicotine group (Fig. 17f, g). The synchrony of firing was significantly altered in all groups (Fig. 17h, i). The somatosensory cortex plays an important role in the processing of sensory input, and it is a part of the interaction between pain and anxiety (Borich et al., 2015; Zhuo, 2016). The primary somatosensory cortex contains neuronal populations associated with pain, and reactivation of these populations has been suggested to induce anxiety-like behavior via projections to

the anterior cingulate cortex (ACC) (Ishikawa et al., 2023). In *Chapters 1* and *2-2*, ACE proposed to induce anxiety-like behavior. Despite the variation in the time elapsed after administration, the concentrations of ACE and nicotine found to increase anxiety-like behaviors in *Chapter 1* altered neuronal firing frequency and amplitude in the somatosensory cortex in this study. This finding suggests the potential involvement of a network extending from the somatosensory cortex to the ACC in these anxieties.

Increased anxiety-like behavior also reportedly occurs with prenatal exposure to ACE (Sano et al., 2016). ACE can be transferred from the mother to child in humans (Ichikawa et al., 2019). This necessitates further information on its toxicity during developmental stages. However, the permeability of ACE may be different in neonates and adults as previous studies have reported that the BBB of newborn rabbits has selective permeability, unlike that of adult rabbits (Braun et al., 1980). *In vitro* BBB models are a commonly used method, but possess some challenges, such as the fact that they are very simplistic and therefore their relevance may be limited (Cho et al., 2015). *In vivo* Ca^{2+} imaging by two-photon microscopy enables the conduction of research that addresses these issues in that actual changes in neuronal activity can be observed *in vivo*. In addition, there are several reports on the developmental neurotoxicity of ACE. The oral administration of ACE in the prenatal and neonatal periods impairs neurogenesis in the hippocampus and neocortex and induces microglial activation (Kagawa et al., 2018; Nakayama et al., 2019). Despite challenges, such as the difficulty of surgery, Ca^{2+} imaging using two-photon microscopy has the potential to detect these disorders and facilitate our understanding of these developmental neurotoxicity.

Changes in the brain's neuronal activity during acute exposure to a drug differed between the ACE and nicotine groups. In addition, from the standpoint of the performance of two-photon microscopy, *in vivo* imaging using two-photon microscopy is currently not capable of analyzing the deep structures of the brain; hence, only the surface layer was imaged and analyzed in the current study. However, the results from this study suggest that *in vivo* imaging of just the surface layer can be useful. More specifically, these results indicated that changes in neuronal activity could be observed even at concentrations that

were shown to have no effect on behavior in *Chapter 1*. These studies, however, are insufficient to elucidate the *in vivo* effects of brain dysfunction. Further research, involving the examination of neural activity in other anxiety-related brain regions, such as the ACC, will provide more detailed insights into these effects.

5. Summary

These results suggest that even at concentrations that did not affect behavior, changes in neuronal activity were detected by Ca^{2+} imaging using two-photon microscopy. In other words, I was able to show that it is possible to detect disturbances in brain function that cannot be captured by behavioral tests. This, in turn, suggests that *in vivo* Ca^{2+} imaging by two-photon microscopy is a promising technique to assess the effects of neurotoxicants.

6. Figures and tables

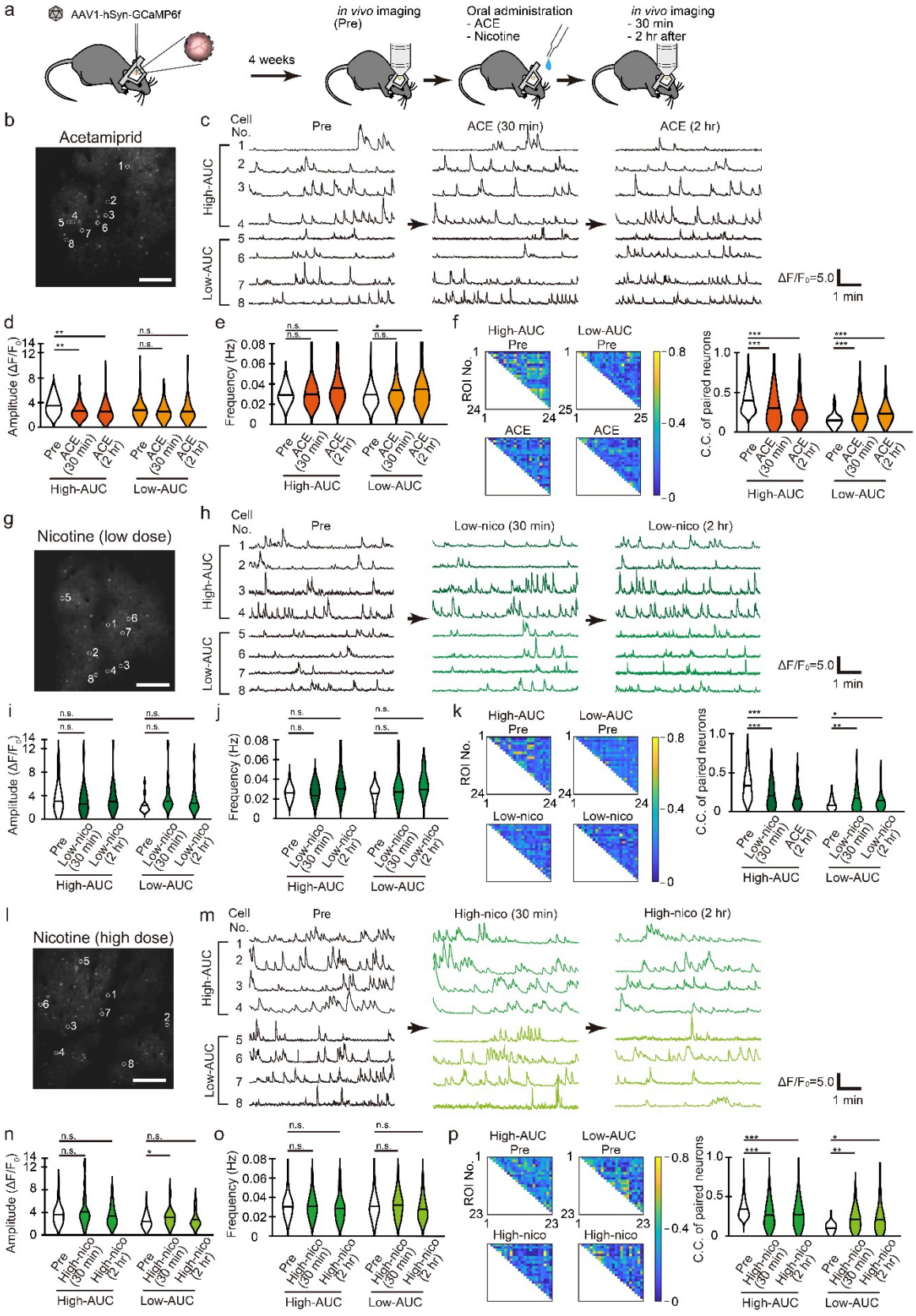

Figure 17. The effect of acute administration of ACE (20 mg/kg, p.o.) and low-dose (0.33 mg/kg, p.o.) or high-dose (1.65 mg/kg, p.o.) of nicotine on the neuronal activity in the somatosensory cortex.

(a) A schematic drawing of the experimental procedure for the two-photon microscopy. Wild-type mice have been injected with adeno-associated virus vector-encoding GCaMP6f into the somatosensory cortex to enable Ca^{2+} imaging of neurons. *In vivo* Ca^{2+} imaging has been performed before and after the oral administration of reagents; (b, g, and l) Representative images of neurons expressing GCaMP6f. Typical Ca^{2+} responses, before and after the administration, recorded from the circled neurons and represented in c, h, and m, respectively. Scale bar, 100 μm; (c, h, and m) Ca^{2+} responses from same neurons; (d, i, and n) The amplitude and (e, j, and o) frequency of Ca^{2+} transient in each group, before and after the administration (group A: 60 neurons per each cell group from 4 mice; group L: 22 and 21 neurons per high- and low-AUC cell group, respectively, from 4 mice; group H: 42 neurons per each cell group from 3 mice); (f, k, and p) Representative results of correlation co-efficiency for paired neurons. Color-coded maps indicate that the typical neuron sets have responded to each reagent.

n.s., not significant. $*P < 0.05$, $**P < 0.01$, $***P < 0.001$, Steel test.

Table 11. Summary of the neuronal activities in the somatosensory cortex before, 30 min, and 2 h after administration (mean ± SEM).

Acetamiprid (n = 4)							
High-AUC group				Low-AUC group			
	Frequency (Hz)	Amplitude ($\Delta F/F_0$)	C.C. of paired neuron		Frequency (Hz)	Amplitude ($\Delta F/F_0$)	C.C. of paired neuron
Pre	0.0248±0.0010	3.40±0.16	0.410±0.0052	Pre	0.0278±0.0024	2.67±0.20	0.152±0.0037
30 min	0.0279±0.0026 (P = 0.9510)	2.74±0.17 (P = 0.0032)	0.310±0.0066 (P < 0.0001)	30 min	0.0321±0.0038 (P = 0.2532)	2.57±0.18 (P = 0.8956)	0.223±0.0052 (P < 0.0001)
2h	0.0299±0.0018 (P = 0.1150)	2.83±0.20 (P = 0.0077)	0.289±0.0059 (P < 0.0001)	2h	0.0335±0.0027 (P = 0.0356)	2.53±0.19 (P = 0.7071)	0.222±0.0045 (P < 0.0001)
Nicotine (low dose) (n = 4)							
High-AUC group				Low-AUC group			
	Frequency (Hz)	Amplitude ($\Delta F/F_0$)	C.C. of paired neuron		Frequency (Hz)	Amplitude ($\Delta F/F_0$)	C.C. of paired neuron
Pre	0.0258±0.0015	3.10±0.45	0.367±0.014	Pre	0.0286±0.0019	2.06±0.27	0.136±0.0065
30 min	0.0223±0.0015 (P = 0.264)	2.66±0.42 (P = 0.5537)	0.294±0.016 (P < 0.0001)	30 min	0.0302±0.0038 (P = 0.6864)	2.75±0.44 (P = 0.1544)	0.201±0.013 (P = 0.0037)
2h	0.0299±0.0028 (P = 0.6713)	3.06±0.48 (P = 0.9991)	0.246±0.013 (P < 0.0001)	2h	0.0330±0.0023 (P = 0.5248)	2.43±0.39 (P = 0.8624)	0.177±0.010 (P = 0.0102)
Nicotine (high dose) (n = 3)							
High-AUC group				Low-AUC group			
	Frequency (Hz)	Amplitude ($\Delta F/F_0$)	C.C. of paired neuron		Frequency (Hz)	Amplitude ($\Delta F/F_0$)	C.C. of paired neuron
Pre	0.0301±0.0015	3.65±0.26	0.354±0.0049	Pre	0.0309±0.0021	2.32±0.18	0.113±0.0026
30 min	0.0303±0.0018 (P = 0.9761)	4.15±0.40 (P = 0.9245)	0.264±0.0068 (P < 0.0001)	30 min	0.0312±0.0020 (P = 0.9197)	3.04±0.24 (P = 0.0431)	0.215±0.0059 (P < 0.0001)
2h	0.0277±0.0020 (P = 0.2190)	3.44±0.27 (P = 0.6009)	0.266±0.0067 (P < 0.0001)	2h	0.0275±0.0019 (P = 0.2850)	2.63±0.23 (P = 0.6657)	0.209±0.0065 (P < 0.0001)

Chapter 4

Screening of brain regions activated *in vivo* by acetamiprid, using red fluorescent protein tdTomato labeling in transgenic mice

1. Introduction

In *Chapter 3*, *in vivo* Ca^{2+} imaging using two-photon microscopy was employed to elucidate the changes in neural activity during arousal. While this technique provides detailed insights into neuronal activity, its invasiveness imposes limitations on the brain regions that can be examined. Consequently, the objective of this chapter is to identify brain regions where neural activity is altered by NNs using transgenic mouse model.

One particularly effective approach for capturing changes in neural activity *in vivo* is targeted recombination in active populations (TRAP). This method utilizes the promoter of the immediate early gene (IEG), which are rapidly expressed in response to cellular stimulation, to induce activity-dependent recombination and label neurons that are activated by stimulation (Guenthner et al., 2013). Among the IEGs employed in TRAP, *Fos* and *Arc* are prevalent markers of neuronal activity. c-Fos, a transcription factor, does not directly influence neuronal function like many other IEGs, whereas the Arc protein (activity-regulated cytoskeleton-associated protein) localizes to neuronal dendrites and modulates synaptic function, suggesting its involvement in neuronal plasticity (Lyford et al., 1995). In short, Arc exhibits high specificity for neurons.

In this study, I employed a mouse model that was generated through the cross-breeding of transgenic mice, which expressed a complex of Cre recombinase and mutant estrogen receptor ER^{T2} under the control of the Arc promoter, with reporter mice that expressed red fluorescent protein tdTomato in a Cre-dependent manner. In this mouse model, active cells expressing Cre-ER^{T2} undergo recombination only in the presence of tamoxifen, thereby resulting in the expression of tdTomato. This labeling facilitates the identification of neurons that are activated following ACE administration.

As detailed in *Chapters 1* and *2*, the administration of ACE has been demonstrated to induce an increase in anxiety-like behavior. Furthermore, *Chapter 3* provides evidence that ACE alters neural activity in layer II/III of the somatosensory cortex. Consequently, this study has focused on the following brain regions: the hippocampus and striatum, where significant correlations between anxiety-like behaviors and MAs was identified in *Chapter 2*; the inferior colliculus, which is innervated by serotonin from the RN and induces the freezing response; the somatosensory cortex layers II/III, as observed in *Chapter 3*; the ACC, which receives projections from these regions and is involved in anxiety; and the

amygdala and septal nucleus, which is involved in anxiety. To assess the impact of ACE administration on neural activity in these brain regions, 4-hydroxytamoxifen (4-OHT), a metabolite of tamoxifen, was administered 30 min following ACE exposure. This approach enabled the assessment of region-specific neural activity changes induced by ACE.

2. Material and methods

2.1. Chemicals

ACE was purchased from Cosmo Bio Co., Ltd. (100% purity, Tokyo, Japan). Isoflurane and sucrose were purchased from Fujifilm Wako Pure Chemicals Co., Inc. (Tokyo, Japan). Tween 80 was purchased from Bio Medical Science Co., Ltd. (Tokyo, Japan), 4-OHT from Sigma-Aldrich Co. LLC (St. Louis, MO, USA), DMSO from Nacalai Tesque, Inc. (Kyoto, Japan), and 4% PFA/PB from Bioenno Lifesciences (Santa Ana, CA, USA). All other chemicals were purchased from Kanto Chemical Co., Inc. (Tokyo, Japan).

2.2. Animals

All animal experiments were approved by the Experimental Committee of the Faculty of Veterinary Medicine, Hokkaido University, as well as Safety Committee on Genetic Recombination Experiments (approval number: 22-0024, 2022-058). All the experiments were conducted in accordance with the Guide for the Care and Use of Laboratory Animals and with the Association for the Assessment and Accreditation of Laboratory Animal Care International (AAALAC) and the Safety Management Regulations on Genetic Recombination Experiments.

Arc^{CreER} mice (Stock #021881) and Ai14 mice (Stock #007914) were purchased from The Jackson Laboratory (Bar Harbor, ME, USA) and maintained strains. These two strains were subsequently crossed, and male Arc^{CreER};Ai14 mice obtained were utilized in this study at 12 weeks of age. All mice were maintained at a temperature of 22 ± 1°C (room temperature) and 70 ± 5% humidity, under a 12-h light/dark cycle (9:00–21:00; light, 21:00–9:00; dark). The food (breeding solid food for mice, rats, and hamsters: CE-2, CLEA

Japan, Inc., Tokyo, Japan) and tap water were provided ad libitum. The food and water were replaced twice a week, and cages were changed once a week.

2.3. TRAP

Male Arc^{CreER};Ai14 mice were randomly divided into the control (n = 4) and ACE (n = 6) groups. Saline was administered orally to the control group using a sonde (FUCHIGAMI, Kyoto, Japan), while ACE dissolved in normal saline was administered at 20 mg/kg BW, which was estimated to be the NOAEL of ACE in mice (Food Safety Commission, 2014). Thirty min after oral administration, mice received an intraperitoneal (i.p.) injection of 4-OHT (10 mg/kg BW) to induce recombination. The 4-OHT was heated at 65°C for 10 min, as previously established (Felker et al., 2016). It was then dissolved in saline containing 3% Tween 80 and a minimal amount of DMSO, yielding a concentration of 1 mg/mL. Each reagent was administered under light anesthesia with isoflurane at a volume of 10 mL/kg BW.

2.4. Brain sectioning

Following an approximate waiting period of one month for the accumulation of the red fluorescent protein tdTomato, the mice were euthanized by cervical dislocation under deep anesthesia with isoflurane. Subsequently, the whole brains were harvested by perfusion with heparinized saline, and fixed by shaking overnight at 4°C in 4% PFA/PB. This was followed by further shaking overnight in 30% sucrose in 0.1 M PB. The fixed brains were then embedded in O.C.T. Compound (Sakura Finetek Japan Co., Ltd., Tokyo, Japan) and sliced into 50 μm sections using a cryostat (Leica CM 1900; Leica Microsystems GmbH, Wetzlar, Germany). These brain slices were washed three times with 0.1 M PB and then mounted in glass slides using the nuclear staining inclusion agent DAPI Fluoromount-G® (Southern Biotechnology Associates Inc., Birmingham, AL, USA).

2.5. Imaging analysis

The red fluorescent was obtained using a fluorescent microscope BZ-X810 and Advanced Observation Module BZ-H4XD (objective lens: × 20, Plan Apochromat 20x; Keyence, Osaka, Japan). The image data was then mixed to ensure the images could not been identified by the researcher. Cell counts were subsequently performed using Fiji Image J (1.53e; NIH, Java 1.8.0_172; 64 bit) (Schindelin et al., 2012).

2.6. Statistical analysis

For statistical analysis, Microsoft Excel (2016) and JMP (SAS Institute Inc., Cary, NC, USA) were used. The number of tdTomato-positive neurons in the ACC, layer II/III of the somatosensory cortex, septum, striatum, dorsal hippocampus CA1 and amygdala were compared by Student's t-test, and those in the dentate gyrus (DG), ventral hippocampus CA1 and inferior colliculus, where normal distribution or equal variance could not be assumed, by exact Wilcoxon rank sum test. It is noteworthy that some mice with data that were identified as outliers by Tukey's IQR method in one or more brain regions were excluded from the data set. All data are presented as mean ± SEM, and the significance level was set at $P < 0.05$.

3. Results

3.1. Number of tdTomato-expressing neurons per area of brain region

Examples of brain regions in which the number of neurons was counted, and the average values of the brain region area and the number of tdTomato-expressing neurons are shown in Figure 18 and Table 12, respectively. In light of the findings on the effects of ACE on anxiety in the preceding three chapters, this chapter focused on the quantification of tdTomato-expressing neurons and the calculation of their density in nine brain regions involved in anxiety and behavior: the ACC, the somatosensory cortex layers II/III, the septal nucleus, the striatum, the dorsal hippocampal DG, the dorsal and ventral hippocampal CA1 region, the amygdala, and the inferior colliculus. It is noteworthy that for the inferior colliculus, the averages for the left and right sides are presented.

The number of tdTomato-expressing neurons per square millimeter was 426 ± 41.4 and 481 ± 47.0 in the ACC of the control and ACE groups, respectively, with no significant difference (Fig. 19a, $P = 0.4369$). Conversely, in layers II/III of the somatosensory cortex, the ACE group exhibited 341 ± 31.0 neurons, while the control group showed 451 ± 38.6 neurons, suggesting a robust, albeit non-significant, tendency towards increased activated neurons following ACE administration (Fig. 19b, $P = 0.0756$). Similarly, a weak increasing trend was observed in the septal nuclei, with 53 ± 8.79 and 78 ± 16.7 neurons in the control and ACE groups, respectively (Fig. 19c, $P = 0.3006$). In the striatum, the control and ACE groups had 122 ± 20.7 and 125 ± 13.9 neurons, respectively, with no significant differences (Fig. 19d, $P = 0.9097$). The DG exhibited the highest density of labeled neurons, with a mean of 613 ± 13.7 in the control group and 611 ± 77.6 in the ACE group, with no significant difference between the groups (Fig. 19e, $P = 0.9143$). The dorsal and ventral hippocampal CA1 regions of the hippocampus were also measured. The mean values obtained for the dorsal hippocampus were 187 ± 26.8 and 178 ± 28.3 for the control and ACE groups, respectively. In the ventral hippocampus, the mean values were 66 ± 7.28 and 77 ± 12.0, respectively. These measurements did not demonstrate significant differences in these brain regions (Fig. 19f, $P = 0.8465$; Fig. 19g, $P = 0.9143$). Conversely, a rising trend was observed in the amygdala and inferior colliculus, with 45 ± 6.87, 69 ± 11.3, 35 ± 0.698, and 58 ± 14.9 cells in the control and ACE groups, respectively (Fig. 19h, $P = 0.1480$; Fig. 19i, $P = 0.3524$).

4. Discussion

Arc^{CreER};Ai14 mice are a transgenic mouse model that employs the TRAP method. This model is generated by crossing Arc^{CreER} mice, which express Cre-ER^{T2} under the control of the Arc promoter, with Ai14 reporter mice (loxP-stop-loxP-tdTomato). The expression of Cre-ER^{T2}, a complex of Cre recombinase and the mutant estrogen receptor ER^{T2}, is induced in a cell activity-dependent manner through the Arc promoter. The Arc protein is a widely used marker of neuronal activity. ER^{T2} does not respond to endogenous estrogen, but it is activated upon the administered tamoxifen, allowing Cre-ER^{T2} to translocate into the nucleus. Within the nucleus, the Cre recombinase interacts with the loxP sequence,

excising the STOP codon upstream of the tdTomato gene. This Cre-loxP mediated recombination results in sustained expression of the red fluorescent protein tdTomato in activated neurons. Consequently, neurons that are active at the time of tamoxifen administration are specifically labeled with red fluorescence in Arc^{CreER};Ai14 mice.

Among the nine brain regions analyzed in this study, four exhibited a trend towards increased neuronal activation following ACE administration: layer II/III of the somatosensory cortex, the septal nucleus, the amygdala, and the inferior colliculus. The respective number of activated neurons in these regions was approximately 1.32, 1.47, 1.53, and 1.66 times those of the control group, with corresponding *P*-values of 0.0756 , 0.3006, 0.1480 and 0.3524, respectively. In *Chapter 3*, the somatosensory cortex layer II/III was identified as containing a population of neurons exhibiting increased firing frequency subsequent to ACE administration, as evidenced by *in vivo* Ca^{2+} imaging using two-photon microscopy. The results of this study may support this finding. In addition, as discussed in *Chapter 3*, the somatosensory cortex has been shown to contain a neuronal population that is involved in anxiety through its projections to the ACC (Ishikawa et al., 2023). The increase in activated neurons observed in the somatosensory cortex in this study may be indicative of heightened activity within this neuronal population.

The ACC is one of the brain regions that receives serotonergic innervation from the RN and input from the somatosensory cortex. It projects to the amygdala and functions as a higher-order center in the processing of emotions and pain, including anxiety (Hao et al., 2023). Given the reported inhibitory effect of serotonin on excitatory synaptic transmission in most ACC neurons via 5-HT1A receptors (Tian et al., 2017), coupled with the increased serotonin production observed in DRN in *Chapters 2-2*, it was hypothesized that neural activity in the ACC might be suppressed. However, no significant differences were found in this study.

One possible explanation for this result, besides the possibility that neuronal activity remained unchanged, lies in the limitations of the TRAP method. Neuronal populations with low Arc expression may not be effectively labeled by this technique. Arc has been shown to have higher specificity for neurons than c-fos, as Arc is abundant in neuronal dendrites (Guenthner et al., 2013; Lyford et al., 1995). In contrast, Arc-mediated

TRAP shows a bias toward forebrain regions, and certain neuronal populations, such as granule cells in the DG, can undergo tamoxifen-independent recombination in age-dependent manner (Guenthner et al., 2013). This tamoxifen-independent recombination occurs primarily in neurons with high Arc expression, which varies between neuronal types. Consequently, neurons with low Arc expression, which may undergo changes in neural activity, may not have been labeled in this study.

Another potential factor is the complexity of detecting short-term neuronal inhibition. In the TRAP method, recombination occurs only in neurons expressing Cre-ER^{T2} during the period when tamoxifen is translocated to the brain, metabolized, and excreted. Consequently, neurons that show constant activity under physiological conditions or during home cage activity are labeled with tdTomato, even when temporarily inhibited by a single dose of ACE. When 4-OHT, a metabolite of tamoxifen, is used instead of tamoxifen itself, the time window for TRAP activation is reduced to less than six hours before and after administration of 4-OHT. However, ACE metabolism is known to be rapid, with a Tmax in male rats ranging from 30 minutes to five hours after oral administration (Food Safety Commission, 2014). Thus, if the activity of ACC neurons were transiently inhibited by ACE and subsequently reactivated in the presence of 4-OHT, such changes would likely fail to be detected by this technique. Further investigation of the ACC is needed to explore these possibilities, particularly to better understand the dynamics of short-term neuronal inhibition and its implications for ACC function under the influence of ACE.

The amygdala, which exhibited the second strongest trend toward increased activation (P = 0.1480) following the somatosensory cortex, is a well-established brain region implicated in anxiety and fear. As previously mentioned, the amygdala receives input from the ACC and is characterized by robust serotonergic activity, with approximately 10% of serotonergic projections from the DRN targeting this region (Asan et al., 2013; Ma et al., 1991). Given its low levels of spontaneous neural activity (LeDoux, 2007), the amygdala is considered a suitable target for detecting neuronal changes using the TRAP method. In the amygdala, serotonin has been demonstrated to induce the release

of GABA via 5-HT2A receptors (Jiang et al., 2008). This mechanism could contribute to the observed upward trend in tdTomato-positive neurons following ACE administration.

An increasing trend in activated neurons was also observed in the septal nucleus, a brain region implicated in anxiety regulation. The septal-hippocampal pathway has been identified as an important circuit for controlling anxiety (Parfitt et al., 2017). Specifically, the lateral septum is closely connected to the hippocampus, and nicotine exposure in the lateral septum has been reported to increase anxiety-like behavior (Ouagazzal et al., 1999). While this study did not identify significant changes in the hippocampus, it is possible that different results might be obtained if behavioral or other tests were conducted prior to the administration of 4-OHT. Such adjustments in the experimental approach could potentially elucidate additional effects of ACE on hippocampal or septal activity.

The inferior colliculus, a brain region critical for auditory perception as well as defensive responses, also showed a tendency toward increased neuronal activation. The stimulation of the inferior colliculus has been demonstrated to induce avoidance responses, including vigilance, freezing, and escape behaviors (Castilho et al., 1999). Given the role of serotonin, a key neurotransmitter in the inferior colliculus, and the observation that most of the serotonergic innervation of this region originates in the DRN (Hurley et al., 2002), it can be hypothesized that ACE, which was demonstrated in *Chapter 2-2* to increase serotonin production in the DRN, may also influence neural activity in the inferior colliculus. However, further studies are needed to determine whether the observed trend is attributable to auditory stimulation in the home cage environment or to defensive responses arising from social interactions with other mice.

While the RN is recognized as a critical component in the regulation of anxiety, the TRAP method in Arc^{CreER};Ai14 mice exhibits a bias toward forebrain regions, preventing direct observations of the RN (Guenthner et al., 2013; Ons et al., 2004). To address this limitation, I propose the utilization of complementary techniques, such as antiserotonin staining or mass spectrometry imaging, to examine RN activity. The integration of these

methods with data from Arc^{CreER};Ai14 mouse brain sections could facilitate a more comprehensive understanding of the circuitry underlying ACE-induced anxiety.

5. Summary

In conclusion, the administration of ACE was associated with a tendency towards heightened neural activity in several brain regions implicated in anxiety, including layer II/III of the somatosensory cortex, the septal nucleus, the amygdala, and the inferior colliculus. These findings underscore the utility of Arc^{CreER};Ai14 mice as a valuable tool for screening brain regions exhibiting elevated neural activity. When combined with complementary techniques, such as staining and mass spectrometry imaging, this approach has the potential to advance the understanding of toxicological mechanisms.

In this study, 4-OHT was administered without any treatment beyond oral administration. To refine this methodology, future studies could incorporate behavioral tests, such as the EPM, conducted following oral administration of ACE and prior to 4-OHT administration. This approach could facilitate the identification of brain regions more specifically associated with anxiety-like behaviors.

6. Figures and tables

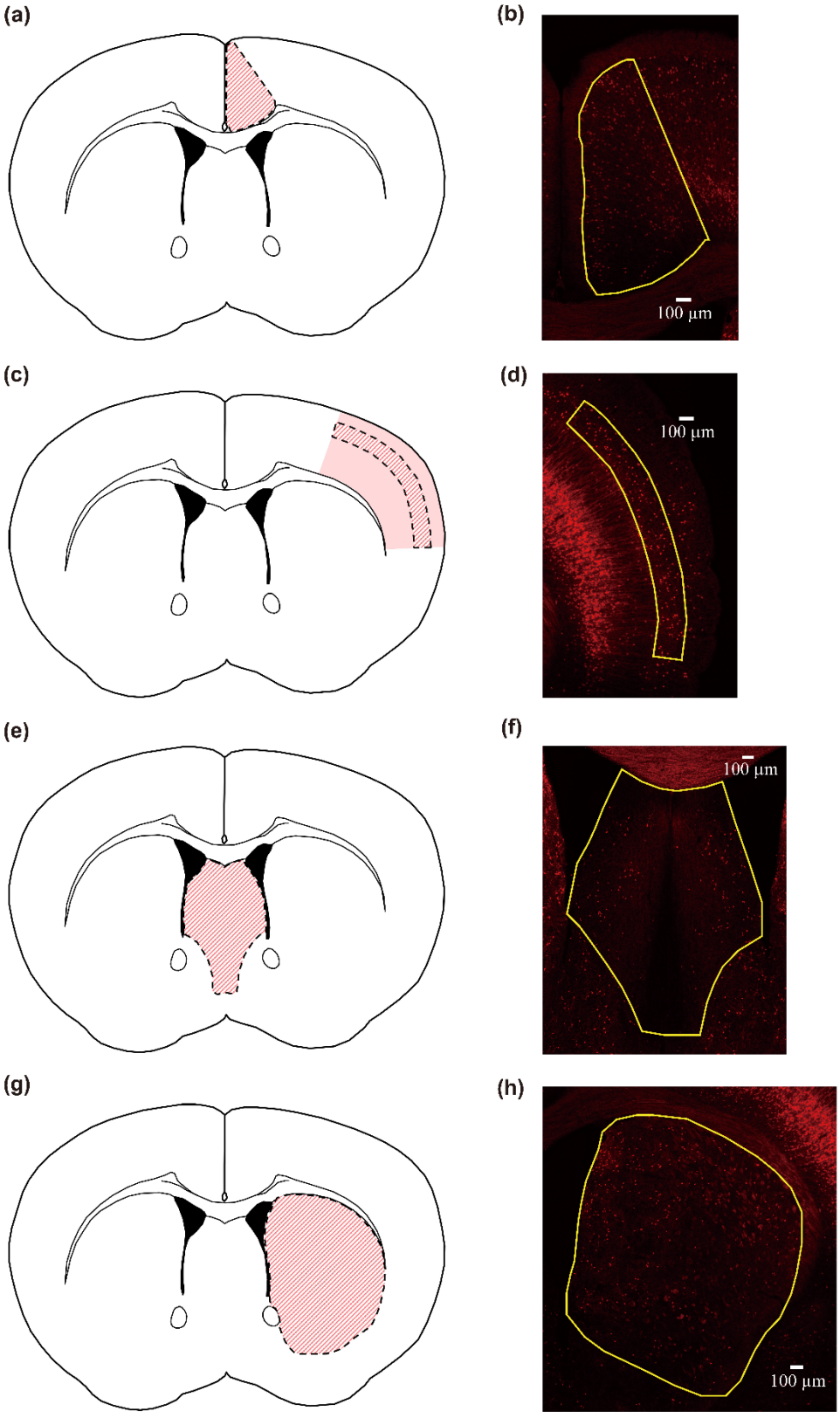

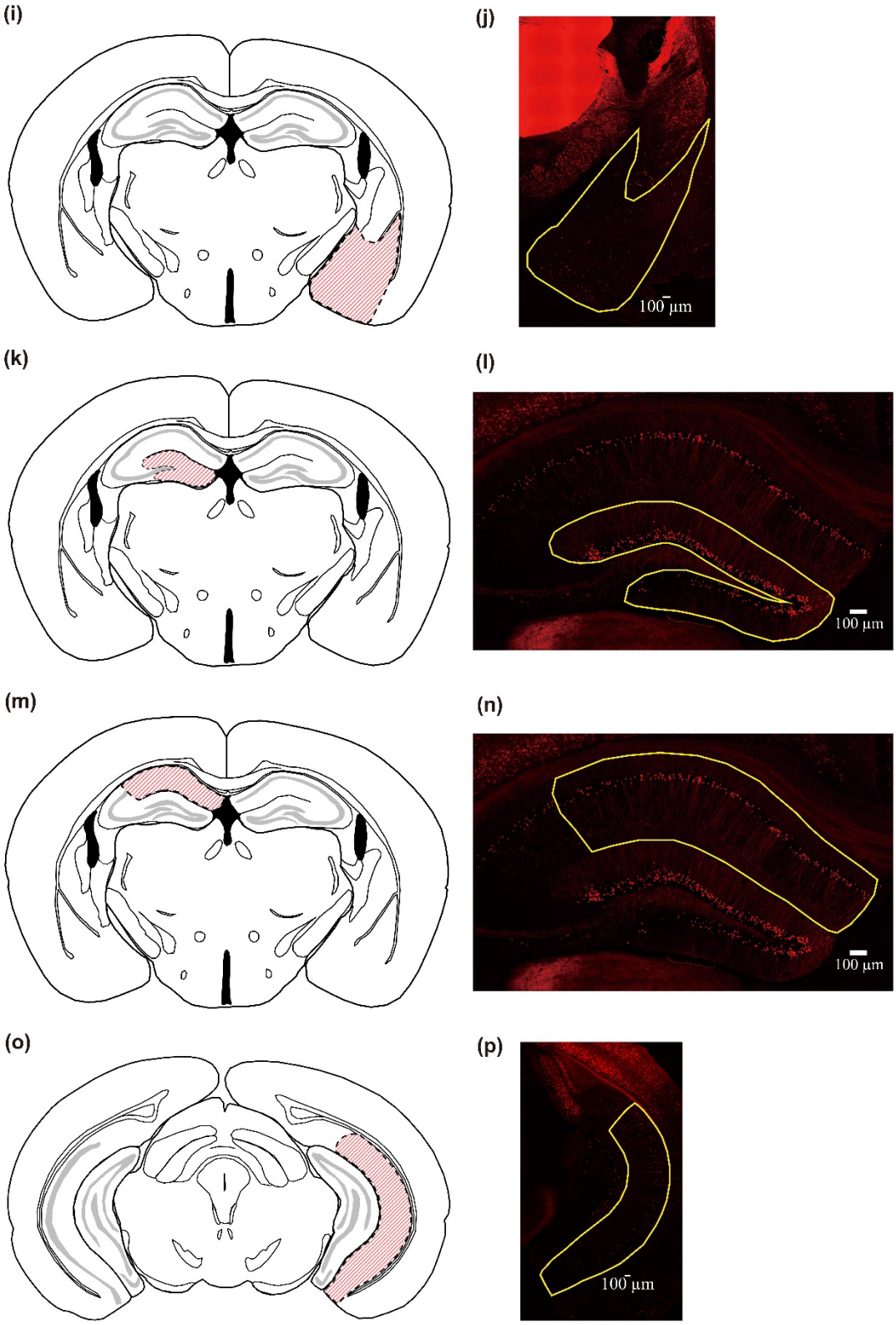
(i)
(j)
100 µm
(k)
(l)
100 µm
(m)
(n)
100 µm
(o)
(p)
100 µm

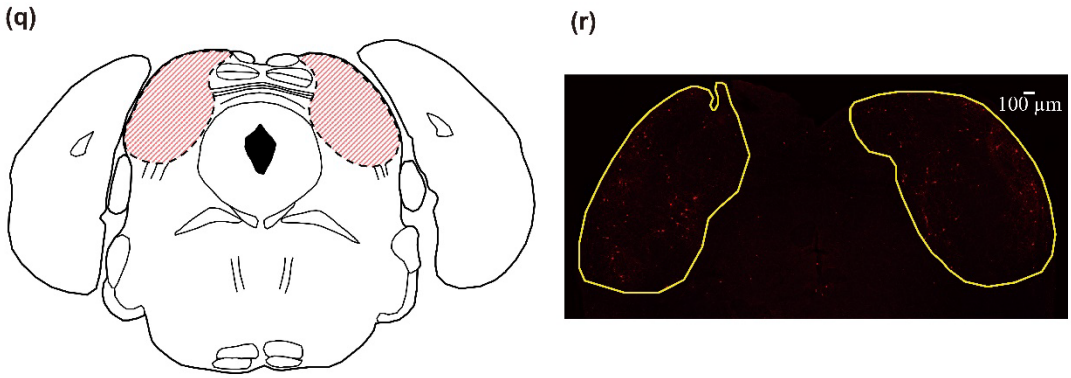

Figure 18. Examples of areas where the number of neurons was counted.

The left side of the figure presents shaded images of brain regions where neurons were counted, while the right side presents examples of brain regions where neurons were actually counted. All section images are from the same one mouse in the control group.

(a) (b) The ACC, (c) (d) the somatosensory cortex layers II/III, (e) (f) septal nucleus and (g) (h) the striatum were sectioned near Bregma 0.62mm; (i) (j) the amygdala, (k) (l) the dorsal DG and (m) (n) the dorsal hippocampus CA1 were sectioned near Bregma -1.82mm; (o) (p) the ventral hippocampus CA1 was sectioned near Bregma -3.40mm; and (q) (r) the inferior colliculus was sectioned near Bregma -4.84mm.

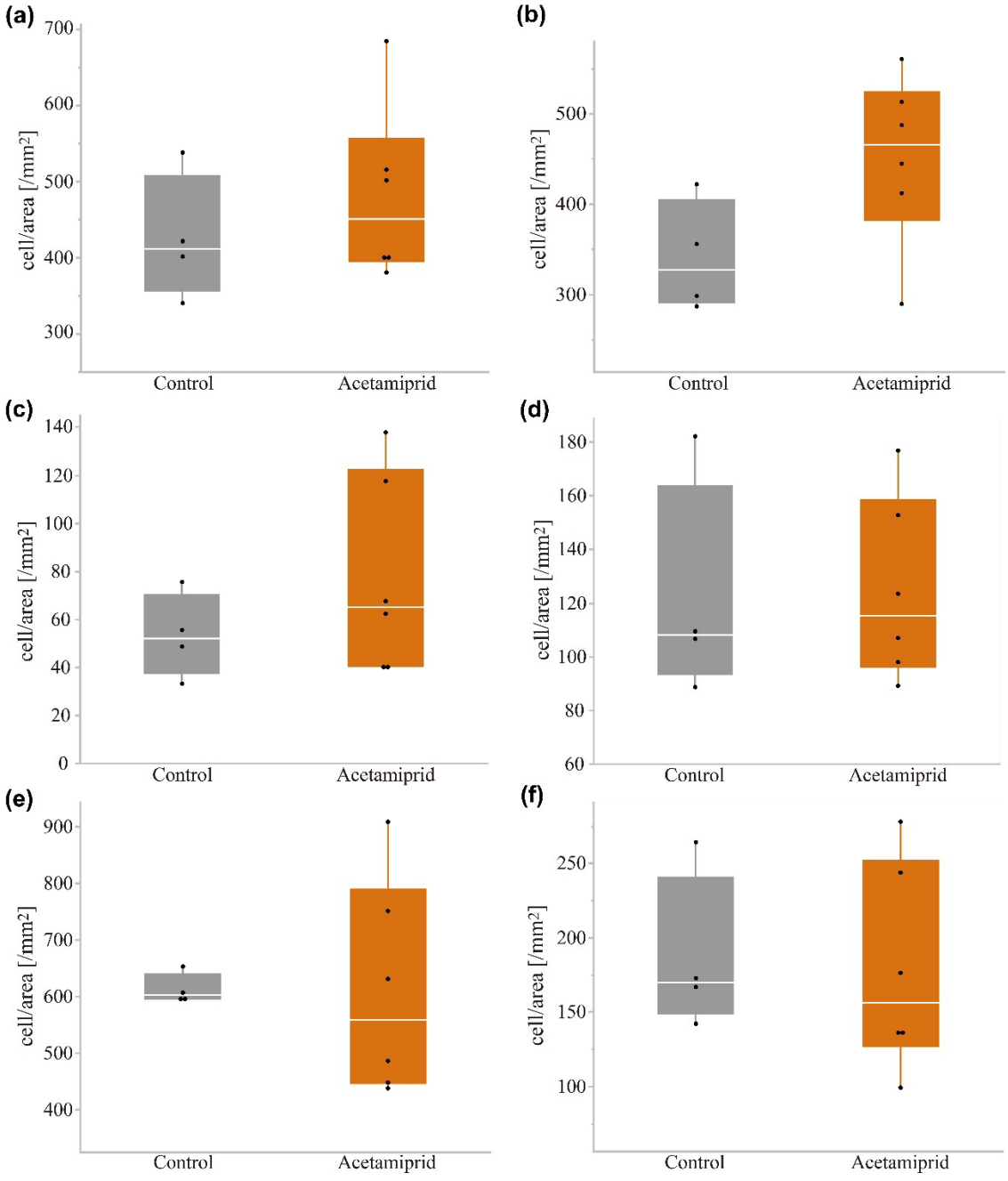
(a)
cell/area [/mm²]
700
600
500
400
300
Control
Acetamiprid
(b)
cell/area [/mm²]
500
400
300
Control
Acetamiprid
(c)
cell/area [/mm²]
140
120
100
80
60
40
20
0
Control
Acetamiprid
(d)
cell/area [/mm²]
180
160
140
120
100
80
60
Control
Acetamiprid
(e)
cell/area [/mm²]
900
800
700
600
500
400
Control
Acetamiprid
(f)
cell/area [/mm²]
250
200
150
100
Control
Acetamiprid

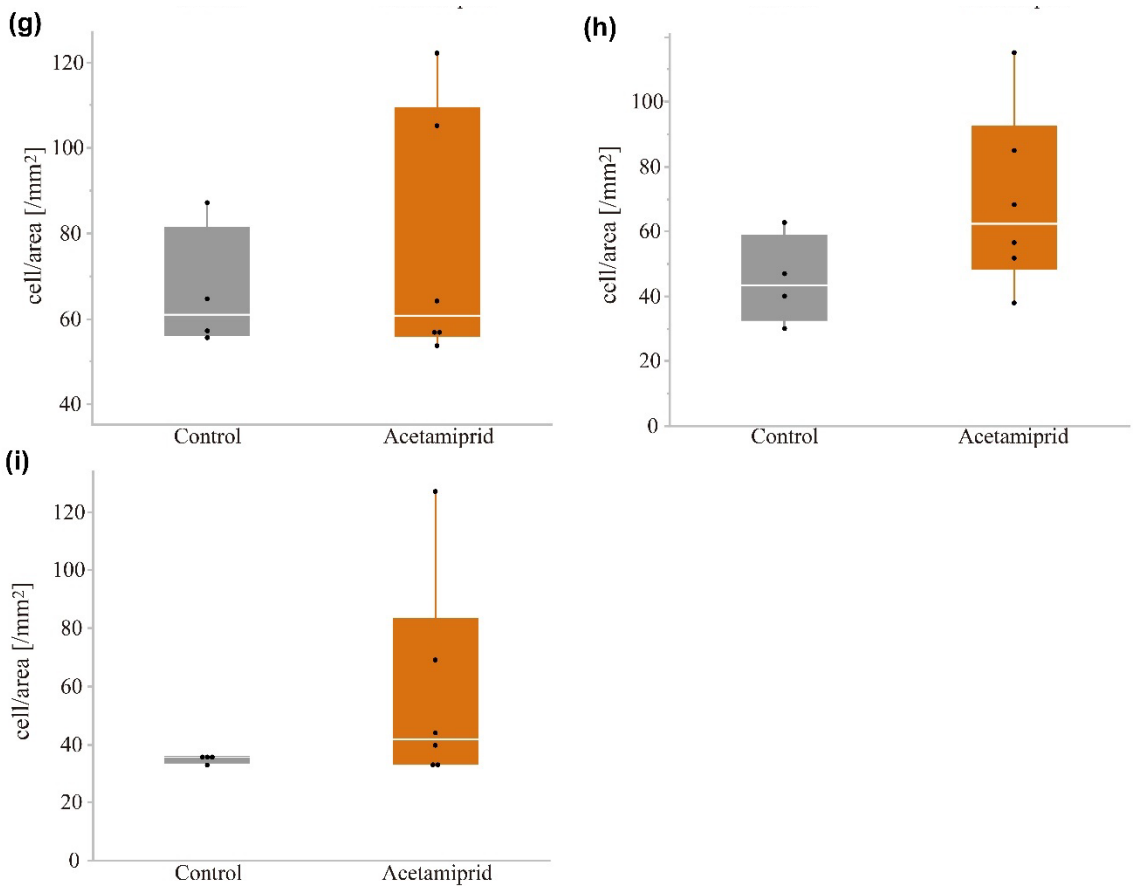

Figure 19. The number of tdTomato expressing neurons per area in each brain region. The neurons expressing tdTomato tended to increase in the (b) somatosensory cortex layers II/III, (c) septal nucleus, (h) amygdala and (i) inferior colliculi ($P = 0.0756$, 0.3006, 0.1480 and 0.3524, respectively). There was no significant change in the (a) ACC, (d) striatum, (e) DG, (f) dorsal hippocampus CA1 and (g) ventral hippocampus CA1.

In each box-and-whisker plot, the box itself indicates the range from the 25th to the 75th percentile, and the white line in the center represents the median data value. The whiskers extend from the edge of the box to 1.5 times the interquartile range, or the minimum or maximum data value (control: $n = 4$, ACE: $n = 6$).

Table 12. The area of the brain regions and the number of neurons expressing tdTomato. All values are presented as mean ± SEM of each group (control: $n = 4$, ACE: $n = 6$).

Brain region		Area [mm^2]	Number of neurons
ACC	control	0.855 ± 0.023	366 ± 44.3
	ACE	0.845 ± 0.029	406 ± 41.0
somatosensory cortex layers II/III	control	0.415 ± 0.038	141 ± 14.9
	ACE	0.487 ± 0.034	222 ± 28.7
septal nucleus	control	2.46 ± 0.14	128 ± 14.9
	ACE	2.02 ± 0.13	150 ± 26.1
striatum	control	3.85 ± 0.55	447 ± 51.0
	ACE	3.46 ± 0.22	427 ± 46.4
DG	control	0.657 ± 0.019	403 ± 13.1
	ACE	0.634 ± 0.021	389 ± 54.2
dorsal hippocampus CA1	control	1.01 ± 0.046	186 ± 19.1
	ACE	0.935 ± 0.043	169 ± 30.9
ventral hippocampus CA1	control	2.73 ± 0.070	180 ± 18.5
	ACE	2.43 ± 0.086	189 ± 34.9
amygdala	control	2.60 ± 0.13	115 ± 14.7
	ACE	2.29 ± 0.12	162 ± 31.4
inferior colliculi	control	1.92 ± 0.19	67 ± 8.14
	ACE	2.03 ± 0.057	116 ± 29.3

Conclusions

In summary, the administration of NNs at NOAEL levels resulted in an increase in anxiety-like behavior, decrease activity, as well as alterations in brain MA concentrations in mice. Notably, ACE administration induced elevated serotonin levels in the hippocampus and dopamine levels in the striatum, both of which showed significant correlations with anxiety-like behavior. This study is the first to demonstrate direct correlations between the effects of NNs on MAs and their impacts on behavior.

Furthermore, the application of *in vivo* Ca^{2+} imaging using two-photon microscopy, combined with Arc^{CreER};Ai14 mice, enabled the identification of changes in neural activity in brain regions, such as the somatosensory cortex and amygdala, without histopathological changes. These findings underscore the utility of advanced imaging techniques and transgenic models in elucidating the neurotoxic effects at the mechanistic level.

In this study, ACE was administered in *Chapters 1* and *2-2*, while IMI was administered in *Chapter 2-1*. However, the behavioral and MA effects of these two NNs were found to differ. These variations can be attributed not only to the type of NN administered but also to procedural differences, such as whether mice were subjected to behavioral testing prior to sampling. Consequently, a direct comparison of the results is not applicable. One potential confounding factor contributing to the observed differences in effects may be the distinct agonist activity and affinity of ACE and IMI for nAChRs. For instance, IMI, a weak partial agonist, elicits approximately 20% of the maximal acetylcholine (Ach) current, while ACE, a more potent agonist, produces around 60% (Tan et al., 2007). The α4β2 and α7 subtypes are the most abundant in the mammalian brain (Gotti et al., 2006), and previous studies have reported that IMI act as a partial agonist for both the α4β2 and α7 subtypes (Ihara et al., 2003; Li, P et al., 2011). In contrast, the function of ACE as a partial agonist for α7 subtype has been demonstrated (Cartereau et al., 2018), but the extent of its agonist activity for the α4β2 subtype in mammals is still lacking. Given the high expression of α4β2 and α7 nAChRs in the hippocampus, which is known to be involved in cognitive function, anxiety, and depression (Arias et al., 2021; Davis et al., 2007; McGranahan et al., 2011; Mineur et al., 2018, 2023; Sabri et al., 2018),

the differential agonist activity of NNs on nAChRs may be one of the factors contributing to the different effects of ACE and IMI observed in this study. Further research is necessary to elucidate the specific interactions of ACE with the α4β2 subtype and to determine their relevance to the observed behavioral and neurochemical outcomes.

As demonstrated in this study and as previously demonstrated by other research, the administration of ACE has been shown to increase hippocampal serotonin and striatal dopamine, both of which are associated with anxiety-like behavior (*Chapter 2-2*). Furthermore, this study revealed that ACE administration enhances serotonin production in the DRN, the primary source of serotonergic projections to forebrain regions, including the hippocampus (*Chapter 2-2*). Nicotine has been observed to activate serotonergic neurons through glutamate release (Garduño et al., 2012), and stimulation of serotonergic neurons in the RN has been reported to increase anxiety-like behavior via enhanced serotonin release in the hippocampus (Abela et al., 2020; Ohmura et al., 2014). Additionally, serotonergic pathways originating from the RN have been demonstrated to dominate dopaminergic pathways (Alex et al., 2007).

In light of these findings, the following pathways are hypothesized to be the primary mechanisms underlying ACE-induced anxiety-like behavior: (i) ACE stimulates α4β2 nAChRs on glutamatergic neurons in the RN, leading to increased glutamate release; (ii) The released glutamate activates post-synaptic serotonergic neurons in the RN; (iii) Serotonergic innervation from the activated RN enhances serotonin release in downstream serotonergic pathways, including the hippocampus, and the released serotonin modulates dopaminergic activity, thereby inducing anxiety-like behavior.

As detailed in *Chapters 3* and *4*, alterations in neural activity were observed in the somatosensory cortex, septal nucleus, amygdala, and inferior colliculus. These regions are also predominantly influenced by serotonergic input from the RN, suggesting that serotonin plays an important role in ACE-induced anxiety-like behavior. However, the function of serotonin in the brain is highly complex. Serotonin receptors are classified into seven families, with the 5-HT1x and 2x families, which are abundantly expressed in the ACC, being particularly implicated in cognition and emotion (Celada et al., 2004; Miranda, 2025). Within these two families, several receptor subtypes exist, which can be further

categorized as autoreceptors or heteroreceptors. These receptor subtypes often co-localize and interact to balance excitatory and inhibitory effects (Santana et al., 2004). While the SSRIs are frequently utilized as a primary treatment for depression, it is important to note that nearly all serotonin receptor subtypes contribute to antidepressant and anxiolytic-like effects. Notably, the 5-HT2C and 5-HT6 subtypes have been shown to induce antidepressant-like effects through both agonist and antagonist mechanisms (Żmudzka et al., 2018). These findings underscore the complexity of serotonergic signaling and the necessity for further investigation into the specific function of each receptor subtype in depression and anxiety. Consequently, further exploration into the distinctions among serotonin receptor subtypes is essential to achieve a more comprehensive understanding of the serotonergic mechanisms underlying ACE-induced anxiety-like behavior. Such insights will enhance our knowledge of the effects of ACE on anxiety and contribute to a more comprehensive understanding of serotonin's role in emotional regulation and psychiatric disorders.

Throughout *Chapters 1-4*, I investigated the correlation between behavioral changes as individual-level effects, alterations in MAs as molecular-level effects, and changes in neural activity as cellular and organ-level effects. By examining findings across multiple levels within the AOP framework, this study proposed a hypothesis for the mechanism by which ACE influences anxiety-like behavior. The findings underscore the necessity of integrating data from multiple levels, rather than relying on observations from a single level, to effectively detect neurotoxicity - particularly in cases involving subtle disruptions, such as those affecting neurotransmitter systems, that occur without observable pathological changes.

Future studies should aim to validate this hypothesis by conducting a more comprehensive examination of alterations within the serotonin system. One proposed approach involves the combination of Arc^{CreER};Ai14 mice with complementary techniques, such as staining and mass spectrometric imaging. This integrative methodological approach would provide a more profound understanding of the molecular and cellular mechanisms underlying ACE-induced anxiety-like behavior and contribute to a more comprehensive understanding of neurotoxic effects.

Acknowledgments

I would like to express my gratitude to the many people who helped me carry out this research, which I conducted in the Laboratory of Toxicology under the supervision of Professor Mayumi Ishizuka during my Ph.D. studies at the Graduate School of Veterinary Medicine, Hokkaido University.

I am very grateful to my supervisors, Professor Mayumi Ishizuka, Professor Yoshinori Ikenaka and Associate Professor Shota M.M. Nakayama (Laboratory of Toxicology, Graduate School of Veterinary Medicine, Hokkaido University), who have guided me throughout the six years since I was an undergraduate student. I was able to complete this research thanks to the advice I received from them from time to time, from planning the research to discussing the results, suggesting ideas and career paths. I would like to continue to devote myself to giving back to future generations what I have received.

I appreciate the precise opinions and guidance of Professor Kenichi Otsuguro (Laboratory of Pharmacology, Graduate School of Veterinary Medicine, Hokkaido University) and Professor Takashi Kimura (Laboratory of Comparative Pathology, Graduate School of Veterinary Medicine, Hokkaido University), who reviewed this thesis from perspectives that I could not have obtained only in my own field of research. I would like to thank them sincerely.

I gratefully acknowledge Associate Professor Chitoku Toda (Faculty of Life Sciences, Kumamoto University) not only for the peer review of this thesis, but also for his great guidance in the research using Arc^{CreER};Ai14 mice. I would like to express my deep appreciation to him for his frequent consultations on experiments after his transfer from Hokkaido University to Kumamoto University.

For the *in vivo* imaging using the two-photon microscope, I greatly thank Professor Hiroaki Wakei (Department of Anatomy and Molecular Cell Biology, Graduate School of Medicine, Nagoya University) for allowing me to use the two-photon microscope and for his advice on the research. I would also like to express my gratitude to Assistant Professor Shota Sugio (Department of Anatomy and Molecular Cell Biology, Graduate School of Medicine, Nagoya University) for his great efforts in taking care of the mice, performing craniotomies, and providing guidance on the techniques.

My undergraduate classmate Ryo Yamazaki, who was from the Laboratory of Comparative Pathology but had done experiments with NNs in the Laboratory of Toxicology like me, gave us many opportunities to discuss together. His knowledge of pathology was also indispensable in helping me to master the sampling of mice. I would like to take this opportunity to thank him.

Dr Akifumi Eguchi (Center for Preventive Medical Sciences, Chiba University), Associate Professor Kei Nomiyama (Center for Marine Environmental Studies, Division of Environmental Chemistry and Ecotoxicology, Ehime University), Professor Emeritus Nobuhiko Hoshi (Laboratory of Animal Molecular Morphology, Graduate School of Agricultural Science, Kobe University), Associate Professor Tetsushi Hirano (Faculty of Pharmaceutical Sciences, University of Toyama) and Associate Professor Shuichi Shimma (Department of Biotechnology, Graduate School of Engineering, Osaka University) have given me advice on many opportunities when presenting at various conferences and publishing papers. I would like to express my deep appreciation to all of them.

I would like to thank everyone in the Department of Toxicology for welcoming me so warmly for almost six years. In particular, I appreciate the technical assistant, Ms. Mai Tamba, who gave me guidance and support for my experiments on many occasions, in addition to her duties. I joined the lab at about the same time, and I consider her to be the person largely responsible for the friendly mood in the lab. Also, Mr. Takahiro Ichise, who was an academic researcher in our laboratory at the time, provided extensive guidance on the basics of LC/MS/MS analysis and laboratory management. In addition, I am grateful to postdoctoral researchers Dr. Nimako Collins and Dr. Yared Beyene Yohannes, academic researchers Dr. Rio Doya and Ms. Satoko Namba, and although they have already graduated from the same graduate school, Dr. Kazuki Takeda, Dr. Mitsuki Kondo, Dr. Kodai Motohira, Dr. Nyei Chan Soe and Dr. So Shinya for their guidance in experiments, advice in seminars and progress meetings, and consultation on the doctoral course. Although I often came to the laboratory late at night, I enjoyed my doctoral course thanks to all the members of the Laboratory of Toxicology who were always helpful and friendly, including many seniors, juniors and staff members who I have not been able to mention here. I would like to take this opportunity to thank them.

I give my deepest thanks and love to my parents who brought me up so far, allowed me to go to university and live alone in a distant place, and supported me, as well as to my late dear dog.

This research was funded by the Hokkaido University School of Veterinary Medicine Wise/Leading Travel and Subsistence Grant, Grant-in-Aid for JSPS Fellows, MEXT Joint Usage/Research Centre - Leading Academia in Marine and Environment Pollution Research (LaMer). Thanks to these financial supports, I was able to focus on my research. I would like to express my appreciation for their support.

Finally, I would like to express my sincerest gratitude to the many animals who have contributed to this research and pray that they may rest in peace. This research would not have been possible without their precious sacrifices, and I will continue to do my best to reduce the number of such sacrifices as much as possible.

References

Abd-Elhakim YM, Mohammed HH, Mohamed WAM. Imidacloprid impacts on neurobehavioral performance, oxidative stress, and apoptotic events in the brain of adolescent and adult rats. J. Agric. Food Chem., 66 (51), 13513–13524, 2018. https://doi.org/10.1021/acs.jafc.8b05793

Abela AR, Browne CJ, Sargin D, Prevot TD, Ji XD, Li Z, Lambe EK, Fletcher PJ. Median raphe serotonin neurons promote anxiety-like behavior via inputs to the dorsal hippocampus. Neuropharmacology, 168 , 107985, 2020. https://doi.org/10.1016/J.NEUROPHARM.2020.107985

Abrams JK, Johnson PL, Hollis JH, Lowry CA. Anatomic and functional topography of the dorsal raphe nucleus. Ann. N. Y. Acad. Sci., 1018 (1), 46–57, 2004. https://doi.org/10.1196/ANNALS.1296.005

Akinola LS, McKiver B, Toma W, Zhu AZX, Tyndale RF, Kumar V, Damaj MI. C57BL/6 substrain differences in pharmacological effects after acute and repeated nicotine administration. Brain Sci., 9 (10)2019. https://doi.org/10.3390/brainsci9100244

Alex KD, Pehek EA. Pharmacologic mechanisms of serotonergic regulation of dopamine neurotransmission. Pharmacol. Ther., 113 (2), 296–320, 2007. https://doi.org/10.1016/J.PHARMTHERA.2006.08.004

Altemus M, Sarvaiya N, Neill Epperson C. Sex differences in anxiety and depression clinical perspectives. Front. Neuroendocrinol., 35 (3), 320–330, 2014. https://doi.org/10.1016/J.YFRNE.2014.05.004

An XL, Zou JX, Wu RY, Ying Y, Tai FD, Zeng SY, Rui J, Xia Z, Liu EQ, Hugh B. Strain and sex differences in anxiety-like and social behaviors in C57BL/6J and BALB/cJ mice. Exp. Anim., 60 (2), 111–123, 2011. https://doi.org/10.1538/EXPANIM.60.111

Anastassiades M, Lehotay SJ, Štajnbaher D, Schenck FJ. Fast and easy multiresidue method employing acetonitrile extraction/partitioning and “dispersive solid-phase extraction” for the determination of pesticide residues in produce. J. AOAC Int., 86 (2), 412–431, 2003. https://doi.org/10.1093/JAOAC/86.2.412

Antón Alvarez X, Franco A, Fernández-Novoa L, Cacabelos R. Blood levels of histamine, IL-1β, and TNF-α in patients with mild to moderate Alzheimer disease. Mol. Chem. Neuropathol., 29 (2–3), 237–252, 1996. https://doi.org/10.1007/bf02815005

Arias HR, Targowska-Duda KM, García-Colunga J, Ortells MO. Is the antidepressant activity of selective serotonin reuptake inhibitors mediated by nicotinic acetylcholine receptors? Mol. 2021, Vol. 26, Page 2149, 26 (8), 2149, 2021. https://doi.org/10.3390/MOLECULES26082149

Arroyo S, Bennett C, Hestrin S. Nicotinic modulation of cortical circuits. Front. Neural Circuits, 8 (MAR), 30, 2014. https://doi.org/10.3389/fncir.2014.00030

Asan E, Steinke M, Lesch K-P, Asan E, Steinke ÁM, Steinke M, Lesch K-P. Serotonergic innervation of the amygdala: targets, receptors, and implications for stress and anxiety. Histochem. Cell Biol. 2013 1396, 139 (6), 785–813, 2013. https://doi.org/10.1007/S00418-013-1081-1

Bal-Price A, Meek ME (Bette. Adverse outcome pathways: Application to enhance mechanistic understanding of neurotoxicity. Pharmacol. Ther., 179 , 84–95, 2017. https://doi.org/10.1016/J.PHARMTHERA.2017.05.006

Bannerman DM, Rawlins JNP, McHugh SB, Deacon RMJ, Yee BK, Bast T, Zhang WN, Pothuizen HHJ, Feldon J. Regional dissociations within the hippocampus—memory and anxiety. Neurosci. Biobehav. Rev., 28 (3), 273–283, 2004. https://doi.org/10.1016/J.NEUBIOREV.2004.03.004

Bass C, Denholm I, Williamson MS, Nauen R. The global status of insect resistance to neonicotinoid insecticides. Pestic. Biochem. Physiol., 121 , 78–87, 2015. https://doi.org/10.1016/J.PESTBP.2015.04.004

Bayer CropScience K.K. Imidacloprid pesticide abstracts (in Japanese). 2017. https://www.acis.famic.go.jp/syouroku/imidacloprid/index.htm

Bhardwaj S, Srivastava MK, Kapoor U, Srivastava LP. A 90 days oral toxicity of imidacloprid in female rats: Morphological, biochemical and histopathological evaluations. Food Chem. Toxicol., 48 (5), 1185–1190, 2010. https://doi.org/10.1016/j.fct.2010.02.009

Biala G, Budzynska B. Effects of acute and chronic nicotine on elevated plus maze in mice: Involvement of calcium channels. Life Sci., 79 (1), 81–88, 2006. https://doi.org/10.1016/j.lfs.2005.12.043

Blanchard DC, Griebel G, Blanchard RJ. The mouse defense test battery: pharmacological and behavioral assays for anxiety and panic. Eur. J. Pharmacol., 463 (1–3), 97–116, 2003. https://doi.org/10.1016/S0014-2999(03)01276-7

Börchers S, Krieger JP, Asker M, Maric I, Skibicka KP. Commonly-used rodent tests of anxiety-like behavior lack predictive validity for human sex differences. Psychoneuroendocrinology, 141 , 105733, 2022. https://doi.org/10.1016/J.PSYNEUEN.2022.105733

Borich MR, Brodie SM, Gray WA, Ionta S, Boyd LA. Understanding the role of the primary somatosensory cortex: Opportunities for rehabilitation. Neuropsychologia, 79 , 246–255, 2015. https://doi.org/10.1016/j.neuropsychologia.2015.07.007

Bouwknecht JA, Spiga F, Staub DR, Hale MW, Shekhar A, Lowry CA. Differential effects of exposure to low-light or high-light open-field on anxiety-related behaviors: Relationship to c-Fos expression in serotonergic and non-serotonergic neurons in the dorsal raphe nucleus. Brain Res. Bull., 72 (1), 32–43, 2007. https://doi.org/10.1016/J.BRAINRESBULL.2006.12.009

Braun LD, Cornford EM, Oldendorf WH. Newborn rabbit blood–brain barrier is selectively permeable and differs substantially from the adult. J. Neurochem., 34 (1), 147–152, 1980. https://doi.org/10.1111/J.1471-4159.1980.TB04633.X

Bruhwyler J. Anxiolytic potential of a microgram dose of chlordiazepoxide in the open-field test. Eur. J. Pharmacol., 187 (3), 547–549, 1990. https://doi.org/10.1016/0014-2999(90)90385-J

Burwick T. The binding problem. Wiley Interdiscip. Rev. Cogn. Sci., 5 (3), 305–315, 2014. https://doi.org/10.1002/wcs.1279

Buzsáki G, Watson BO. Brain rhythms and neural syntax: Implications for efficient coding of cognitive content and neuropsychiatric disease. Dialogues Clin. Neurosci., 14 (4), 345–367, 2012. https://doi.org/10.31887/dcns.2012.14.4/gbuzsaki

Cachope R, Cheer JF. Local control of striatal dopamine release. Front. Behav. Neurosci., 8 (MAY), 1–7, 2014. https://doi.org/10.3389/fnbeh.2014.00188

Calafat AM, Ye X, Silva MJ, Kuklenyik Z, Needham LL, Kolossa M, Tuomisto J, Astrup Jensen A. Human exposure assessment to environmental chemicals using biomonitoring. Int. J. Androl., 29 (1), 166–171, 2006. https://doi.org/10.1111/J.1365-2605.2005.00570.X

Cartereau A, Martin C, Thany SH. Neonicotinoid insecticides differently modulate acetycholine-induced currents on mammalian α7 nicotinic acetylcholine receptors. Br. J. Pharmacol., 175 (11), 1987–1998, 2018. https://doi.org/10.1111/bph.14018

Castilho VM, Avanzi V, Brandão ML. Antinociception elicited by aversive stimulation of the inferior colliculus. Pharmacol. Biochem. Behav., 62 (3), 425–431, 1999. https://doi.org/10.1016/S0091-3057(98)00197-X

Celada P, Puig ; M Victoria, Amargós-Bosch M, Adell A, Artigas F. The therapeutic role of 5-HT 1A and 5-HT 2A receptors in depression. Rev Psychiatr Neurosci, 29 (4)2004.

Chen T-W, Wardill TJ, Sun Y, Pulver SR, Renninger SL, Baohan A, Schreiter ER, Kerr RA, Orger MB, Jayaraman V, Looger LL, Svoboda K, Kim DS. Ultrasensitive fluorescent proteins for imaging neuronal activity. Nat. 2013 4997458, 499 (7458), 295–300, 2013. https://doi.org/10.1038/nature12354

Cho H, Seo JH, Wong KHK, Terasaki Y, Park J, Bong K, Arai K, Lo EH, Irimia D. Three-dimensional blood-brain barrier model for in vitro studies of neurovascular pathology. Sci. Reports 2015 51, 5 (1), 15222, 2015. https://doi.org/10.1038/srep15222

Claudio L, Kwa WC, Russell AL, Wallinga D. Testing methods for developmental neurotoxicity of environmental chemicals. Toxicol. Appl. Pharmacol., 164 (1), 1–14, 2000. https://doi.org/10.1006/taap.2000.8890

Coelho MH, Silva IJ, Azevedo MS, Manso CF. Decrease in blood histamine in drug-treated Parkinsonian patients. Mol. Chem. Neuropathol. 1991 142, 14 (2), 77–85, 1991. https://doi.org/10.1007/BF03159928

Costa LG, Guizzetti M, Lu H, Bordi F, Vitalone A, Tita B, Palmery M, Valeri P, Silvestrini B. Intracellular signal transduction pathways as targets for neurotoxicants. Toxicology, 160 (1–3), 19–26, 2001. https://doi.org/10.1016/S0300-483X(00)00435-2

da Silva Soares R, Falconi-Sobrinho LL, dos Anjos-Garcia T, Coimbra NC. 5-Hydroxytryptamine 2A receptors of the dorsal raphe nucleus modulate panic-like behaviours and mediate fear-induced antinociception elicited by neuronal activation in the central nucleus of the inferior colliculus. Behav. Brain Res., 357–358 , 71–81, 2019. https://doi.org/10.1016/J.BBR.2017.07.016

Dailly E, Chenu F, Renard CE, Bourin M. Dopamine, depression and antidepressants. Fundam. Clin. Pharmacol., 18 (6), 601–607, 2004. https://doi.org/10.1111/J.1472-8206.2004.00287.X

Davis JA, Kenney JW, Gould TJ. Hippocampal α4β2 nicotinic acetylcholine receptor involvement in the enhancing effect of acute nicotine on contextual fear conditioning. J. Neurosci., 27 (40), 10870–10877, 2007. https://doi.org/10.1523/JNEUROSCI.3242-07.2007

de Oliveira IM, Nunes BVF, Barbosa DR, Pallares AM, Faro LRF. Effects of the neonicotinoids thiametoxam and clothianidin on in vivo dopamine release in rat striatum. Toxicol. Lett., 192 (3), 294–297, 2010. https://doi.org/10.1016/J.TOXLET.2009.11.005

Degroot A, Treit D. Dorsal and ventral hippocampal cholinergic systems modulate anxiety in the plus-maze and shock-probe tests. Brain Res., 949 (1–2), 60–70, 2002. https://doi.org/10.1016/S0006-8993(02)02965-7

Djemil S, Chen X, Zhang Z, Lee J, Rauf M, Pak DTS, Dzakpasu R. Activation of nicotinic acetylcholine receptors induces potentiation and synchronization within in vitro hippocampal networks. J. Neurochem., 153 (4), 468–484, 2020. https://doi.org/10.1111/jnc.14938

Doty RL. Olfaction in Parkinson's disease and related disorders. Neurobiol. Dis., 46 (3), 527–552, 2012. https://doi.org/10.1016/j.nbd.2011.10.026

Erro R, Pappatà S, Amboni M, Vicidomini C, Longo K, Santangelo G, Picillo M, Vitale C, Moccia M, Giordano F, Brunetti A, Pellecchia MT, Salvatore M, Barone P. Anxiety is associated with striatal dopamine transporter availability in newly diagnosed untreated Parkinson's disease patients. Parkinsonism Relat. Disord., 18 (9), 1034–1038, 2012. https://doi.org/10.1016/J.PARKRELDIS.2012.05.022

Esteve C, Tolner EA, Shyti R, van den Maagdenberg AMJM, McDonnell LA. Mass spectrometry imaging of amino neurotransmitters: a comparison of derivatization methods and application in mouse brain tissue. Metabolomics, 12 (2), 1–9, 2016. https://doi.org/10.1007/s11306-015-0926-0

European Food Safety Authority. Scientific opinion on the developmental neurotoxicity potential of acetamiprid and imidacloprid. EFSA J., 11 (12)2013. https://doi.org/10.2903/j.efsa.2013.3471

European Food Safety Authority. Peer review of the pesticide risk assessment of the active substance acetamiprid. EFSA J., 14 (11)2016. https://doi.org/10.2903/j.efsa.2016.4610

Faro LRF, Tak-Kim H, Alfonso M, Durán R. Clothianidin, a neonicotinoid insecticide, activates α4β2, α7 and muscarinic receptors to induce in vivo dopamine release from rat striatum. Toxicology, 426 , 152285, 2019. https://doi.org/10.1016/j.tox.2019.152285

Felker A, Nieuwenhuize S, Dolbois A, Blazkova K, Hess C, Low LWL, Burger S, Samson N, Carney TJ, Bartunek P, Nevado C, Mosimann C. In vivo performance and properties of tamoxifen metabolites for CreERT2 control. PLOS ONE, 11 (4), e0152989, 2016. https://doi.org/10.1371/JOURNAL.PONE.0152989

Fernández-Novoa L, Cacabelos R. Histamine function in brain disorders. Behav. Brain Res., 124 (2), 213–233, 2001. https://doi.org/10.1016/S0166-4328(01)00215-7

Flace P, Livrea P, Basile GA, Galletta D, Bizzoca A, Gennarini G, Bertino S, Branca JJV, Gulisano M, Bianconi S, Bramanti A, Anastasi G. The cerebellar dopaminergic system. Front. Syst. Neurosci., 15 , 650614, 2021. https://doi.org/10.3389/FNSYS.2021.650614/BIBTEX

Food Safety Commission. Pesticide evaluation report acetamiprid (3rd edition) (in Japanese). 2014.

Ford KA, Casida JE. Chloropyridinyl neonicotinoid insecticides: Diverse molecular substituents contribute to facile metabolism in mice. Chem. Res. Toxicol., 19 (7), 944–951, 2006. https://doi.org/10.1021/tx0600696

Freire C, Koifman S. Pesticide exposure and Parkinson's disease: Epidemiological evidence of association. Neurotoxicology, 33 (5), 947–971, 2012. https://doi.org/10.1016/J.NEURO.2012.05.011

Garduño J, Galindo-Charles L, Jiménez-Rodríguez J, Galarraga E, Tapia D, Mihailescu S, Hernandez-Lopez S. Presynaptic α4β2 nicotinic acetylcholine receptors increase glutamate release and serotonin neuron excitability in the dorsal raphe nucleus. J. Neurosci., 32 (43), 15148–15157, 2012. https://doi.org/10.1523/JNEUROSCI.0941-12.2012

Gholipoor P, Saboory E, Roshan-Milani S, Fereidoni J. Effect of hyperthermia on histamine blood level and convulsive behavior in infant rats. Epilepsy Behav., 29 (2), 269–274, 2013. https://doi.org/10.1016/J.YEBEH.2013.07.026

González RR, Fernández RF, Vidal JLM, Frenich AG, Pérez MLG. Development and validation of an ultra-high performance liquid chromatography-tandem mass-spectrometry (UHPLC-MS/MS) method for the simultaneous determination of neurotransmitters in rat brain samples. J. Neurosci. Methods, 198 (2), 187–194, 2011. https://doi.org/10.1016/j.jneumeth.2011.03.023

Gotti C, Zoli M, Clementi F. Brain nicotinic acetylcholine receptors: Native subtypes and their relevance. In Trends Pharmacol. Sci.2006. https://doi.org/10.1016/j.tips.2006.07.004

Gray CM. Synchronous oscillations in neuronal systems: Mechanisms and functions. J. Comput. Neurosci., 1 (1–2), 11–38, 1994. https://doi.org/10.1007/BF00962716

Guenthner CJ, Miyamichi K, Yang HH, Heller HC, Luo L. Permanent genetic access to transiently active neurons via TRAP: Targeted recombination in active populations. Neuron, 78 (5), 773–784, 2013. https://doi.org/10.1016/J.NEURON.2013.03.025/ATTACHMENT/A3903006-5A28-447E-8D0E-FCB0168AE8D5/MMC1.PDF

Haas HL, Sergeeva OA, Selbach O. Histamine in the nervous system. Physiol. Rev., 88 (3), 1183–1241, 2008. https://doi.org/10.1152/PHYSREV.00043.2007/ASSET/IMAGES/LARGE/Z9J0030824830021.JPEG

Hagino Y, Kasai S, Fujita M, Setogawa S, Yamaura H, Yanagihara D, Hashimoto M, Kobayashi K, Meltzer HY, Ikeda K. Involvement of cholinergic system in hyperactivity in dopamine-deficient mice. Neuropsychopharmacology, 40 (5), 1141–1150, 2015. https://doi.org/10.1038/npp.2014.295

Hamon M, Blier P. Monoamine neurocircuitry in depression and strategies for new treatments. Prog. Neuro-Psychopharmacology Biol. Psychiatry, 45 , 54–63, 2013. https://doi.org/10.1016/J.PNPBP.2013.04.009

Hao S, Shi W, Liu W, Chen QY, Zhuo M. Multiple modulatory roles of serotonin in chronic pain and injury-related anxiety. Front. Synaptic Neurosci., 15 , 1122381, 2023. https://doi.org/10.3389/FNSYN.2023.1122381/BIBTEX

He YC, Wu GY, Li D, Tang B, Li B, Ding Y, Zhu JN, Wang JJ. Histamine promotes rat motor performances by activation of H2 receptors in the cerebellar fastigial nucleus. Behav. Brain Res., 228 (1), 44–52, 2012. https://doi.org/10.1016/J.BBR.2011.11.029

Hirano T, Miyata Y, Kubo S, Ohno S, Onaru K, Maeda M, Kitauchi S, Nishi M, Tabuchi Y, Ikenaka Y, Ichise T, Nakayama SMM, Ishizuka M, Arizono K, Takahashi K, Kato K, Mantani Y, Yokoyama T, Hoshi N. Aging-related changes in the sensitivity of behavioral effects of the neonicotinoid pesticide clothianidin in male mice. Toxicol. Lett., 342 , 95–103, 2021. https://doi.org/10.1016/J.TOXLET.2021.02.010

Hirano T, Yanai S, Takada T, Yoneda N, Omotehara T, Kubota N, Minami K, Yamamoto A, Mantani Y, Yokoyama T, Kitagawa H, Hoshi N. NOAEL-dose of a neonicotinoid pesticide, clothianidin, acutely induce anxiety-related behavior with human-audible vocalizations in male mice in a novel environment. Toxicol. Lett., 282 , 57–63, 2018. https://doi.org/10.1016/j.toxlet.2017.10.010

Höglinger GU, Alvarez-Fischer D, Arias-Carrión O, Djufri M, Windolph A, Keber U, Borta A, Ries V, Schwarting RKW, Scheller D, Oertel WH. A new dopaminergic nigro-olfactory projection. Acta Neuropathol., 130 (3), 333–348, 2015. https://doi.org/10.1007/s00401-015-1451-y

Houchat JN, Cartereau A, Le Mauff A, Taillebois E, Thany SH. An overview on the effect of neonicotinoid insecticides on mammalian cholinergic functions through the activation of neuronal nicotinic acetylcholine receptors. In Int. J. Environ. Res. Public Health2020. https://doi.org/10.3390/ijerph17093222

Hritcu L, Clicinschi M, Nabeshima T. Brain serotonin depletion impairs short-term memory, but not long-term memory in rats. Physiol. Behav., 91 (5), 652–657, 2007. https://doi.org/10.1016/j.physbeh.2007.03.028

Huang F, Li J, Shi H lian, Wang T ting, Muhtar W, Du M, Zhang B bei, Wu H, Yang L, Hu Z bi, Wu X jun. Simultaneous quantification of seven hippocampal neurotransmitters in depression mice by LC-MS/MS. J. Neurosci. Methods, 229 , 8–14, 2014. https://doi.org/10.1016/j.jneumeth.2014.04.004

Hurley LM, Thompson AM, Pollak GD. Serotonin in the inferior colliculus. Hear. Res., 168 (1–2), 1–11, 2002. https://doi.org/10.1016/S0378-5955(02)00365-9

Ichikawa G, Kuribayashi R, Ikenaka Y, Ichise T, Nakayama SMM, Ishizuka M, Taira K, Fujioka K, Sairenchi T, Kobashi G, Bonmatin JM, Yoshihara S. LC-ESI/MS/MS analysis of neonicotinoids in urine of very low birth weight infants at birth. PLOS ONE, 14 (7), e0219208, 2019. https://doi.org/10.1371/journal.pone.0219208

Ihara M, Matsuda K, Otake M, Kuwamura M, Shimomura M, Komai K, Akamatsu M, Raymond V, Sattelle DB. Diverse actions of neonicotinoids on chicken α7, α4β2 and Drosophila–chicken SADβ2 and ALSβ2 hybrid nicotinic acetylcholine receptors expressed in Xenopus laevis oocytes. Neuropharmacology, 45 (1), 133–144, 2003. https://doi.org/10.1016/S0028-3908(03)00134-5

Ikenaka Y, Miyabara Y, Ichise T, Nakayama S, Nimako C, Ishizuka M, Tohyama C. Exposures of children to neonicotinoids in pine wilt disease control areas. Environ. Toxicol. Chem., 38 (1), 71–79, 2019. https://doi.org/10.1002/etc.4316

Ioka E. Synchronous firing. J. Japan Soc. Fuzzy Theory Intell. Informatics, 26 (3), 113–113, 2014. https://doi.org/10.3156/jsoft.26.3_113_1

Ishikawa T, Murata K, Okuda H, Potapenko I, Hori K, Furuyama T, Yamamoto R, Ono M, Kato N, Fukazawa Y, Ozaki N. Pain-related neuronal ensembles in the primary somatosensory cortex contribute to hyperalgesia and anxiety. IScience, 26 (4)2023. https://doi.org/10.1016/j.isci.2023.106332

Ito C. The role of brain histamine in acute and chronic stresses. Biomed. Pharmacother., 54 (5), 263–267, 2000. https://doi.org/10.1016/S0753-3322(00)80069-4

Jeschke P, Nauen R, Schindler M, Elbert A. Overview of the status and global strategy for neonicotinoids. J. Agric. Food Chem., 59 (7), 2897–2908, 2011. https://doi.org/10.1021/jf101303g

Jiang X, Xing G, Yang C, Verma A, Zhang L, Li H. Stress impairs 5-HT2A receptor-mediated serotonergic facilitation of GABA release in juvenile rat basolateral amygdala. Neuropsychopharmacol. 2009 342, 34 (2), 410–423, 2008. https://doi.org/10.1038/npp.2008.71

Jones N, King SM. Influence of circadian phase and test illumination on pre-clinical models of anxiety. Physiol. Behav., 72 (1–2), 99–106, 2001. https://doi.org/10.1016/S0031-9384(00)00388-7

Kagawa N, Nagao T. Neurodevelopmental toxicity in the mouse neocortex following prenatal exposure to acetamiprid. J. Appl. Toxicol., 38 (12), 1521–1528, 2018. https://doi.org/10.1002/jat.3692

Kanno J. Introduction to the concept of signal toxicity. J. Toxicol. Sci., 41 (Special Issue), SP105–SP109, 2016. https://doi.org/10.2131/jts.41.SP105

Kenny PJ, Cheeta S, E. File S. Anxiogenic effects of nicotine in the dorsal hippocampus are mediated by 5-HT1A and not by muscarinic M1 receptors. Neuropharmacology, 39 (2), 300–307, 2000. https://doi.org/10.1016/S0028-3908(99)00114-8

Khidkhan K, Ikenaka Y, Ichise T, Nakayama SMM, Mizukawa H, Nomiyama K, Iwata H, Arizono K, Takahashi K, Kato K, Ishizuka M. Interspecies differences in cytochrome P450-mediated metabolism of neonicotinoids among cats, dogs, rats, and humans. Comp. Biochem. Physiol. C Toxicol. Pharmacol., 239 , 108898, 2021. https://doi.org/10.1016/j.cbpc.2020.108898

Kim TH, Choi J, Kim HG, Kim HR. Quantification of neurotransmitters in mouse brain tissue by using liquid chromatography coupled electrospray tandem mass spectrometry. J. Anal. Methods Chem., 2014 (Lc)2014. https://doi.org/10.1155/2014/506870

Kimura-Kuroda J, Komuta Y, Kuroda Y, Hayashi M, Kawano H. Nicotine-like effects of the neonicotinoid insecticides acetamiprid and imidacloprid on cerebellar neurons from neonatal rats. PLOS ONE, 7 (2), e32432, 2012. https://doi.org/10.1371/journal.pone.0032432

Klingelhöfer D, Braun M, Brüggmann D, Groneberg DA. Neonicotinoids: A critical assessment of the global research landscape of the most extensively used insecticide. Environ. Res., 213 , 113727, 2022. https://doi.org/10.1016/J.ENVRES.2022.113727

Koukouli F, Rooy M, Tziotis D, Sailor KA, O'Neill HC, Levenga J, Witte M, Nilges M, Changeux JP, Hoeffer CA, Stitzel JA, Gutkin BS, Digregorio DA, Maskos U. Nicotine reverses hypofrontality in animal models of addiction and schizophrenia. Nat. Med., 23 (3), 347–354, 2017. https://doi.org/10.1038/nm.4274

Kubo S, Hirano T, Miyata Y, Ohno S, Onaru K, Ikenaka Y, Nakayama SMM, Ishizuka M, Mantani Y, Yokoyama T, Hoshi N. Sex-specific behavioral effects of acute exposure to the neonicotinoid clothianidin in mice. Toxicol. Appl. Pharmacol., 456 , 116283, 2022. https://doi.org/10.1016/J.TAAP.2022.116283

Landoni JH de. *Nicotine*. 1991. http://www.inchem.org/documents/pims/chemical/nicotine.htm#SubSectionTitle:7.2.2 Relevant animal data

Lansdell SJ, Millar NS. The influence of nicotinic receptor subunit composition upon agonist, α-bungarotoxin and insecticide (imidacloprid) binding affinity. Neuropharmacology, 39 (4), 671–679, 2000. https://doi.org/10.1016/S0028-3908(99)00170-7

LeDoux J. The amygdala. Curr. Biol., 17 (20), R868–R874, 2007. https://doi.org/10.1016/j.cub.2007.08.005

Lehotay SJ, O'Neil M, Tully J, García AV, Contreras M, Mol H, Heinke V, Anspach T, Lach G, Fussell R, Mastovska K, Poulsen ME, Brown A, Hammack W, Cook JM, Alder L, Lindtner K, Vila MG, Hopper M, … Parker A. Determination of pesticide residues in foods by acetonitrile extraction and partitioning with magnesium sulfate: Collaborative study. J. AOAC Int., 90 (2), 485–520, 2007. https://doi.org/10.1093/JAOAC/90.2.485

Li D, Zhang H, Chang M, Shen K, Zhang N, Zhu K, Zhou Z, Zhang W, Wang Q, Liu X, Zhang W. Neonicotinoid insecticide and their metabolite residues in fruit juices: Implications for dietary intake in China. Chemosphere, 261 , 127682, 2020. https://doi.org/10.1016/J.CHEMOSPHERE.2020.127682

Li P, Ann J, Akk G. Activation and modulation of human α4β2 nicotinic acetylcholine receptors by the neonicotinoids clothianidin and imidacloprid. J. Neurosci. Res., 89 (8), 1295–1301, 2011. https://doi.org/10.1002/JNR.22644

Liu R xia, Xian Y yan, Liu S, Yu F, Mu H jie, Sun K xiang, Liu W hui. Development, validation and comparison of surrogate matrix and surrogate analyte approaches with UHPLC–MS/MS to simultaneously quantify dopamine, serotonin and γ-aminobutyric acid in four rat brain regions. Biomed. Chromatogr., 32 (9), 1–10, 2018. https://doi.org/10.1002/bmc.4276

Liu X, Wang X, Xu J, Dong F, Song W, Zheng Y. Determination of tebuconazole, trifloxystrobin and its metabolite in fruit and vegetables by a Quick, Easy, Cheap, Effective, Rugged and Safe (QuEChERS) method using gas chromatography with a nitrogen–phosphorus detector and ion trap mass spectrometry. Biomed. Chromatogr., 25 (10), 1081–1090, 2011. https://doi.org/10.1002/BMC.1575

Lonare M, Kumar M, Raut S, Badgujar P, Doltade S, Telang A. Evaluation of imidacloprid-induced neurotoxicity in male rats: A protective effect of curcumin. Neurochem. Int., 78 , 122–129, 2014. https://doi.org/10.1016/j.neuint.2014.09.004

Lucki I. The spectrum of behaviors influenced by serotonin. Biol. Psychiatry, 44 (3), 151–162, 1998. https://doi.org/10.1016/S0006-3223(98)00139-5

Ly TK, Behra P, Nhu-Trang TT. Quantification of 397 pesticide residues in different types of commercial teas: Validation of high accuracy methods and quality assessment. Food Chem., 370 , 130986, 2022. https://doi.org/10.1016/J.FOODCHEM.2021.130986

Lyford GL, Yamagata K, Kaufmann WE, Barnes CA, Sanders LK, Copeland NG, Gilbert DJ, Jenkins NA, Lanahan AA, Worley PF. Arc, a growth factor and activity-regulated gene, encodes a novel cytoskeleton-associated protein that is enriched in neuronal dendrites. Neuron, 14 , 433–445, 1995.

Ma QP, Yin GF, Ai MK, Han JS. Serotonergic projections from the nucleus raphe dorsalis to the amygdala in the rat. Neurosci. Lett., 134 (1), 21–24, 1991. https://doi.org/10.1016/0304-3940(91)90499-J

Mabrouk OS, Li Q, Song P, Kennedy RT. Microdialysis and mass spectrometric monitoring of dopamine and enkephalins in the globus pallidus reveal reciprocal

interactions that regulate movement. J. Neurochem., 118 (1), 24–33, 2011. https://doi.org/10.1111/j.1471-4159.2011.07293.x

Maeda N, Sato M, Haeno S, Yokota H. Simultaneous determination of the neurotransmitters and free amino acids in rat organs by LC-MS analysis. Sci. J. Grad. Sch. Rakuno Gakuen Univ., 2016/March , 1–7, 2016.

Masamizu Y, Tanaka YR, Tanaka YH, Hira R, Ohkubo F, Kitamura K, Isomura Y, Okada T, Matsuzaki M. Two distinct layer-specific dynamics of cortical ensembles during learning of a motor task. Nat. Neurosci., 17 (7), 987–994, 2014. https://doi.org/10.1038/nn.3739

Matsuda K, Buckingham SD, Kleier D, Rauh JJ, Grauso M, Sattelle DB, Buckingham SD. Neonicotinoids: insecticides actingon insect nicotinic acetylcholinereceptors. Trends Pharmacol. Sci., 22 (11), 573–580, 2001.

Matsuda K, Ihara M, Sattelle DB. Neonicotinoid insecticides: Molecular targets, resistance, and toxicity. Annu. Rev. Pharmacol. Toxicol., 60 (1), 241–255, 2020. https://doi.org/10.1146/annurev-pharmtox-010818-021747

McGranahan TM, Patzlaff NE, Grady SR, Heinemann SF, Booker TK. α4β2 nicotinic acetylcholine receptors on dopaminergic neurons mediate nicotine reward and anxiety relief. J. Neurosci., 31 (30), 10891–10902, 2011. https://doi.org/10.1523/JNEUROSCI.0937-11.2011

Merdas M, Lagarrigue M, Vanbellingen Q, Umbdenstock T, Da Violante G, Pineau C. On-tissue chemical derivatization reagents for matrix-assisted laser desorption/ionization mass spectrometry imaging. J. Mass Spectrom., 56 (10), e4731, 2021. https://doi.org/10.1002/JMS.4731

Metherate R. Nicotinic acetylcholine receptors in sensory cortex. In Learn. Mem.2004. https://doi.org/10.1101/lm.69904

Mihailescu S, Guzmán-Marín R, Frías Domínguez M del C, Drucker-Coliín R. Mechanisms of nicotine actions on dorsal raphe serotoninergic neurons. Eur. J. Pharmacol., 452 (1), 77–82, 2002. https://doi.org/10.1016/S0014-2999(02)02244-6

Mihailescu S, Palomero-Rivero M, Meade-Huerta P, Maza-Flores A, Drucker-Colín R. Effects of nicotine and mecamylamine on rat dorsal raphe neurons. Eur. J. Pharmacol., 360 (1), 31–36, 1998. https://doi.org/10.1016/S0014-2999(98)00658-X

Mineur YS, Mose TN, Blakeman S, Picciotto MR. Hippocampal α7 nicotinic ACh receptors contribute to modulation of depression-like behaviour in C57BL/6J mice. Br. J. Pharmacol., 175 (11), 1903–1914, 2018. https://doi.org/10.1111/bph.13769

Mineur YS, Obayemi A, Wigestrand MB, Fote GM, Calarco CA, Li AM, Picciotto MR. Cholinergic signaling in the hippocampus regulates social stress resilience and anxiety- and depression-like behavior. Proc. Natl. Acad. Sci. U. S. A., 110 (9), 3573–3578, 2013. https://doi.org/10.1073/PNAS.1219731110/SUPPL_FILE/PNAS.201219731SI.PDF

Mineur YS, Soares AR, Etherington IM, Abdulla ZI, Picciotto MR. Pathophysiology of nAChRs: Limbic circuits and related disorders. Pharmacol. Res., 191 , 106745, 2023. https://doi.org/10.1016/J.PHRS.2023.106745

Miranda L. Antidepressant and anxiolytic effects of activating 5HT2A receptors in the anterior cingulate cortex and the theoretical mechanisms underlying them – A scoping review of available literature. Brain Res., 1846 , 149226, 2025. https://doi.org/10.1016/J.BRAINRES.2024.149226

Mohammad-Zadeh LF, Moses L, Gwaltney-Brant SM. Serotonin: a review. J. Vet. Pharmacol. Ther., 31 (3), 187–199, 2008. https://doi.org/10.1111/J.1365-2885.2008.00944.X

Moore RY, Halaris AE. Hippocampal innervation by serotonin neurons of the midbrain raphe in the rat. J. Comp. Neurol., 164 (2), 171–183, 1975. https://doi.org/10.1002/CNE.901640203

Morilak DA, Frazer A. Antidepressants and brain monoaminergic systems: a dimensional approach to understanding their behavioural effects in depression and anxiety disorders. Int. J. Neuropsychopharmacol., 7 (2), 193–218, 2004. https://doi.org/10.1017/S1461145704004080

Morse DE. Neuroendocrine responses to nicotine and stress: enhancement of peripheral stress responses by the administration of nicotine. Psychopharmacology (Berl)., 98 (4), 539–543, 1989. https://doi.org/10.1007/BF00441956/METRICS

Moser VC. Functional assays for neurotoxicity testing. Toxicol. Pathol., 39 (1), 36–45, 2010. https://doi.org/10.1177/0192623310385255

Nabekura J, Eto K. In vivo imaging of the brain by two-photon laser microscopy. Folia Pharmacol. Jpn., 135 (3), 104–108, 2010. https://doi.org/10.1254/fpj.135.104

Nakayama A, Yoshida M, Kagawa N, Nagao T. The neonicotinoids acetamiprid and imidacloprid impair neurogenesis and alter the microglial profile in the hippocampal dentate gyrus of mouse neonates. J. Appl. Toxicol., 39 (6), 877–887, 2019. https://doi.org/10.1002/jat.3776

Nasehi M, Mafi F, Oryan S, Nasri S, Zarrindast MR. The effects of dopaminergic drugs in the dorsal hippocampus of mice in the nicotine-induced anxiogenic-like response. Pharmacol. Biochem. Behav., 98 (3), 468–473, 2011. https://doi.org/10.1016/J.PBB.2011.02.011

Nieoullon A, Coquerel A. Dopamine: A key regulator to adapt action, emotion, motivation and cognition. Curr. Opin. Neurol., 16 (SUPPL. 2), 3–9, 2003. https://doi.org/10.1097/00019052-200312002-00002

OECD. Test No. 424: Neurotoxicity study in rodents. 1997. https://doi.org/10.1787/9789264071025-en

OECD. Guidance document for neurotoxicity testing. 2004. https://doi.org/10.1787/16D23A96-EN

Ohama E, Ikuta F. Parkinson's disease: Distribution of Lewy bodies and monoamine neuron system. Acta Neuropathol., 34 (4), 311–319, 1976. https://doi.org/10.1007/BF00696560/METRICS

Ohmura Y, Tanaka KF, Tsunematsu T, Yamanaka A, Yoshioka M. Optogenetic activation of serotonergic neurons enhances anxiety-like behaviour in mice. Int. J. Neuropsychopharmacol., 17 (11), 1777–1783, 2014. https://doi.org/10.1017/S1461145714000637

Okada T, Kato D, Nomura Y, Obata N, Quan X, Morinaga A, Yano H, Guo Z, Aoyama Y, Tachibana Y, Moorhouse AJ, Matoba O, Takiguchi T, Mizobuchi S, Wake H. Pain induces stable, active microcircuits in the somatosensory cortex that provide a therapeutic target. Sci. Adv., 7 (12), 8261, 2021. https://doi.org/10.1126/SCIADV.ABD8261

Ons S, Martí O, Armario A. Stress-induced activation of the immediate early gene Arc (activity-regulated cytoskeleton-associated protein) is restricted to telencephalic areas in the rat brain: relationship to c-fos mRNA. J. Neurochem., 89 (5), 1111–1118, 2004. https://doi.org/10.1111/J.1471-4159.2004.02396.X

Ouagazzal AM, Kenny PJ, File SE. Stimulation of nicotinic receptors in the lateral septal nucleus increases anxiety. Eur. J. Neurosci., 11 (11), 3957–3962, 1999. https://doi.org/10.1046/J.1460-9568.1999.00823.X

Parfitt GM, Nguyen R, Bang JY, Aqrabawi AJ, Tran MM, Seo DK, Richards BA, Kim JC. Bidirectional control of anxiety-related behaviors in mice: role of inputs arising from the ventral hippocampus to the lateral septum and medial prefrontal cortex. Neuropsychopharmacol. 2017 428, 42 (8), 1715–1728, 2017. https://doi.org/10.1038/npp.2017.56

Petersen DR, Norris KJ, Thompson JA. A comparative study of the disposition of nicotine and its metabolites in three inbred strains of mice. Drug Metab. Dispos., 12 (6), 725–731, 1984.

Pignatelli A, Kobayashi K, Okano H, Belluzzi O. Functional properties of dopaminergic neurones in the mouse olfactory bulb. J. Physiol., 564 (2), 501–514, 2005. https://doi.org/10.1113/jphysiol.2005.084632

Prus AJ, Vann RE, Rosecrans JA, James JR, Pehrson AL, O'Connell MM, Philibin SD, Robinson SE. Acute nicotine reduces and repeated nicotine increases spontaneous activity in male and female Lewis rats. Pharmacol. Biochem. Behav., 91 (1), 150–154, 2008. https://doi.org/10.1016/j.pbb.2008.06.024

Rahman MA, Rahman MS, Uddin MJ, Mamum-Or-Rashid ANM, Pang MG, Rhim H. Emerging risk of environmental factors: insight mechanisms of Alzheimer's diseases. Environ. Sci. Pollut. Res., 27 (36), 44659–44672, 2020. https://doi.org/10.1007/S11356-020-08243-Z/FIGURES/5

Robinson SE, James JR, Lapp LN, Vann RE, Gross DF, Philibin SD, Rosecrans JA. Evidence of cellular nicotinic receptor desensitization in rats exhibiting nicotine-induced acute tolerance. Psychopharmacology (Berl)., 184 (3–4), 306–313, 2006. https://doi.org/10.1007/s00213-005-0049-9

Rodrigues KJA, Santana MB, Do Nascimento JLM, Picanço-Diniz DLW, Maués LAL, Santos SN, Ferreira VMM, Alfonso M, Durán R, Faro LRF. Behavioral and biochemical effects of neonicotinoid thiamethoxam on the cholinergic system in rats. Ecotoxicol. Environ. Saf., 73 (1), 101–107, 2010. https://doi.org/10.1016/j.ecoenv.2009.04.021

Rostami P, Hajizadeh-Moghaddam A, Zarrindast MR. The effects of histaminergic agents in the ventral hippocampus of rats in the plus-maze test of anxiety-like behaviours. Physiol. Behav., 87 (5), 891–896, 2006. https://doi.org/10.1016/J.PHYSBEH.2006.02.001

Sabri O, Meyer PM, Gräf S, Hesse S, Wilke S, Becker GA, Rullmann M, Patt M, Luthardt J, Wagenknecht G, Hoepping A, Smits R, Franke A, Sattler B, Tiepolt S, Fischer S, Deuther-Conrad W, Hegerl U, Barthel H, … Brust P. Cognitive correlates of α4β2 nicotinic acetylcholine receptors in mild Alzheimer's dementia. Brain, 141 (6), 1840–1854, 2018. https://doi.org/10.1093/BRAIN/AWY099

Sánchez-Bayo F, Goulson D, Pennacchio F, Nazzi F, Goka K, Desneux N. Are bee diseases linked to pesticides? - A brief review. In Environ. Int.2016. https://doi.org/10.1016/j.envint.2016.01.009

Sano K, Isobe T, Yang J, Win-Shwe TT, Yoshikane M, Nakayama SF, Kawashima T, Suzuki G, Hashimoto S, Nohara K, Tohyama C, Maekawa F. In utero and lactational exposure to acetamiprid induces abnormalities in socio-sexual and anxiety-related behaviors of male mice. Front. Neurosci., 10 (JUN), 228, 2016. https://doi.org/10.3389/fnins.2016.00228

Santana N, Bortolozzi A, Serrats J, Mengod G, Artigas F. Expression of serotonin1A and serotonin2A receptors in pyramidal and GABAergic neurons of the rat prefrontal cortex. Cereb. Cortex, 14 (10), 1100–1109, 2004. https://doi.org/10.1093/CERCOR/BHH070

Schindelin J, Arganda-Carreras I, Frise E, Kaynig V, Longair M, Pietzsch T, Preibisch S, Rueden C, Saalfeld S, Schmid B, Tinevez JY, White DJ, Hartenstein V, Eliceiri K, Tomancak P, Cardona A. Fiji: An open-source platform for biological-image analysis. In Nat. Methods2012. https://doi.org/10.1038/nmeth.2019

Shariatgorji M, Nilsson A, Goodwin RJA, Källback P, Schintu N, Zhang X, Crossman AR, Bezard E, Svenningsson P, Andren PE. Direct targeted quantitative molecular imaging of neurotransmitters in brain tissue sections. Neuron, 84 (4), 697–707, 2014. https://doi.org/10.1016/j.neuron.2014.10.011

Shariatgorji M, Nilsson A, Källback P, Karlsson O, Zhang X, Svenningsson P, Andren PE. Pyrylium salts as reactive matrices for MALDI-MS imaging of biologically active primary amines. J. Am. Soc. Mass Spectrom., 26 (6), 934–939, 2015. https://doi.org/10.1007/s13361-015-1119-9

Shepherd JK, Grewal SS, Fletcher A, Bill DJ, Dourish CT. Behavioural and pharmacological characterisation of the elevated "zero-maze" as an animal model of anxiety. Psychopharmacology (Berl)., 116 (1), 56–64, 1994. https://doi.org/10.1007/BF02244871/METRICS

Shikano H, Ikeda A, Maejima Y, Kobayashi S, Terauchi T, Yokoyama J, Shimomura K, Taira S. Optimization of the use of Py–Tag for next generation derivatization reagents in imaging mass spectrometry. J. Biosci. Bioeng., 134 (3), 264–268, 2022. https://doi.org/10.1016/J.JBIOSC.2022.06.007

Shimma S, Takeo E, Fukusaki E. Protocol for quantitative imaging mass spectrometry. Bunseki Kagaku, 65 (12), 745–750, 2016. https://doi.org/10.2116/bunsekikagaku.65.745

Song YN, Li HZ, Zhu JN, Guo CL, Wang JJ. Histamine improves rat rota-rod and balance beam performances through H2 receptors in the cerebellar interpositus nucleus. Neuroscience, 140 (1), 33–43, 2006. https://doi.org/10.1016/J.NEUROSCIENCE.2006.01.045

Sørensen LK, Johannsen M. Sensitive determination of monoamine neurotransmitters, their main metabolites and precursor amino acids in different mouse brain components by liquid chromatography–electrospray tandem mass spectrometry after selective sample clean-up. Biomed. Chromatogr., 33 (4), 1–12, 2019. https://doi.org/10.1002/bmc.4479

Stehle S, Ovcharova V, Wolfram J, Bub S, Herrmann LZ, Petschick LL, Schulz R. Neonicotinoid insecticides in global agricultural surface waters – Exposure, risks and regulatory challenges. Sci. Total Environ., 867 , 161383, 2023. https://doi.org/10.1016/J.SCITOTENV.2022.161383

Suzuki T, Hirai A, Khidkhan K, Nimako C, Ichise T, Takeda K, Mizukawa H, Nakayama SMM, Nomiyama K, Hoshi N, Maeda M, Hirano T, Sasaoka K, Sasaki N, Takiguchi M, Ishizuka M, Ikenaka Y. The effects of fipronil on emotional and cognitive behaviors in mammals. Pestic. Biochem. Physiol., 104847, 2021. https://doi.org/10.1016/j.pestbp.2021.104847

Taillebois E, Cartereau A, Jones AK, Thany SH. Neonicotinoid insecticides mode of action on insect nicotinic acetylcholine receptors using binding studies. Pestic. Biochem. Physiol., 151 , 59–66, 2018. https://doi.org/10.1016/J.PESTBP.2018.04.007

Taira K, Kawakami T, Weragoda SK, Herath HMAS, Ikenaka Y, Fujioka K, Hemachandra M, Pallewatta N, Aoyama Y, Ishizuka M, Bonmatin JM, Komori M. Urinary concentrations of neonicotinoid insecticides were related to renal tubular dysfunction and neuropsychological complaints in Dry-zone of Sri Lanka. Sci. Reports 2021 111, 11 (1), 1–12, 2021. https://doi.org/10.1038/s41598-021-01732-2

Taira S, Ikeda A, Kobayashi S, Shikano H, Ikeda R, Maejima Y, Horita S, Yokoyama J, Shimomura K. Comparative analysis of derivatization reagents for catecholamines and amino acids. Appl. Sci. 2021, Vol. 11, Page 6217, 11 (13), 6217, 2021. https://doi.org/10.3390/APP11136217

Tan J, Galligan JJ, Hollingworth RM. Agonist actions of neonicotinoids on nicotinic acetylcholine receptors expressed by cockroach neurons. Neurotoxicology, 28 (4), 829–842, 2007. https://doi.org/10.1016/J.NEURO.2007.04.002

Tareke E, Bowyer JF, Doerge DR. Quantification of rat brain neurotransmitters and metabolites using liquid chromatography/electrospray tandem mass spectrometry and comparison with liquid chromatography/electrochemical detection. Rapid Commun. Mass Spectrom., 21 (23), 3898–3904, 2007. https://doi.org/10.1002/rcm.3295

Terayama H, Endo H, Tsukamoto H, Matsumoto K, Umezu M, Kanazawa T, Ito M, Sato T, Naito M, Kawakami S, Fujino Y, Tatemichi M, Sakabe K. Acetamiprid accumulates in different amounts in murine brain regions. Int. J. Environ. Res. Public Health, 13 (10)2016. https://doi.org/10.3390/ijerph13100937

Thévenaz P, Ruttimann UE, Unser M. A pyramid approach to subpixel registration based on intensity. IEEE Trans. Image Process., 7 (1), 27–41, 1998. https://doi.org/10.1109/83.650848

Thompson DA, Lehmler HJ, Kolpin DW, Hladik ML, Vargo JD, Schilling KE, Lefevre GH, Peeples TL, Poch MC, Laduca LE, Cwiertny DM, Field RW. A critical review on the potential impacts of neonicotinoid insecticide use: current knowledge of environmental fate, toxicity, and implications for human health. Environ. Sci. Process. Impacts, 22 (6), 1315–1346, 2020. https://doi.org/10.1039/C9EM00586B

Tian Z, Yamanaka M, Bernabucci M, Zhao MG, Zhuo M. Characterization of serotonin-induced inhibition of excitatory synaptic transmission in the anterior cingulate cortex. Mol. Brain, 10 (1), 1–10, 2017. https://doi.org/10.1186/S13041-017-0303-1/FIGURES/8

Tomizawa M, Casida JE. Selective toxicity of neonicotinoids attributable to specificity of insect and mammalian nicotinic receptors. Annu. Rev. Entomol., 48 , 339–364, 2003. https://doi.org/10.1146/annurev.ento.48.091801.112731

Tomizawa M, Casida JE. Neonicotinoid insecticide toxicology: Mechanisms of selective action. In Annu. Rev. Pharmacol. Toxicol.2005. https://doi.org/10.1146/annurev.pharmtox.45.120403.095930

Tomizawa M, Lee DL, Casida JE. Neonicotinoid insecticides: Molecular features conferring selectivity for insect versus mammalian nicotinic receptors. J. Agric. Food Chem., 48 (12), 6016–6024, 2000. https://doi.org/10.1021/JF000873C/ASSET/IMAGES/LARGE/JF000873CF00004.JPEG

Ueyama J, Harada KH, Koizumi A, Sugiura Y, Kondo T, Saito I, Kamijima M. Temporal levels of urinary neonicotinoid and dialkylphosphate concentrations in Japanese women between 1994 and 2011. In Environ. Sci. Technol.2015. https://doi.org/10.1021/acs.est.5b03062

Umeda T, Isa T, Nishimura Y. The somatosensory cortex receives information about motor output. Sci. Adv., 5 (7), eaaw5388, 2019. https://doi.org/10.1126/sciadv.aaw5388

Vellingiri B, Chandrasekhar M, Sri Sabari S, Gopalakrishnan AV, Narayanasamy A, Venkatesan D, Iyer M, Kesari K, Dey A. Neurotoxicity of pesticides – A link to

neurodegeneration. Ecotoxicol. Environ. Saf., 243 , 113972, 2022. https://doi.org/10.1016/J.ECOENV.2022.113972

Walf AA, Frye CA. The use of the elevated plus maze as an assay of anxiety-related behavior in rodents. Nat. Protoc. 2007 22, 2 (2), 322–328, 2007. https://doi.org/10.1038/nprot.2007.44

Yamaguchi T, Togashi H, Matsumoto M, Yoshioka M. Evaluation of anxiety-related behavior in elevated plus-maze test and its applications. Nihon Yakurigaku Zasshi, 126 (2), 99–106, 2005. ahttps://doi.org/10.1254/fpj.126.99

Yamaguchi T, Togashi H, Matsumoto M, Yoshioka M. Evaluation of anxiety - related behavior in elevated plus-maze test and its applications. Folia Pharmacol. Jpn., 126 , 99–105, 2005. b

Yamaguchi T, Yoshioka M. Evaluation for anxiety-related behaviors in rodents. Folia Pharmacol. Jpn., 130 (2), 105–111, 2007. https://doi.org/10.1254/fpj.130.105

Yeganeh-Doost P, Gruber O, Falkai P, Schmitt A. The role of the cerebellum in schizophrenia: from cognition to molecular pathways. Clinics, 66 (SUPPL.1), 71–77, 2011. https://doi.org/10.1590/S1807-59322011001300009

Yoneda N, Takada T, Hirano T, Yanai S, Yamamoto A, Mantani Y, Yokoyama T, Kitagawa H, Tabuchi Y, Hoshi N. Peripubertal exposure to the neonicotinoid pesticide dinotefuran affects dopaminergic neurons and causes hyperactivity in male mice. In J. Vet. Med. Sci.2018. https://doi.org/10.1292/jvms.18-0014

Yoshikawa T, Nakamura T, Shibakusa T, Sugita M, Naganuma F, Iida T, Miura Y, Mohsen A, Harada R, Yanai K. Insufficient intake of L-histidine reduces brain histamine and causes anxiety-like behaviors in male mice. J. Nutr., 144 (10), 1637–1641, 2014. https://doi.org/10.3945/jn.114.196105

Yoshimura S. 神経毒性試験. Pharm. Soc. Japan, 29 (1), 35–37, 1993. https://doi.org/10.14894/faruawpsj.29.1_35

Yoshitomi I, Itoh Y, Oishi R, Saeki K. Brain histamine turnover enhanced by footshock. Brain Res., 362 (1), 195–198, 1986. https://doi.org/10.1016/0006-8993(86)91418-6

Zarrindast MR, Homayoun H, Babaie A, Etminani A, Gharib B. Involvement of adrenergic and cholinergic systems in nicotine-induced anxiogenesis in mice. Eur. J. Pharmacol., 407 (1–2), 145–158, 2000. https://doi.org/10.1016/S0014-2999(00)00628-2

Zarrindast MR, Khakpai F. The modulatory role of dopamine in anxiety-like behavior. Arch. Iran. Med., 18 (9), 591–603, 2015. http://journalaim.com/Article/884

Zarrindast MR, Khalifeh S, Rezayof A, Rostami P, Aghamohammadi Sereshki A, Zahmatkesh M. Involvement of rat dopaminergic system of nucleus accumbens in nicotine-induced anxiogenic-like behaviors. Brain Res., 1460 , 25–32, 2012. https://doi.org/10.1016/J.BRAINRES.2012.04.036

Zarrindast MR, Naghdi-Sedeh N, Nasehi M, Sahraei H, Bahrami F, Asadi F. The effects of dopaminergic drugs in the ventral hippocampus of rats in the nicotine-induced

anxiogenic-like response. Neurosci. Lett., 475 (3), 156–160, 2010. https://doi.org/10.1016/J.NEULET.2010.03.069

Zarrindast MR, Torabi M, Rostami P, Fazli-Tabaei S. The effects of histaminergic agents in the dorsal hippocampus of rats in the elevated plus-maze test of anxiety. Pharmacol. Biochem. Behav., 85 (3), 500–506, 2006. https://doi.org/10.1016/J.PBB.2006.09.019

Zhang D, Lu S. Human exposure to neonicotinoids and the associated health risks: A review. Environ. Int., 163 , 107201, 2022. https://doi.org/10.1016/J.ENVINT.2022.107201

Zhu KY, Fu Q, Leung KW, Wong ZCF, Choi RCY, Tsim KWK. The establishment of a sensitive method in determining different neurotransmitters simultaneously in rat brains by using liquid chromatography-electrospray tandem mass spectrometry. J. Chromatogr. B Anal. Technol. Biomed. Life Sci., 879 (11–12), 737–742, 2011. https://doi.org/10.1016/j.jchromb.2011.02.011

Zhuo M. Neural mechanisms underlying anxiety-chronic pain interactions. In Trends Neurosci.2016. https://doi.org/10.1016/j.tins.2016.01.006

Żmudzka E, Sałaciak K, Sapa J, Pytka K. Serotonin receptors in depression and anxiety: Insights from animal studies. Life Sci., 210 , 106–124, 2018. https://doi.org/10.1016/J.LFS.2018.08.050

Abstract

Humans are routinely exposed to various chemicals, including neonicotinoid pesticides (NNs), through daily products, food, and the environment. NNs, such as acetamiprid (ACE) and imidacloprid (IMI), have been implicated in neurotoxicity, affecting emotional and cognitive behaviors, even at doses below the no observed adverse effect level (NOAEL). However, conventional neurotoxicity tests often fail to detect these effects due to the absence of histopathological changes. This study aimed to develop high-sensitivity methods for detecting neurotransmission disruptions and to elucidate the neurotoxic mechanisms of NNs by integrating findings across multiple levels of the adverse outcome pathway (AOP) framework.

In *Chapter 1*, it was demonstrated that ACE rapidly distributed to the hippocampus and striatum within one hour of oral administration. In addition, behavioral tests indicated that ACE induced anxiety-like behavior at NOAEL doses in the elevated plus maze (EPM) tests, highlighting the necessity for further investigation into its underlying mechanisms.

Chapter 2 examined the effects of IMI and ACE on monoamine neurotransmitters (MAs) and their association with anxiety-like behavior. IMI was found to reduce dopamine in the olfactory bulb and serotonin in the striatum at NOAEL doses, suggesting that even low doses of NNs can disrupt MAs. ACE increased hippocampal serotonin and striatal dopamine, which correlated with anxiety-like behavior observed 30 minutes after administration. Furthermore, serotonergic neurons in the dorsal raphe nuclei (DRN), which have been shown to be a critical origin of serotonergic projections, exhibited increased serotonin production. These findings underscore the importance of serotonergic pathways in ACE-induced behavioral changes.

In *Chapter 3*, *in vivo* Ca^{2+} imaging using two-photon microscopy detected changes in neuronal activity in the somatosensory cortex at ACE concentrations that did not influence behavior in *Chapter 1*. These findings demonstrate the utility of two-photon microscopy in identifying neurotoxicity undetectable through conventional neurotoxicity tests.

Chapter 4 utilized Arc^{CreER};Ai14 transgenic mice to screen for brain regions with elevated neuronal activity following ACE administration. The results indicated increased neural activity in anxiety-associated regions, including the somatosensory cortex, septal nucleus, amygdala, and inferior colliculus, many of which are innervated by serotonergic projections from the DRN. The combination of this approach with complementary techniques, such as staining and mass spectrometry imaging, may provide a more comprehensive understanding of the toxicological mechanisms involved.

This study proposes a hypothesis that ACE activates serotonergic neurons in the DRN, increasing serotonin release in the hippocampus and other downstream serotonergic pathways, resulting in anxiety-like behavior. These findings underscore the limitations of conventional toxicity tests, which may overlook neurotransmission disruptions affecting emotional and cognitive behaviors. This study emphasizes the importance of investigating AOPs across multiple levels, integrating novel techniques for the toxicology field, including two-photon microscopy and Arc^{CreER};Ai14 mice model.

The findings of this study provide a more profound comprehension of NNs-induced neurotoxicity and support the development of high-sensitivity neurotoxicity tests, which will advance chemical risk assessment and the discovery of biomarkers for subtle neurotoxic effects.

Japanese abstract

ヒトは、職業的に化学物質を扱わない場合でも、日用品や食品、環境などを通じて日常的に様々な化学物質に曝露されている。疫学研究によれば、こうした化学物質への曝露がパーキンソン病やアルツハイマー病といった精神疾患に関与する可能性が示唆されている。しかし、これらの知見はリスク管理への十分な活用には至っておらず、化学物質のリスク評価における重要なフレームワークである有害性発現経路（AOP）に関するデータの蓄積が求められている。また、 ネオニコチノイド系農薬（NNs）を含む一部の化学物質は、病理組織学的な変化を伴わないような低濃度でも、神経情報伝達の攪乱によって情動認知行動に影響を及ぼす可能性があるが、現行の神経毒性試験法ではこうした影響を検出することは困難である。特にNNsは、世界中で広く使用されている農薬であるにもかかわらず、神経系への影響やその機序については十分に解明されていない。本研究では、NNsの一種であるアセタミプリド（ACE）とイミダクロプリド（IMI）に焦点を当て、AOPの複数のレベルにわたる知見を提供することで、これらのNNsが情動認知行動に影響を与えるメカニズムを解明するとともに、神経情報伝達の攪乱を高感度に検出することを試みた。

まず、*Chapter 1*では、ACEがマウスの不安様行動に与える影響と、脳および血漿中のACE濃度を評価した。その結果、無毒性量（NOAEL）レベルのACEが高架式十字迷路試験（EPM）において不安様行動を誘発すること、さらに経口投与から1時間後にACEが海馬や線状体などの脳領域に移行することが示された。この結果は、ACEの神経毒性作用を解明するためのさらなる研究の必要性を強調している。

*Chapter 2*では、IMIおよびACEのモノアミン神経伝達物質（MAs）に対する影響を調べるとともに、この影響が不安様行動に関連するかどうかを明らかにした。まず*Chapter 2-1*において、LC/MS/MS分析によりMAsを高感度で検出するための誘導体化条件を検討した。検討した条件でMAs分析を実施したところ、NOAELレベルのIMIが嗅球のドーパミンや線条体のセロトニンを減少させることが明らかとなり、低濃度のNNsでもMAsを変化させる可能性が示唆された。*Chapter 2-2*では、MAsの変化と不安様行動について相関解析を実施した。その結果、ACEが海馬のセロトニンと線条体のドーパミンレベルを増加させ、これは投与後30分

の不安様行動と相関していることが示された。さらに、 海馬などの前脳領域に投射するセロトニン作動性神経の大半が起始することが知られている背側縫線核（DRN）について、抗セロトニン染色を行ったところ、セロトニン産生の増加が観察された。これらの結果から、ACE誘発性の不安様行動にセロトニン作動性経路が関与している可能性が示唆された。

*Chapter 3*では、二光子顕微鏡を用いた生体内Ca^{2+}イメージングを実施し、*Chapter 1*で行動に影響を及ぼさなかった濃度のACEが、覚醒下で体性感覚野の神経活動を変化させることを明らかにした。この結果は、二光子顕微鏡により、従来の毒性試験では検出できない神経毒性影響を検出できることを示している。

最後に*Chapter 4*では、活性化細胞を赤色蛍光タンパクtdTomatoで標識するように設計された遺伝子組換えマウスであるArc^{CreER};Ai14マウスを用いて、ACEの投与により神経活動が亢進した脳領域をスクリーニングした。その結果、主に不安や行動に関連する脳領域である体性感覚野、中隔核、扁桃体、下丘において、神経活動が増加する傾向が観察された。これらの脳領域はDRNからのセロトニン支配を受けることも知られており、ACEの神経毒性においてセロトニン系が重要な役割を果たす可能性が改めて示唆された。このアプローチを染色や質量分析イメージングなどの技術と組み合わせることで、毒性メカニズムのさらなる解明に大きく寄与できると考えられる。

以上の結果から、ACEによる神経毒性のメカニズムとして、DRNのセロトニン作動性神経が活性化され、これが海馬などのセロトニン経路を通じて不安様行動を誘発する、という仮説が提案された。本研究は、病理組織学的変化を伴わない神経情報伝達の攪乱を検出し、そのメカニズムを解明するためには、AOPの複数のレベルにわたる知見を統合することが重要であることを示している。今後、本研究で使用した二光子顕微鏡やArc^{CreER};Ai14マウスなど、毒性学分野でいまだ活用されていない技術も組み合わせながらAOPの複数のレベルにおける影響を調べることで、神経毒性のメカニズムを明らかにし、有用なバイオマーカーの発見などにつなげていく必要がある。本研究で得られた知見は、NNsによる神経毒性への理解を深めるとともに、高感度な神経毒性試験法の確立に貢献することが期待される。